Advanced School and Conference on Quantum Matter | (SMR 4114)

01 Dec 2025 - 12 Dec 2025
ICTP, Trieste, Italy

P01 - ABBRUCIATI Federico

Pressure control of magnetic frustration in spin liquid putative material Y-Kapellasite

P02 - ADIRA Mohitha

Gapless topological behaviour - a signature of Deconfined quantum criticality?

P03 - ALI Asad

Quantum Mpemba Effect in a Dirty Bose-Hubbard Model under Stark Potential

P04 - ANDREONI Riccardo

Stochastic Sampling-Based Classification of Quantum States of Matter

P05 - ARILDSEN Mark Jesse

Unambiguous diagnostic of chirality in the entanglement spectrum of (2+1)-dimensional topological spin liquids: Demonstration in the Abelian chiral SU(4) spin liquid setting

P06 - ASAFOV Daniil

Microscopic derivation of effective field theory for hydrodynamics in U(1)-symmetric Brownian circuits

P07 - BACCICONI Zeno

Theory of fractional Quantum Hall liquids coupled to quantum light and emergent graviton polaritons

P08 - BANERJEE Archi

Multiplicative Chern Insulator

P09 - BARARI Saeed

Quantum Phase Diagram of the Kitaev–Heisenberg Model on the Square–Hexagonal–Dodecagonal Lattice

P10 - BAUER Tim Yannik

Compact localized fermions and Ising anyons in a chiral spin liquid

P11 - BIEDERMANN Jan

Twist-tuned quantum criticality in moire bilayer graphene

P12 - BORUTTA JANARTHANARAMAN Hariprasaad

Exact valence bond ground states of a spin-1 model on the checkerboard and pyrochlore lattices

P13 - BREDA ZACHE' Victor

Spin-nematic phases for multipolar Kondo interactions in heavy-fermions materials

P14 - BUDARAJU Sasank

Triangular Heisenberg model under a magnetic field: monte carlo approach

P15 - BUENO XAVIER Hernan Guillermo

Chiral gravitons on the lattice

P16 - CAI Peiyuan

Symmetry-protected topological order identified via Gutzwiller-guided density-matrix-renormalization-group: SO(n) spin chains

P17 - CAPELO DOMINGUES Gabriel

Magnetization plateaux in the Kagome antiferromagnet

P18 - CARREIRA DE JES TORRES Rafael

Tricriticality in 4D U(1) Lattice Gauge Theory

P19 - CHAKRABORTY Nilotpal

Fractional diffusion without disorder in two dimensions

P20 - CHANDA Titas

A cornucopia of emergence in classical frustrated systems

P21 - CHATTERJEE Sourin

Projective symmetry group classification of Abrikosov fermion mean-field ansatze on the trellis lattice

P22 - DAKIR Yassine

Characterizing non-Markovianity via quantum coherence based on Kirkwood-Dirac quasiprobability

P23 - DARWISH Esa

Investigation of Periodic TI-NI/TI-S Multilayers in the Presence of a Transverse Magnetic Field to Realize Weyl Semimetal/Weyl Superconductor with Tilted Weyl Cones

P24 - DAS Ankur

Topological Semimetals via Internal Symmetry

P25 - DAS Hiranmay

Critical States of Fermions with Z2 Flux Disorder

P26 - DASH Gaurab Kumar

Floquet exceptional Topological Insulator

P27 - DASH Soumyaranjan

Vacancy induced expansion of spin-liquid regime in J1-J2 Heisenberg model

P28 - DATTA Soujanya

Anomalous Landau Levels in Inhomogeneous Fluxes and Emergent Supersymmetry

P29 - DE Ayush

Phases of the "Odd" Toric Code in a tilted field

P30 - DEBNATH Shreya

Topological characterization of magnon-polaron bands and thermal Hall conductivity in a frustrated kagome antiferromagnet

P31 - DEB Rohit

Classification and Energy Minimization of Spin Liquids via the Projective Symmetry Group Approach

P32 - DE CASTRO BELLINATI Carlo

Towards more efficient matrix product state representations of fermionic Gaussian states

P33 - DE OLIVEIRA CARVALHO Bruno

Classification of locality preserving symmetries on spin chains

P34 - DUSEL Felix Michael

Chiral Gapless Spin Liquid in Hyperbolic Space

P35 - ESMER Berna

Spin-liquid candidate based on S=1/2 Ti3+ ions with a langbeinite structure

P36 - FENG Shi

Transient localization from fractionalization in gapless quantum magnets

P37 - FLORES CALDERON Rafael Alvaro

Unconventional Spin Dynamics and Supersolid Excitations in the Triangular-Lattice XXZ Model

P38 - FRANCHINI Fabio

The Frustration of Being Odd

P39 - FRANCUZ Anna Elzbieta

Topological Order in the Rydberg Blockade on the Kagome Lattice with PEPS

P40 - GARRE RUBIO Jose

Boundary-bulk maps of topological phases via gauging.

P41 - GHORAI Debabrata

Quantum geometry from fidelity expansion

P42 - GIUDICI Giuliano

Adiabatic echo protocols for robust many-body state preparation

P43 - GONZALEZ Matias Gabriel

Spin Liquids on the Tetratrillium Lattice

P44 - GRANBERG CAUCHI Sabastian Charles Jan

Chiral spin liquid in external magnetic field: Phase diagram of the decorated-honeycomb Kitaev model

P45 - GUPTA Manoj

Emergent SU (4) Symmetry and Gapless Spin-Orbital Liquid in ZrCl3 inspired model

P46 - HABEL Jonas

Understanding the Hamiltonian of alpha-RuCl3 through Nonlinear Spin-Wave Analysis

P47 - HALDER Dipendu

Controlled probing of localization effects in the non-Hermitian Aubry-André model via topolectrical circuits

P48 - HASSAN Noah Medhat Mohammed Louis

The Pseudo-Majorana Functional Renormalization Group: An efficient tool for treating frustrated systems

P49 - HILLE Simon Hans

TeMFpy: a Python library for converting fermionic mean-field states into tensor networks

P50 - JADIDI KOUHBANANI Fatemeh

Quantum manipulation of energy transfer in quantum materials

P51 - JONES Joseph

A New, Exact Perturbation Theory for Operators Related by the Baker-Campbell-Hausdorff identity; Applied to the Ising model on the Square, Cubic and Hypercubic Lattices

P52 - KALINOWSKI Stanislaw

Stability of the Spin Polaron Solution in the J1-J2 Doped Quantum Spin Liquid

P53 - KAROLIYA Shubhanshu

Majorana polarization in disordered heterostructures

P54 - KHAN Sakil

Emergence of distinct relaxation behaviour and Quantum Regression Theorem in the Ultra-strong Coupling Limit

P55 - KHOSROJERDI Mehran

Quantum Machine Learning for Quantum Phase Recognition in Many-Body Systems

P56 - KOLLER Eduard Ferdinand Vitus

Spin-phonon coupling induced chiral phonons and their signature in Raman Circular Dichroism

P57 - KOMAR Rafal

Understanding the limits of the linear spin wave theory

P58 - KONDAKOR Mark

Symmetry Study of Elemental Rhenium

P59 - SHIMIZU Kotaro

Quasi-isotropic magnetic interaction in Yb and Ce compounds

P60 - KRANITZ Peter

SU(2) symmetric Hamiltonian for the four-color states on the pyrochlore lattice

P61 - KUMAR Sankalp

Pseudocriticality in antiferromagnetic spin chains

P62 - KUNDU Souvik

Thermal quenches in spin-3/2 ice

P63 - LAHIRI Srijata

Emergent topological phases and coexistence of gapless and spectral-localized Floquet quantum spin Hall states mediated via electron-phonon interaction.

P64 - LEITAO SOUSA RIBEIRO Afonso

Dissipative quantum spin ice

P65 - LIN Jonathan

Probing Spinon Interactions in the Bilinear-Biquadratic Spin-1 Chain

P66 - LISANDRINI Franco Thomas

Superconductivity in the repulsive Hubbard model on different geometries induced by density-assisted hopping

P67 - LI Yahui

Highly entangled statioanry states from strong symmetries

P68 - LOZANO GOMEZ Daniel

An Atlas of Classical Pyrochlore Spin Liquids

P69 - MAITY Atanu

Fermionic parton theory of Rydberg $\mathbb{Z}_2$ quantum spin liquids

P70 - MAITY Avijit

Thermal Hall response of an abelian chiral spin liquid at finite temperatures

P71 - MAJUMDER Ritwika

Dynamical signatures of fractionalization in spin-1/2 1d Kitaev chain

P72 - MAKRIS Grigorios

Extraordinary-log phase in the Heisenberg spin chain

P73 - MALLADI Ananth Venkatesh Narasimha

Cold quantum gases of many flavors

P74 - MANGEOLLE Leo Charles Henri Maurice Albert

Extrinsic contribution to bosonic thermal Hall transport

P75 - MAO Dan

Exotic Gapless Mott Insulator with Tile-invariant Symmetry

P76 - MARINHO PEREIRA DE MELO Marcus Vinicius

Quantum Spin Liquids in Spin Ice Pyrochlores Stabilized by Disorder

P77 - MARTINS CARVALHO Isaac

Single-site entanglement unveils superconducting transition in a correlated fermionic system

P78 - MOHAMMADI Sepideh

Quantum Fisher Information, Dynamical Susceptibility, and Topological Non-Fermi Liquids in the interacting SSH chain

P79 - MOUSAVI Zahra

Phase diagram of the hard-core bosonic Hubbard model for frustrated dipolar bosons using Neural Network Quantum States (NQS)

P80 - MUKHERJEE Arkaprava

Controlling Chaos in Finite Mean Sachdev-Ye-Kitaev Model

P81 - MUELLER-GROELING Mark Henrik

SU(2) Gauge Theory for Fluctuating Stripes in the Pseudogap Regime

P82 - NEEHUS Avedis Eric Albert

Projectively implemented altermagnetism in an exactly solvable quantum spin liquid

P83 - NIGAM Harsh

Phases and phase transitions in a dimerized spin-1/2 XXZ chain

P84 - NINA CARREIRA FERREIRA DA CRUZ José Maria

Generalized Dimer Physics in Multi-Level Rydberg Atom Arrays

P85 - OVCHINNIKOV Anatolii

Lattice local integrable regularization of the Sine-Gordon model.

P86 - PACHHAL Subrata

Symmetry protected topological wire in a topological vacuum

P87 - PAL Adipta

Topological finite-size effects in magnetic topological insulators

P88 - PAL Sudeshna

Magnetic superconductors in Metal-Organic framework hybrids with flat-bands

P89 - PANAHI Yasamin Sadat

Topology, anomaly, and 2d criticality at strong randomness

P90 - PANDEY Jay

Flux-fractionalization transition in two dimensional non-bipartite lattices

P91 - PARK Jemin

Reallocation of Nonlocal Entanglement in Incommensurate Cold Atom Arrays

P92 - PARTHASARATHY Manikandan

Thermal coherence of the Heisenberg model with Dzyaloshinsky–Moriya interactions in an inhomogenous externalfield

P93 - PATEL Nishit Belaben

Field Induced Enhancement of Spin Excitations in the Frustrated Magnet LiYbW2O8

P94 - PATEL Rahul Pratap

Quantum phases of two-dimensional Z2 gauge theory coupled to Double-component spin-full fermionic matter in SSH model

P95 - PATIL Pranay Mahesh

Tunable topological protection in Rydberg lattices via a novel quantum Monte Carlo approach

P96 - PATIL Vinay Rajendra

Effective field theory for Quantum Skyrmion Hall effect

P97 - PATRICOLO Miriam

Functional Renormalization Group treatment of the spiral phase

P98 - PEARCE John Solis

Magnetic Anisotropies of RuX_3 (X = Br, I) Probed by Torque Magnetometry

P99 - PEREIRA DE BARROSFORNI Paulo

Spin susceptibility in a pseudogap state with fluctuating spiral magnetic order

P100 - PUSHKAR Arnav

Eigenstate thermalization in <> quantum spin liquids

P101 - PUTZER Bernhard Gabriel

Eliashberg theory and superfluid stiffness of band-off-diagonal pairing in twisted graphen

P102 - RABELO Lucas Gabriel

Kondo screening and random singlet formation in highly disordered systems

P103 - RAIKOS Andreas

Variational study of the magnetization plateaux in the spin-1/2 kagome Heisenberg antiferromagnet: a neural network quantum state approach

P104 - RAI Kshiti Sneh

A Hierarchy of Spectral Gap Certificates for Frustration-Free Spin Systems

P105 - RAJA Alwyn Jose

Spin-basis wavefunctions for 1D Kitaev Spin Models

P106 - RAJ Anoop

Dynamics of magnetic monopoles in the presence of domain walls

P107 - RITU -

Characterising Quantum Magic in Topological Many-Body Quantum Systems

P108 - ROUXEL Malo Clement Yohann

Multipartite entanglement in the spin-1 bilinear-biquadratic chain

P109 - ROY Koustav

Unveiling Floquet Skin Modes via Generalized Brillouin zone in a Driven Non-Hermitian Ladder

P110 - RUDNER Laszlo

Emergence of Nematic Ordering from Two-Magnon Bound States on Frustrated Triangular Lattices

P111 - SAHU Dibyajyoti

Majorana Bound States in Nanowires: Identifying Topological Signatures and Overcoming Transport Challenges

P112 - SAHU Krushna Chandra

Z2 spin liquids in Bilayer Kagome

P113 - SALGADO LINARES Ignacio

Spin Dynamics Approach to Thermal Hall Conductivity in Kitaev Magnets

P114 - SAMANTA Diganta

Dynamics of Periodically Driven Spin Liquid

P115 - SANDERS Alaric Luca

Defect poisoning in quantum spin ice

P116 - SAU Indrajit

Anomalous dynamics of a fermion coupled to a constrained gauge background

P117 - SCHMIDT Otto Theodor Primus

Geometry of tensor network varieties for quantum condensed matter physics

P118 - SEETHARAMAN Siddharth

Properties of Krylov State Complexity in Qubit Dynamics

P119 - SEN Snehasish

Fermionic Bands of the Heisenberg Antiferromagnetic Spin-1/2 Trimer Chain

P120 - SKURATIVSKA Anastasiia

Machine learning symmetry protected topological phases from randomized measurements

P121 - SOYOUF JAHROMI Seyed Saeed

Phase diagram of the Kitaev-Heisenberg model on the Amorphous and hyperbolic lattices

P122 - SRIDHARAN Srinidhi

Entanglement Signatures of Gapless Topological Phases in a 2D BdG Superconductor

P123 - SRIVASTAVA Pritesh

Revealing Flat-Band Tunability through Orbital-Selective Hopping in Kagome Materials

P124 - STAFFIERI Gregorio

Signatures of the Fermi surface reconstruction of a doped Mott insulator in a slab geometry

P125 - STERN Matthew Samuel

Classical Fracton Spin Liquid on the Octochlore Lattice

P126 - STOCKER Lidia

Kondo effect in atomic gases: suppression of screening clouds by potential scattering

P127 - SZABO Attila

Rainbow chains and numerical renormalisation group for accurate conformal spectra

P128 - TAGLIENTE Antonio Maria

revealing spinons by proximity effect

P129 - TEXCA GARCIA Julio Cesar

Adiabatic gauge potential approach to characterize the onset of chaos in a many-body quantum system with a quasiperiodical potential

P130 - TOROK Matyas

Stabilizing Altermagnetism via Interaction-Induced Octupolar Order in a Two-Orbital Model

P131 - ULAGA Martin

Anisotropic spin models on frustrated lattices: from spin liquids to supersolids

P132 - VARMA K Gautham

Strain-induced Ettingshausen effect in spin orbit coupled non-centrosymmetric metals

P133 - VEDULA Ramana Bharadwaj

Probing Topological Phase Transitions in Disordered SSH Chains via Entanglement Entropy and Lyapunov Exponents

P134 - VISWANATHAN Balakrishnan

Quantum imaging with undetected photons

P135 - WALICKI Mikołaj Marek

Realisaton of the ancilla concept in cuprate-like systems

P136 - WALKLING James Ross

Sierpinski Spin Ice

P137 - WALTHER Luis Benedikt

Persistence of the BKT transition with long-range couplings

P138 - WILLSHER Josef David

Dynamics and stability of critical spin liquids

P139 - YANG Qi

QRCTM: Efficient iPEPS Simulation for Quantum Spin Models

P140 - YOUCEF KHODJA Selma

Polaron formation in bosonic flux ladders

P141 - ZENG Zhongda

Adiabatic echo protocols for robust quantum many-body state preparation

P142 - ZUENDEL Martina

Second order phase transition in dissipative cat qubits

P01

Pressure control of magnetic frustration in spin liquid putative material Y-Kapellasite

Federico Abbruciati [1,2] , **Pascal Puphal** [3] , **Aleksandar Razpopov**[4], **Roser Valenti**[4], **Matthieu Le Tacon**[2], **and Bjorn Wehinger** [1]

[1]*European Synchrotron Radiation Facility, ESRF, Grenoble*
[2] *Institute for quantum materials and technologies, KIT, Karlsruhe*
[3] *Max Planck Institute for solid state research, Stuttgart*
[4] *Institute for Theoretical physics, Goethe University Frankfurt*

Low-dimensional materials with strong magnetic interaction, such as antiferromagnetic kagome layered systems, embody the characteristics of the perfect candidate for the research of the long-dreamt QSL (quantum spin liquid). The strong magnetic frustration arising from interacting spins in a kagome system might be the key to this novel phase, where disorder prevails over any magnetic ordering and where fractional excitations and entanglement are predicted. In this scenario, the recent realization of the Y3Cu9(OH)19Cl8 anisotropic kagome lattice system caught the attention. The anisotropy leads to three different Cu-O-Cu super-exchange interactions between the non-equivalent copper atoms [1]. The discovery of this compound prompted a detailed theoretical study, which highlighted two long-range magnetic ordering phases with propagation vector Q = (1/3,1/3) and Q = (0,0) and a classical spin liquid phase [2]. This paper focuses on how to tune the three different couplings with state-of-the-art high-pressure and low temperature single crystal x-ray diffraction measurements at the ID27 beamline of ESRF and to show how the pressure-induced modifications in Cu-O-Cu angle can directly influence the magnitude of the magnetic exchange. Moreover, the paper addresses these changes from an ab-initio perspective, further corroborating the trend towards the spin liquid phase with increased hydrostatic pressure and proving how the magnetic couplings are sensitive to the Cu-O-Cu angle and hydrogen position. Remarkably, complementary µSR data under pressure shows that the magnetic ground state is surprisingly sensitive to the applied pressure, and that under a moderate 2 GPa pressure, the frustration increase is sufficient to induce a fluctuating ground state [3]. The suppression of long-range ordering with pressure tuning is a remarkable step towards the realization of a well-control spin liquid ground state.

[1] Puphal, Pascal, et al. Journal of Materials Chemistry C 5.10 (2017): 2629-2635.

[2] Hering, Max, et al. npj Computational Materials 8.1 (2022): 10.

[3] Chatterjee, Dipranjan, et al, arXiv preprint arXiv:2502.09733 (2025).

P02

Gapless topological behaviour - a signature of Deconfined quantum criticality?

Mohitha Adira, Pinaki Sengupta

School of Physical and Mathematical Sciences, Nanyang Technological University, Singapore

The Takhtajan–Babujian point in the bilinear-biquadratic spin-1 chain has long been recognized as a candidate for achieving a deconfined quantum critical (DQC) point between the symmetry protected topological (SPT) phase and a dimerized phase [1]. On the other hand, a recent study on the spin-12 cluster Ising model showed unambiguously that gapless SPT-like behavior emerges at the transition between an SPT phase and an antiferromagnetic (AFM) phase in the presence of long-range interactions [2].

By adding a long-range interaction term to the JQ_2 spin-1 chain or introducing a singlet-projecting Q term to a long-range Heisenberg spin-1 chain, we can access regimes where DQC behavior and algebraic SPT signatures coexist. In this work, we investigate the spin-1 JQ_2 chain with decaying staggered long-range interactions using large-scale stochastic series expansion (SSE) quantum Monte Carlo simulations. We perform systematic finite-size scaling of local-order parameters to extract critical exponents. Furthermore, we compute the Rényi entanglement entropy via the non-equilibrium increment method [3] and analyze its scaling to identify the universality class. Our results provide insights into the realization of deconfined quantum criticality and emergent gapless topological behavior in one-dimensional spin-1 systems.

[1] Rakov, M. & Weyrauch, M. Bilinear-biquadratic spin-1 model in the Haldane and dimerized phases. *Phys. Rev. B*. **105**, 024424 (2022,1)

[2] Yang, S., Lin, H. & Yu, X. Gapless topological behaviors in a long-range quantum spin chain. *Communications Physics*. **8**, 27 (2025,1,18)

[3] D'Emidio, J. Entanglement Entropy from Nonequilibrium Work. *Phys. Rev. Lett.*. **124**, 110602 (2020,3)

P03

Quantum Mpemba Effect in a Dirty Bose-Hubbard Model under Stark Potential

Asad Ali, Saif Al-Kuwari

[1] *(Presenting author) Qatar Center for Quantum Computing, College of Science and Engineering, Hamad Bin Khalifa University, Doha, Qatar*

We investigate the quantum Mpemba effect [1, 2, 3] in a one-dimensional four-site Bose-Hubbard model under Lindblad dynamics with local dephasing noise, using exact numerical techniques. By varying hopping strength, onsite interactions, Stark potentials, and random disorder, we track relaxation to a common steady state via trace distance, relative entropy, entanglement asymmetry, and ℓ_1-norm coherence. QME emerges in the clean interacting regime, where many-body correlations drive nonlinear relaxation, enabling initially distant states to overtake closer ones. Stark potentials and random disorder suppress QME by inducing localization, with disorder causing milder delays. Entanglement asymmetry sensitively probes symmetry restoration underlying QME. These findings highlight the critical role of interactions in anomalous relaxation and provide insights for controlling quantum thermalization in ultracold atomic systems.

[1] L. K. Joshi et al., Phys. Rev. Lett. **132**, 140401 (2024).
[2] H. Zhang et al., Nature **625**, 68 (2025).
[3] F. Carollo et al., Phys. Rev. Lett. **127**, 060401 (2021).

P04

Stochastic Sampling-Based Classification of Quantum States of Matter

R. Andreoni[1], **V. Vitale**[1,2], **R. Verdel, and M. Dalmonte**[2]

[1]*International School for Advanced Studies (SISSA)*
[2]*The Abdus Salam International Centre for Theoretical Physics (ICTP)*
[3]*Pasqal, 24 rue Emile Baudot, 91120 Palaiseau, France*

Classifying phases of matter traditionally requires knowledge of the symmetries and properties of the system in question. However, inspired by experimental capabilities for stochastic sampling of wave functions via projective measurements, we explore whether classification can be achieved based solely on these measurements, without prior system knowledge.

We introduce a novel classification method for states of matter based on stochastic sampling of the system's wave function. This method employs two distinct analyses. The first involves examining the intrinsic dimension of the dataset derived from the samples, which effectively discriminates between different phases. The second analysis constructs networks from the sample dataset, where the network properties are sensitive to phase transitions. Notably, we observe the emergence of scale-free networks near critical points and within critical phases.

This method offers a practical way to classify phases of matter using only measurement data.

P05

Unambiguous diagnostic of chirality in the entanglement spectrum of $(2+1)$-dimensional topological spin liquids: Demonstration in a $\mathrm{SU}(4)$ PEPS

Mark J. Arildsen[1], **Ji-Yao Chen**[2], **Norbert Schuch**[1,3], **and Andreas W.W. Ludwig**[4]

[1]*University of Vienna, Faculty of Physics, Boltzmanngasse 5, 1090 Wien, Austria*
[2]*Guangdong Provincial Key Laboratory of Magnetoelectric Physics and Devices, Center for Neutron Science and Technology, School of Physics, Sun Yat-sen University, Guangzhou 510275, China*
[3]*University of Vienna, Faculty of Mathematics, Oskar-Morgenstern-Platz 1, 1090 Wien, Austria*
[4]*Department of Physics, University of California, Santa Barbara, California 93106, USA*

We address the key question of representation of chiral topological quantum states in $(2+1)$ dimensions by Projected Entangled Pair States (PEPS). A noted result (due to Wahl, Tu, Schuch, and Cirac [1] and Dubail and Read [2]) says this is possible for non-interacting fermions, but the answer is as yet unknown for interacting systems. Characteristic counting of degeneracies of low-lying states in the entanglement spectrum (ES) at fixed transverse momentum of bipartitioned long cylinders ("Li-Haldane counting") provides often-used supporting evidence for chirality. However, non-chiral states (with zero chiral central charge), yet strongly breaking time-reversal and reflection symmetries (i.e., "apparently" chiral states), are known [3], whose low-lying ES exhibits the same Li-Haldane counting as a chiral state (with non-zero chiral charge) in certain topological sectors. We recently identified [4] a hallmark of chirality of a wave function in the ES in SU(3) chiral spin liquids, which is a finer diagnostic than Li-Haldane counting: The exact degeneracies of entanglement-energy levels in the ES corresponding to paired conjugate representations, which are split in non-chiral states. Here we identify an analogous hallmark of chirality of wave functions of SU(4) spin liquids and demonstrate its use in SU(4) PEPS and DMRG numerics.

[1] T.B. Wahl, H.-H. Tu, N. Schuch, and J.I. Cirac, Phys. Rev. Lett. **111**, 236805 (2013).
[2] J. Dubail, N. Read, Phys. Rev. B **92**, 205307 (2015).
[3] M.J. Arildsen, N. Schuch, and A.W.W. Ludwig, Phys. Rev. B **108**, 245150 (2023).
[4] M.J. Arildsen, J.-Y. Chen, N. Schuch, and A.W.W. Ludwig, Phys. Rev. B **110**, 235147 (2024).

P06

Microscopic derivation of effective field theory for hydrodynamics in U(1)-symmetric Brownian Ciruits

Dani Asafov[1,2], **Olexei Motrunich**[2]

[1] *Institute for Theoretical Physics, KU Leuven, Celestijnenlaan 200D, 3001 Leuven, Belgium*

[2] *Department of Physics and Institute for Quantum Information and Matter, California Institute of Technology, Pasadena, California 91125, USA*

Late times dynamics of a symmetry-preserving Browinan circuit can be described by low-energy states of effective frustration-free Hamiltonian in a doubled Hilbert space [1, 2]. For $U(1)$ circuit such states are magnon-like excitations on top of the groundstate manifold [1]. It has been shown that such Brownian circuits exibit Strong-to-Weak symmetry breaking [3], and it can be argued that the low-energy states can be identified with excitations of it's goldstone bosons and the late time behaviour should be described by the corresponding EFT [4]. In this work we derive a field theoretical description of a Super-Hamiltonian for a $U(1)$ Brownian circuit. We find that simplest spin-$\frac{1}{2}$ and related free-fermion models can be described as two independent spin-$\frac{1}{2}$ chains coupled to a non-dynamical "projector" field. We show that this system reduces to a Heisenberg model at late times and describes diffusion of a "fermionic pair" formed by fermions of "top" and "botom" layers of the doubled space. This model supports a ferromagnet - like symmetry breaking, which we identify with strong-to-weak symmetry breaking. Using this field theoretical description, we investigate Brownian circuits with more general terms and emergence of KMS symmetry. We also discuss generalisation of our findings for models with larger N.
In addition, our work provides an alternative derivation of Non-Linear Sigma Model description of monitored dynamics of free fermions [5, 6].

[1] Sanjay Moudgalya, Olexei I. Motrunich, PRX Quantum **5**, 040330 (2024).

[2] Olumakinde Ogunnaike, Johannes Feldmeier and Jong Yeon Lee Phys. Rev. Lett. **131**, 220403 (2023).

[3] Niklas Ziereis, Sanjay Moudgalya,and Michael Knap, arXiv:2509.09669 (2025).

[4] Xiaoyang Huang, Marvin Qi, Jian-Hao Zhang, and Andrew Lucas, Phys. Rev. B **111**, 125147 (2025).

[5] Igor Poboiko, Paul Pöpperl, Igor V. Gornyi, and Alexander D. Mirlin Physical Review X **13**, 041046 (2023).

[6] Michele Fava, Lorenzo Piroli, Tobias Swann, Denis Bernard, and Adam Nahum, Phys. Rev. X **13**, 041045 (2023).

P07

Theory of fractional Quantum Hall liquids coupled to quantum light and emergent graviton polaritons

Z.Bacciconi [1,2] , **H. Xavier**[1,2] , **I. Carusotto**[3], **T. Chanda**[4] **and M. Dalmonte**[2]

[1] *International School of Advanced Studies (SISSA), via Bonomea 265, 34136 Trieste, Italy*

[2] *The Abdus Salam International Centre for Theoretical Physics (ICTP), Strada Costiera 11, 34151 Trieste, Italy*

[3] *INO-CNR Pitaevskii BEC Center and Dipartimento di Fisica, Universit` a di Trento, 38123 Povo, Italy*

[4] *Department of Physics, Indian Institute of Technology Madras, Chennai 600036, India*

Recent breakthrough experiments have demonstrated how it is now possible to explore the dynamics of quantum Hall states interacting with quantum electromagnetic cavity fields [1-3]. While the impact of strongly coupled non-local cavity modes on integer quantum Hall physics has been recently addressed, the effects on fractional quantum Hall (FQH) liquids– and, more generally, fractionalized states of matter– remain largely unexplored.
In our recent work [4], we develop a theoretical framework for the understanding of FQH states coupled to quantum light. In particular, combining analytical arguments with tensor network simulations, we study the dynamics of a $\nu = 1/3$ Laughlin state in a single-mode cavity with finite electric field gradients. We find that the topological signatures of the FQH state remain robust against the non-local cavity vacuum fluctuations. By exploring the low-energy excited spectrum inside the FQH phase, we identify a new neutral quasiparticle, the graviton-polariton, arising from the hybridization between quadrupolar FQH collective excitations (known as gravitons) and light.

[1] F. Appugliese, J. Enkner, G.L. Paravicini-Bagliani, M. Beck, C. Reichl, W. Wegscheider, G. Scalari, C. Ciuti, J. Faist; Breakdown of topological protection by cavityvacuum fields in the integer quantum Hall effect, *Science* **375** (2022) 1030-1034
[2] J. Enkner, L. Graziotto, D. Boriçi, F. Appugliese, C. Reichl, G. Scalari, N. Regnault, W. Wegscheider, C. Ciuti, J. Faist; Enhanced fractional quantum Hall gaps in a two-dimensional electron gas coupled to a hovering split-ring resonator, arxiv 2405.18362
[3] Z. Bacciconi, H. Xavier, T. Chanda, I.Carusotto and M. Dalmonte; Theory of fractional quantum Hall liquids coupled to quantum light and emergent graviton-polaritons, arxiv 2405.12292 (accepted in PRX)

P08

Multiplicative Chern Insulator

Archi Banerjee[1,2,3], **Ashley M. Cook**[1,2]

[1] *Max Planck Institute for the Physics of Complex Systems, Nöthnitzer Strasse 38, 01187 Dresden, Germany*

[2] *Max Planck Institute for Chemical Physics of Solids, Nöthnitzer Strasse 40, 01187 Dresden, Germany*

[3] *SUPA, School of Physics and Astronomy, University of St Andrews, St Andrews KY16 9SS, United Kingdom*

We study multiplicative Chern insulators (MCIs) as canonical examples of multiplicative topological phases of matter [1]. Constructing the MCI Bloch Hamiltonian as a symmetry-protected tensor product of two topologically non-trivial parent Chern insulators (CIs), we study two-dimensional (2D) MCIs and introduce 3D mixed MCIs, constructed by requiring the two 2D parent Hamiltonians share only one momentum component. We study the 2D MCI response to time reversal symmetric flux insertion, observing a 4π Aharonov-Bohm effect, relating these topological states to fractional quantum Hall states via the effective field theory of the quantum skyrmion Hall effect [2,3]. As part of this response, we observe evidence of quantisation of a proposed topological invariant for compactified many-body states, to a rational number, suggesting higher-dimensional topology may also be relevant. Finally, we study effects of bulk perturbations breaking the symmetry-protected tensor product structure of the child Hamiltonian, finding the MCI evolves adiabatically into a topological skyrmion phase [4].

[1] A. M. Cook and J. E. Moore, Multiplicative topological phases, Communications Physics 5, 262 (2022).

[2] A. M. Cook, Quantum skyrmion hall effect, Phys. Rev. B 109, 155123 (2024).

[3] V. Patil, R. Flores-Calder´on, and A. M. Cook, Effective field theory of the quantum skyrmion hall effect (2024), arXiv:2412.19565 [hep-th].

[4] A. M. Cook, Topological skyrmion phases of matter, Journal of Physics: Condensed Matter 35, 184001 (2023).

P09

Quantum Phase Diagram of the Kitaev–Heisenberg Model on the Square–Hexagonal–Dodecagonal Lattice

P10

Compact localized fermions and Ising anyons in a chiral spin liquid

Tim Bauer [1,2], **and Johannes Reuther** [1]

[1]Dahlem Center for Complex Quantum Systems and Institut für Theoretische Physik, Freie Universität Berlin, Arnimallee 14, 14195 Berlin, Germany and Helmholtz-Zentrum Berlin für Materialien und Energie, Hahn-Meitner-Platz 1, 14109 Berlin, Germany

[2] Department of Applied Physics, The University of Tokyo, Hongo, Tokyo 113-8656, Japan

Quasiparticle hybridization remains a major challenge to realizing and controlling exotic states of matter in existing quantum simulation platforms. We report the absence of hybridization for compact localized states (CLS) emerging in a chiral spin liquid. The CLS form due to destructive quantum interference at fine-tuned coupling constants and populate perfectly flat quasiparticle bands. Using a formalism for generic Majorana-hopping Hamiltonians, we derive exact expressions for CLS for various flux configurations and both for the topological and trivial phases of the studied spin model. In addition to finite-energy matter fermions with characteristic spin-spin correlations, we construct compact localized Majorana zero modes attached to π-flux excitations, which enable non-Abelian braiding of Ising anyons with minimal separation. Our results inform the quantum simulation of topologically ordered states of matter and open avenues for exploring flat-band physics in quantum spin liquids.

P11

Twist-tuned quantum criticality in moiré bilayer graphene

Jan Biedermann[1] and Lukas Janssen[1]

[1] *Institut für Theoretische Physik and Würzburg-Dresden Cluster of Excellence ct.qmat, TU Dresden, 01062 Dresden, Germany*

We argue that moiré bilayer graphene at charge neutrality hosts a continuous semimetal-to-insulator quantum phase transition that can be accessed experimentally by tuning the twist angle between the two layers. For small twist angles near the first magic angle, the system realizes a Kramers intervalley-coherent insulator, while above a critical twist angle, we identify a fully symmetric Dirac semimetal ground state. We argue that the quantum critical behavior belongs to the relativistic Gross-Neveu-XY universality class.

Additional calculations help clarify recent experimental observations of a similar quantum phase transition in twisted double bilayer WSe2 [1]. We show that this transition is of Gross-Neveu-Heisenberg type and can be accessed experimentally by varying the twist angle or pressure. Pressure-tuning in particular can readily be performed in situ, raising the exciting possibility of experimentally measuring critical exponents of a relativistic universality class for the first time.

[1] L. Ma, et al., arXiv:2412.07150 (2024).
[2] J. Biedermann, L. Janssen, Phys. Rev. B. **112**, L041109 (2025).
[3] J. Biedermann, L. Janssen, arXiv:2509.04561 (2025).

P12

Exact valence bond ground states of a spin-1 model on the checkerboard and pyrochlore lattices

Hari Prasaad J Borutta[1,*], Yasir Iqbal[1], Kirill Shtengel[2,1]

[1]Department of Physics and Quantum Center for Diamond and Emergent Materials
Indian Institute of Technology, Madras, India
[2]University of California, Riverside, California, USA

[*]haripbj@physics.iitm.ac.in

Following the famous Affleck-Kennedy-Lieb-Tasaki model (AKLT) [1], Klein model [2], and the analysis of ground state order of extended AKLT Hamiltonians on 3D lattices [3], we construct an AKLT-like model/Hamiltonian — spin-projector Hamiltonian — on pyrochlore lattice. We consider a local spin value of $S = 1$ on each lattice site, which is less than the minimum value $S = 3$ (half of the coordination number of the lattice) required for the case of AKLT valence bond ground state (VBS). The Hamiltonian we set up is the sum of projectors onto spin 3 subspace for every triangular face, $P_3\left(\vec{S}_\triangle\right)$, of the tetrahedra forming the lattice. In such a model, we identify the degenerate manifold of ground states and compute an orthogonal basis in this degenerate space. Finally, we study the equal-time two-point spin correlation function to ascertain the nature of order/disorder in the ground state space.

References

[1] I. Affleck, T. Kennedy, E. H. Lieb, and H. Tasaki. Rigorous results on valence-bond ground states in antiferromagnets. *Phys. Rev. Lett.*, 59:799–802, 1987.

[2] D. J. Klein. Exact ground states for a class of antiferromagnetic Heisenberg models with short-range interactions. *J. Phys. A: Math. Gen.*, 15:661–71, 1982.

[3] S. A. Parameswaran, S. L. Sondhi, and D. P. Arovas. Order and disorder in aklt antiferromagnets in three dimensions. *Phys. Rev. B*, 79(2):024408, Jan. 2009.

– Manuscript under preparation

P13

Spin nematic phases for multipolar Kondo interactions in heavy-fermions materials

Victor B. Zaché[1], **Rodrigo G. Pereira**[1,2]

[1]*Departamento de Física Teórica e Experimental, Universidade Federal do Rio Grande do Norte, Natal, RN, 59078-970, Brazil*

[2]*International Institute of Physics, Universidade Federal do Rio Grande do Norte, Natal, RN, 59078-970, Brazil*

Heavy fermion compounds are typical examples of strongly correlated systems in condensed matter physics. Although these materials have been studied for many years, there remains much to explore regarding their spin nematic (SN) phases - an exotic magnetic phase characterized by the breaking of rotational symmetry in spin space while preserving other symmetries. Moreover, these phases can coexist with traditional magnetic orders (e.g. Néel states) and may emerge in strongly interacting quantum phases, as seen in the cuprates. One promising candidate for exhibiting SN behavior is the compound $CeRhIn_5$, whose rich phase diagram - unconventional superconductivity, magnetic transitions, nematicity etc - recently attracted a lot of attention in the literature offering an excellent opportunity to test models explaining these exotic phases.

In this work, starting from a two-dimensional microscopic model considering p and f orbitals, we develop an effective model for SN using perturbation theory in the strong-coupling limit until third order, treating the f orbitals as quasi-localized. The effective third-order operator has quadrupolar order in the bond of two localized spins. We also study the phase diagram of the model employing a parton mean-field technique wich consider this quadrupolar operator as the order parameter. In doing so, we hope to identify the necessary conditions for a spontaneous rotational symmetry breaking due to the coupling of conduction electrons with the quadrupole tensor of two localized spins. Such a mechanism has potential applications in controlling properties like the anisotropy of electrical resistivity in the presence of strong magnetic fields. Furthermore, our model provides a useful framework for future studies on the low-energy effective field theory of nematic phases and their dynamics. It may also serve as a platform to explore other exotic phases, such as the Fractionalized Fermi Liquid (FL*), where spin and charge degrees of freedom become fractionalized, leading to a violation of the conventional Luttinger theorem. In this scenario, the localized f electrons remain decoupled from the Fermi surface, which only accounts for the itinerant conduction electrons, despite the system remaining metallic and symmetric.

P14

Triangular Heisenberg Model under a magnetic field: Monte carlo approach

Sasank Budaraju[1], **Federico Becca, Frank Pollmann, and Johannes Knolle**

[1]*Department of Physics, Technische Universität München, 85748 Garching, Germany*

Understanding the behavior of strongly interacting spin systems under external perturbations such as applied magnetic fields has been a significant and extensively studied topic, both from an experimental and theoretical point of view. Recent experimental studies of triangular lattice materials (e.g certain organic salts and chalcogenides) have observed behavior characteristic of a quantum spin liquid ground state. Understanding the unique signatures of spin liquids under applied magnetic fields would be crucial to reconcile with experimental results, and shed light on the nature of the spin liquid in these compounds.

Our work explores the phase diagram of the $J_1 - J_2$ triangular Heisenberg model under a magnetic field, which we investigate using the variational quantum monte carlo approach. The various possible magnetically ordered phases are parametrized using simple variational wavefunctions, and transitions among these phases are probed using standard monte carlo optimization techniques, As a result, we obtain a intuitive understanding of the evolution of the ground state as a function of applied field. I will present results both in the small J_2 regime where the system has 120 degree Neel order at no applied field, and in the spin liquid regime around $J_2 = 1/8$, where the ground state is a QSL whose exact nature is still debated.

P15

Chiral gravitons on the lattice

Hernan B. Xavier[1,2], **Zeno Bacciconi**[2,1], **Titas Chanda**[3,4], **Dam Thanh Son**[5], **and Marcello Dalmonte**[1]

[1] *ICTP — The Abdus Salam International Centre for Theoretical Physics, Trieste, Italy*
[2] *SISSA — International School for Advances Studies, Trieste, Italy*
[3] *Department of Physics, Indian Institute of Technology Madras, Chennai, India*
[4] *Center for Quantum Information, Communication and Computation (CQuICC), Indian Institute of Technology Madras, Chennai, India*
[5] Kadanoff Center for Theoretical Physics, University of Chicago, Chicago, Illinois 60637, USA

Fractional quantum Hall states host emergent chiral graviton modes, arising from their underlying quantum geometry. It remains unclear, however, whether this picture extends to lattice models, where continuum translations are broken and additional quasiparticle decay channels arise. We present a framework in which we explicitly derive a field theory incorporating lattice chiral graviton operators within the paradigmatic bosonic Harper-Hofstadter model. Extensive numerical evidence suggests that chiral graviton modes persist away from the continuum, and are well captured by the proposed lattice operators. We identify geometric quenches as a viable experimental probe, paving the way for the exploration of chiral gravitons in near-term quantum simulation experiments.

[1] HB Xavier, Z Bacciconi, T Chanda, DT Son, and M Dalmonte, arXiv:2505.02905.

P16

Symmetry-protected topological order identified via Gutzwiller-guided density-matrix-renormalization-group: SO(n) spin chains

P17

Magnetization plateaux in the Kagome antiferromagnet

Gabriel Capelo [1], **Eric C. Andrade** [1]

[1]*Instituto de Física, Universidade de São Paulo*

In the context of systems with localized magnetic moments, we refer to frustration as the inability to satisfy all constraints imposed by the minimization of local interaction energies. Frustration is intimately related to a macroscopic degeneracy in the ground state, which can be lifted by what is known as the order-by-disorder mechanism. One example of this phenomenon is observed in the magnetization process of a triangular lattice antiferromagnet, where quantum fluctuations favor colinear phases, resulting in an incompressible phase of magnetization plateau within a finite range of magnetic fields [1], corresponding to 1/3 of the magnetization of the fully polarized system. More recently, magnetization plateaus have been discussed in the Kagome antiferromagnet, both with numerical methods[2] and in experiments[3]. Taking the J_1-J_2 Heisenberg model in the kagome lattice coupled with an external magnetic field, we employ nonlinear spin-wave theory to show how this plateau phase can be described semiclassically, in close analogy with the same description in the triangular lattice. We discuss the dependence of the plateau width on the spin size and the strength of J_2. It's also predicted that the model exhibits a 7/9 magnetization plateau [4], followed by a magnetization jump to the saturated phase. This phase transition is understood as a crystallization of localized magnons, based on the flat band in the magnon dispersion. We investigate here the stability of the plateau when next-nearest neighbor interactions are considered, causing the band to acquire a small dispersion.

.

[1] A Chubukov, I Golosov J. Phys.: Condens. Matter 3, 69 (1991).
[2] S. Capponi, *et al.,* Phys. Rev. B vol. 88, p.144416 (2013)
[3] W. Ishikawa, *et al.*, Phys. Rev. B vol. 114, p.227202 (2015)
[4] R. Okuma, *et al.*, Nat Commun 10, 1229(2019)

P18

Tricriticality in 4D U(1) Lattice Gauge Theory

Rafael C. Torres[1], **Nuno Cardoso**[1], **Pedro Bicudo**[1], **Pedro Ribeiro**[1,2] **and Paul McClarty**[3]

[1]*CeFEMA, Instituto Superior Técnico, Universidade de Lisboa, Av. Rovisco Pais, 1049-001 Lisboa, Portugal*

[2]*Beijing Computational Science Research Center, Beijing 100084, China*

[3] Laboratoire Léon Brillouin, CEA, CNRS, Université Paris-Saclay, CEA Saclay, 91191 Gif-sur-Yvette, France

The 4D compact U(1) gauge theory has a well-established phase transition between a confining and a Coulomb phase. In this paper, we revisit this model using state-of-the-art Monte Carlo simulations on anisotropic lattices. We map out the coupling-temperature phase diagram, and determine the location of the tricritical point, $T/K_0 \approx 0.19$, below which the first-order transition is observed. We find the critical exponents of the high-temperature second-order transition to be compatible with those of the 3-dimensional O(2) model. Our results at higher temperatures can be compared with literature results and are consistent with them. Surprisingly, below $T/K_0 \approx 0.05$ we find strong indications of a second tricritical point where the first-order transition becomes continuous. These results suggest an unexpected second-order phase transition extending down to zero temperature, contrary to the prevailing consensus. If confirmed, these findings reopen the question of the detailed characterization of the transition including a suitable field theory description.

[1] R. C. Torres, N. Cardoso, P. Bicudo, P. Ribeiro, P. McClarty, Phys. Rev. D **110**, 034518 (2024).

P19

Fractional diffusion without disorder in two dimensions

P20 **Title:** A cornucopia of emergence in classical frustrated systems

Abstract:
Modern many-body physics is replete with examples of emergence wherein collective behavior of a many-body system as described via a long-wavelength or coarse-grained description hosts a higher symmetry in comparison to the bare microscopic theory. Field theoretically such emergence are typically predicated on the presence of an operator that becomes irrelevant (in the renormalization group sense) in the infrared regime, leading to either a critical point or even an entire critical phase hosting a higher symmetry than the short-wavelength microscopic theory. In this talk, I will present a comprehensive study on the frustrated $J_1 - J_2$ classical q-state clock model with even $q > 4$ on a two dimensional square lattice and reveal a rich tapestry of emergent properties driven by competing interactions. The unfrustrated regime, similar to the standard clock model with $q > 4$, features an critical XY-like intermediate critical phase with emergent $U(1)$ symmetry that separates the low-temperature ordered phase and the high-temperature paramagnetic phase. On the other hand, frustration stabilizes five distinct regimes: a low-temperature stripe order phase that breaks $\mathbb{Z}_q \times \mathbb{Z}_2$ symmetry, the high-temperature paramagnetic phase, two $\mathbb{Z}_2$-broken nematic phases (one with and one without the XY-like quasi-long-range order), and finally an exotic stripe phase with emergent discrete $\mathbb{Z}_q$ spin variables with shifted angle that are absent in the microscopic Hamiltonian. Interestingly, this exotic emergent $\mathbb{Z}_q$ symmetry arises not from an operator becoming irrelevant but rather from an particular operator becoming relevant in the infrared limit —highlighting a nonstandard route to emergent behavior. Using large-scale corner transfer matrix renormalization group calculations, complemented by classical Monte Carlo simulations, we map the complete phase diagram and classify all transitions — including Berezinskii–Kosterlitz–Thouless, Ising, first-order, and Landau-incompatible deconfined transitions between different phases. Finally, we outline an effective field-theoretic framework that captures these emergent orders, symmetries and their interwoven transitions.

P21

Projective symmetry group classification of Abrikosov fermion mean-field ansätze on the trellis lattice

Sourin Chatterjee[1],**Atanu Maity**[2,1],**Ronny Thomale**[2,1],**Karlo Penc**[3,1], **Yasir Iqbal**[1]

[1] *Department of Physics and Quantum Center for Diamond and Emergent Materials (QuCenDiEM), Indian Institute of Technology Madras, Chennai 600036, India*

[2] Institut für Theoretische Physik und Astrophysik and Würzburg-Dresden Cluster of Excellence ct.qmat, Julius-Maximilians-Universität Würzburg, Am Hubland Campus Süd, Würzburg 97074, Germany

[3] *Institute for Solid State Physics and Optics, Wigner Research Centre for Physics, Hungary*

Unlike conventional magnets, highly frustrated quantum spin systems may not exhibit long-range magnetic order. Instead, they can host exotic ground states such as quantum spin liquids. These phases are particularly likely to emerge in two-dimensional spin-$\frac{1}{2}$ systems, where strong quantum fluctuations play a crucial role. One promising platform for exploring such physics is the trellis lattice—a highly frustrated two-dimensional geometry first introduced in Ref. [1].

In this work, we perform a fully symmetric Projective Symmetry Group (PSG) classification on the trellis lattice, following the framework developed by Wen [2]. Using the Abrikosov fermion representation for spin operators, we identify 256 algebraic PSGs associated with a Z_2 invariant gauge group (IGG), along with 448 distinct $U(1)$ PSGs. By restricting our analysis to the three nearest neighbour symmetry-inequivalent, we further narrow down the possibilities to 7 $U(1)$ and 25 Z_2 mean-field Anstze.

We investigate the different phases that emerge as we vary the hopping parameters and the coupling strengths. Additionally, we compute the dynamical and static structure factor, facilitating direct comparisons with experimental results.

[1] Normand, B. and Penc, K. and Albrecht, M. and Mila, F, Phys. Rev. B **56**, R5736 (1997).

[2] Xiao-Gang Wen, Phys. Rev. B **65**, 165113 (2002).

P22

Characterizing non-Markovianity via quantum coherence based on Kirkwood-Dirac quasiprobability

Yassine Dakir[1*], Abdallah Slaoui[1,2], and Rachid Ahl Laamara[1,2]

[1] LPHE-Modeling and Simulation, Faculty of Sciences, Mohammed V University in Rabat, Rabat, Morocco.
[2] Centre of Physics and Mathematics, CPM, Faculty of Sciences, Mohammed V University in Rabat, Rabat, Morocco.

***yassine.dakiryd20@gmail.com**

We present a new measure of non-Markovianity based on the property of nonincreasing quantum coherence via Kirkwood-Dirac (KD) quasiprobability under incoherent completely positive trace-preserving maps. Quantum coherence via the KD quasiprobability is defined as the imaginary part of the KD quasiprobability, which is maximized over all possible second bases and evaluated using an incoherent reference basis. A measure non Markovianity based on KD quasiprobability coherence would capture memory effects via the time evolution of the imaginary part of the KD quasiprobability, providing an experimentally accessible and physically intuitive alternative to traditional measures relying on quantum Fisher information or trace distance. This approach is applied to the study of dissipation and dephasing dynamics in single- and two-qubit systems. The results obtained show that, in the cases studied, our measure based on coherence via Kirkwood-Dirac quasiprobability performs at least as well as $\ell 1$-norm coherence in detecting non-Markovianity, this provides a novel perspective on the analysis of non-Markovian dynamics

Keywords:
Non-Markovianity, Quantum coherence, Kirkwood-Dirac quasiprobability

P23

Investigation of Periodic TI-NI/TI-S Multilayers in the Presence of a Transverse Magnetic Field to Realize Weyl Semimetal/Weyl Superconductor with Tilted Weyl Cones

Esa Darwish[1], Zahra Faraei[2]

[1] Department of Physics, Institute for Advanced Studies in Basic Sciences (IASBS), Zanjan 45137-66731, Iran
International Center for Theoretical Phyiscs and Physics Without Frontiers (ICTP-PWF), Trieste 34151, Italy

[2]Institute for Advanced Studies in Basic Sciences (IASBS), Zanjan 45137-66731, Iran

Weyl semimetals and superconductors have remained at the forefront of condensed matter research due to their distinctive topological characteristics. Since their discovery, significant efforts have been devoted to developing methodologies for engineering their electronic properties to harness their potential in quantum technologies. Among these approaches, heterostructures comprising alternating topological and trivial insulator/ s-wave superconductor layers (TI-NI/S) have emerged as a promising platform for realizing Weyl semimetals/superconductors. In this work, we present a comprehensive theoretical analysis of such heterostructures, examining the emergent electronic spectra arising from their periodic multilayer configurations. We demonstrate that applying a transverse magnetic field perpendicular to the side surface of the structure makes a Weyl semimetal state, which subsequently evolves into a Weyl superconductor with tilted Weyl cones. The tilt angle exhibits a direct dependence on both the magnitude of the transverse field and its orientation relative to the layer-normal axis. Furthermore, we establish the necessary conditions for the anisotropy-driven tilting mechanism of the Weyl cones. Our results underscore the efficacy of external magnetic fields as a versatile means of manipulating the electronic properties of Weyl semimetals and superconductors, offering new pathways for their functional control in quantum devices.

Key words: Weyl semimetals, Weyl superconductor, Weyl wave equation in solids, chirality, Weyl point in momentum-energy space, tilted Weyl cones.

[1] A. A. Burkov and L. Balents, Weyl semimetal in a topological insulator multilayer, Phys. Rev. Lett. 107, 127205 (2011).
[2] T. Meng and L. Balents, Weyl superconductors, Phys. Rev. B 86, 054504 (2012).
[3] H. Weyl, Electron and gravitation, Z. Phys. 56, 330–352 (1929).
[4] S.-Y. Xu et al., Discovery of a Weyl fermion semimetal and topological Fermi arcs, Science 349, 613–617 (2015).
[5] B. Q. Lv et al., Experimental discovery of Weyl semimetal TaAs, Phys. Rev. X 5, 031013 (2015).
[6] N. P. Armitage, E. J. Mele, and A. Vishwanath, Weyl and Dirac semimetals in three-dimensional solids, Rev. Mod. Phys. 90, 015001 (2018).
[7] B. Q. Lv, T. Qian, and H. Ding, Experimental perspective on three-dimensional topological semimetals, Rev. Mod. Phys. 93, 025002 (2021).
[8] S. Rao, Weyl semi-metals: a short review, arXiv:1603.02821 (2016).
[9] A. A. Burkov, Topological semimetals, Nat. Mater. 15, 1145–1148 (2016).
[10] B. Yan and C. Felser, Topological materials: Weyl semimetals, Annu. Rev. Condens. Matter Phys. 8, 337–354 (2017).
[11] A. A. Burkov, M. D. Hook, and L. Balents, Topological nodal semimetals, Phys. Rev. B 84, 235126 (2011).

[12] S.-H. Zheng et al., Origin of planar Hall effect on the surface of topological insulators: Tilt of Dirac cone by an in-plane magnetic field, Phys. Rev. B 101, 041408 (2020).
[13] T. O. Wehling, A. M. Black-Schaffer, and A. V. Balatsky, Dirac materials, Adv. Phys. 63, 1–76 (2014).
[14] S.-M. Huang et al., A Weyl Fermion semimetal with surface Fermi arcs in the transition metal monopnictide TaAs class, Nat. Commun. 6, 7373 (2015).
[15] X. Wan, A. M. Turner, A. Vishwanath, and S. Y. Savrasov, Topological semimetal and Fermi-arc surface states in the electronic structure of pyrochlore iridates, Phys. Rev. B 83, 205101 (2011).
[16] F. R. Klinkhamer and G. E. Volovik, Emergent CPT violation from the splitting of Fermi points, Int. J. Mod. Phys. A 20, 2795–2812 (2005).
[17] K.-Y. Yang, Y.-M. Lu, and Y. Ran, Quantum Hall effects in a Weyl semimetal: Possible application in pyrochlore iridates, Phys. Rev. B 84, 075129 (2011).

P24

Topological Semimetals via Internal Symmetry

Faruk Abdulla[1,2], Gapathy Murthy[3], and Ankur Das[4,5]

[1]Harish-Chandra Research Institute, A CI of Homi Bhabha National Institute, Chhatnag Road, Jhunsi, Prayagraj (Allahabad), India
[2]Physics Department, Technion - Israel Institute of Technology, Haifa, Israel
[3]Department of Physics and Astronomy, University of Kentucky, Lexington, KY, USA
[4]Department of Condensed Matter Physics, Weizmann Institute of Science, Rehovot, Israel
[5]Department of Physics, Indian Institute of Science Education and Research (IISER) Tirupati, India

It has been realized over the past two decades that topological nontriviality can be present not only in insulators but also in gapless semimetals, the most prominent example being Weyl semimetals in three dimensions. Key to topological classification schemes are the three "internal" symmetries, time reversal T, charge conjugation C, and their product, called chiral symmetry $S=TC$. In this work, we show that robust topological semimetal phases occur in d=3 in systems without invoking crystalline symmetries other than translations. These topological semimetals naturally appear as an intermediate gapless phase between the topological and the trivial insulators; a sufficient condition for topological semimetals to exist is that the symmetry class must have a nontrivial topological insulator in d=3. We argue and show that the topological semimetals can be classified using winding number on a loop for nodal line semimetals and Chern number for point node semimetals (i.e. Weyl Semimetals). A nonzero winding number on a nodal loop implies robust gapless drumhead states on the surface Brillouin zone. Similarly, for point nodes, it will be Fermi arcs.

[1] Topological nodal line semimetals with chiral symmetry, arXiv: 2311.18667
[2] Stable nodal line semimetals in the chiral classes in three dimensions, arXiv: 2401.02966

P25

Abstract template for Poster Presentation..

Hiranmay Das[1], **Naba P. Nayak**[2], **Soumya Bera**[2], **and Vijay B. Shenoy**[1]

[1]*(Presenting author underlined) Centre for Condensed Matter Theory, Physics Department, Indian Institute of Science, Bengaluru 560012, India*

[2] *Department of Physics, Indian Institute of Technology Bombay, Powai, Mumbai 400 076, India*

We investigate the physics of fermions on a square lattice with π-flux, subjected to disordered random $\mathbb{Z}_2$ gauge fields that arise from flux defects, i. e., plaquettes with zero flux. At half-filling, where the system possesses BDI symmetry, we show that a new class of critical states is realized, with the states at zero energy showing a multifractal character that depends on the flux defect concentration c and local correlation between defects. For any concentration of flux defects, we find that the multi-fractal spectrum shows termination, but *not freezing*. We characterize this class of critical states by uncovering a robust relation between the conductivity and the Lyapunov exponent, which is satisfied by the states irrespective of the concentration or the local correlations between the flux defects. We demonstrate that renormalization group methods, based on perturbing the Dirac point, fail to capture this new class of critical states. This work not only offers new challenges to the theory of disordered systems in the chiral classes, but is also likely to be useful in understanding a variety of problems where fermions interact with discrete gauge fields.

[1] H. Das, N. P. Nayak, S. Bera, V. B. Shenoy, Critical States of Fermions with $\mathbb{Z}_2$ Flux Disorder, arXiv:2505.06689

P26

Floquet Exceptional Topological

Gaurab Kumar Dash and Manisha Thakurat

Indian Institute of Technology, Delhi

Motivation of the research

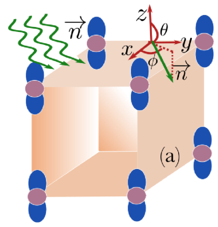

- Time periodic driving can cause a single Dirac cone to emerge as a surface state which represents an anomaly.
- What could be non-hermitian counterpart of such anomaly?

Static Model

- $H_0\ k) = \sum_{j=x,y,z}\ \ \cos k_j\ \ M)\,\tau_z\sigma_0 + \lambda \sin k_j \tau_x \sigma_j] + i\delta\,\tau_x\sigma_0$.

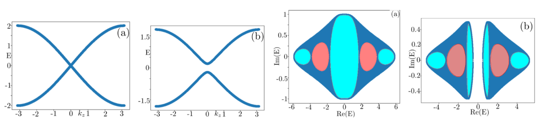

Defectiveness of the surface state

- *conjecture*: discontinuous jump in E from 0 to finite value in thermodynamic limit

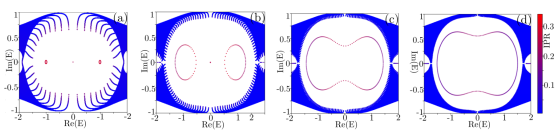

Floquet Perturbation Theory

- Time periodic Fourier series in Floquet Models $\rightarrow$ Tight binding model of Schrodinger's equation
- $H_j\ \ _j' = H_n = \frac{1}{\tau}\int_{\ \tau/2}^{\tau/2} H\ \ k,t)e^{in\omega t}$
- $H_{eff} = H_F^0 + \sum_{n=1}^{\infty} \frac{1}{\omega^n}[H_F{}^{\ n}, H_F^n]$

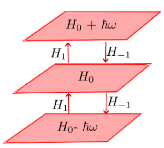

Shining light on 3DNHTI

- MINIM L COUPLING DESCRIPTION : $H'\ \ t, k_x, k_y, k_z) = H\ \ k_x\ \ \ \ _x\ t), k_y\ \ \ \ _y\ t)$
- $H^F\ \ k) = \sum_j\ \cos k_j\ \ \underbrace{M\ \ \ \frac{2}{4}\ 1+\eta^2))}_{\text{photo-tuning}}\tau_z\sigma_0 + \lambda \sum_j \sin k_j \tau_x \sigma_j + \underbrace{\tau_0\ \ \ \ \sigma)}_{\text{photo-dressed magnetic field}} + i\delta\tau_x\sigma_0,$
- $\ \ = \frac{\lambda^2\ \ ^2\eta}{\omega}\ \sin\theta\cos\phi, \sin\theta\sin\phi, \cos\theta)$

Morphing of Weyl nodes along imaginary energy

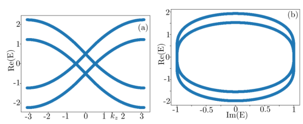

single sheet structure in the surface

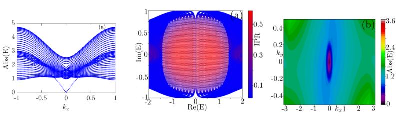

- vortex without the otherwise required anti-vortex

Single second order Exceptional point and Generation of higher order point in the surface

- $H^F\ \ k) = \sum_{j=x,y,z}\ \left(\cos k_j\ \ \ M\ \ \ \frac{2}{2}\right)\tau_z\sigma_0 + \lambda \sin k_j \tau_x \sigma_j] +\ \ \tau_z B + \tau_0 n)\ \sigma + i\,\delta\,\tau_x\sigma_0$
- $\chi = \mathrm{t\ \ n}\ ^{1}\frac{\lambda\ \ ^{2}_{0}}{\omega B}$

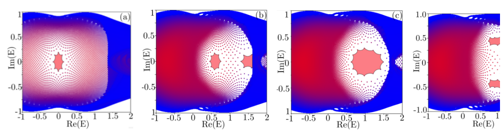

P27

Vacancy induced expansion of spin-liquid regime in $J_1 - J_2$ Heisenberg model

Soumyaranjan Dash[1], **Anish Koley**[1,2], **Sanjeev Kumar**[1]

[1]*Department of Physical Sciences, Indian Institute of Science Education and Research (IISER) Mohali, Sector 81, S.A.S. Nagar, Manauli PO 140306, India*

[2]*Institut für Theoretische Physik, Universität Leipzig, 04103 Leipzig, Germany*

We study the spin-1/2 J_1/J_2 Heisenberg antiferromagnet on the square lattice in the presence of spin vacancies. In the limit of no vacancy, this model exhibits Néel order for small J_2/J_1, stripe antiferromagnetic order for large J_2/J_1, and a quantum disordered phase at intermediate couplings. The extent and nature of this non-magnetic regime remain debated, especially in systems with disorder. We develop a semi-classical Monte Carlo method in which singlet dimers are treated as effective classical variables, and thermally driven updates allow for their dynamical formation and annihilation. This captures the competition between magnetic order and local singlet formation within a tractable framework. Our method reproduces known phase boundaries in the zero-vacancy limit and reveals a significant broadening of the disordered region in the presence of vacancies. The results indicate that spin dilution enhances local singlet correlations and suppresses long-range order, effectively stabilizing a spin-liquid-like regime. This provides theoretical support for the observed suppression of magnetic order in doped frustrated antiferromagnets such as Zn- or Mg-substituted cuprates. Our work suggests that controlled introduction of non-magnetic impurities may offer an experimental route to tune ground states toward quantum disordered phases in two-dimensional frustrated spin systems.

[1] Soumyaranjan Dash, Anish Koley, Sanjeev Kumar , “Vacancy induced expansion of spin-liquid regime in $J_1 - J_2$ Heisenberg model”. (arXiv:2507.20561 [cond-mat.str-el])

[2] Soumyaranjan Dash, Sanjeev Kumar , “Semiclassical approach to partial magnetic order in Kondo lattices”. (Phys. Rev. B 2025, 111, 174443)

P28

Anomalous Landau Levels in Inhomogeneous Fluxes and Emergent Supersymmetry

Soujanya Datta[1], **Krishanu Roychowdhury**[1,2,3]

[1] *Theory Division, Saha Institute of Nuclear Physics, 1/AF Bidhannagar, Kolkata 700064, India*

[2] *Homi Bhabha National Institute, Training School Complex, Anushaktinagar, Mumbai 400094, India*

[3] *Max-Planck-Institut für Physik komplexer Systeme, Nöthnitzer Strasse 38, 01187 Dresden, Germany*

Two-dimensional (2D) systems in magnetic fields host rich physics, most notably the quantum Hall effect arising from Landau level (LL) quantization. In a broad class of 2D models, flat bands with topologically nontrivial band degeneracies give rise to anomalous LL quantization under homogeneous fields[1]. Ascribed to the underlying quantum geometry, these are classified as *singular flat bands* (SFBs)[2], exhibiting unusual wavefunction localization, and anomalous quantization of LLs. We discover new hallmarks in models of SFBs beyond the essential characteristics by investigating their response to inhomogeneous magnetic fluxes, bridging continuum and lattice descriptions. Our analysis reveals a mechanism to controllably manipulate the anomalous LLs (ALLs) via flux inhomogeneity. In particular, we identify "sweet spots" in the parameter space where the entire tower of ALLs collapses to zero energy, rendering a *lattice analog of the Aharonov–Casher theorem*[3] on the counting of zero modes in perpendicular fluxes. Remarkably, these special flux configurations feature an emergent supersymmetry[4] and partial Aharonov–Bohm caging[5] due to re-entrant compact localization. With the addition of strong correlations, these findings will have implications for realizing exotic topological and charge-ordered phases in flat-band lattice models.

[1] J.-W. Rhim, K. Kim, and B.-J. Yang, Nature, **584**, 59 (2020).

[2] J.-W. Rhim and B.-J. Yang, Physical Review B **99**, 045107 (2019).

[3] Y. Aharonov and A. Casher, Physical Review A **19**, 2461 (1979).

[4] K. Roychowdhury, J. Attig, S. Trebst, and M. J. Lawler, Phys- ical Review Research **6**, 043273 (2024).

[5] J. Vidal, R. Mosseri, and B. Doucot, Physical Review Letters **81**, 5888 (1998).

P29

Phases of the "Odd" Toric Code in a tilted field

Umberto Borla , Ayush De , and Snir Gazit

Hebrew University of Jerusalem

In our study [1], we investigate the phases of the "odd" variant of the 2D Z_2 Fradkin–Shenker lattice gauge theory [2], which, in the absence of tilted fields, coincides with the "odd" Toric Code model [3]. The "odd" nature refers to the positive signs of the plaquette and vertex couplings, which can be interpreted as the "even" theory placed in a uniform background of static Z_2 charges and fluxes on each vertex and plaquette, respectively.

Using large-scale density matrix renormalization group (DMRG) and exact diagonalization (ED) techniques, we map out the phase diagram as a function of tilted field strengths h_x and h_z. We identify a deconfined topological phase at low fields, which transitions continuously into confined and Higgs phases exhibiting valence bond solid (VBS) order. At large fields, the system enters a trivial paramagnetic phase. Notably, along the self-dual line $h_x=h_z=h$, we uncover a novel multicritical point where confinement and Higgs transitions coincide, resulting in the spontaneous breaking of both translational symmetry and Z_2 duality, forming a VBS phase. At intermediate fields beyond this point, we observe a continuous cascade of first-order transitions between VBS phases of differing periodicity, suggestive of frustration-induced incommensurate order. The overall topology of the phase diagram is summarized in Fig. 1.

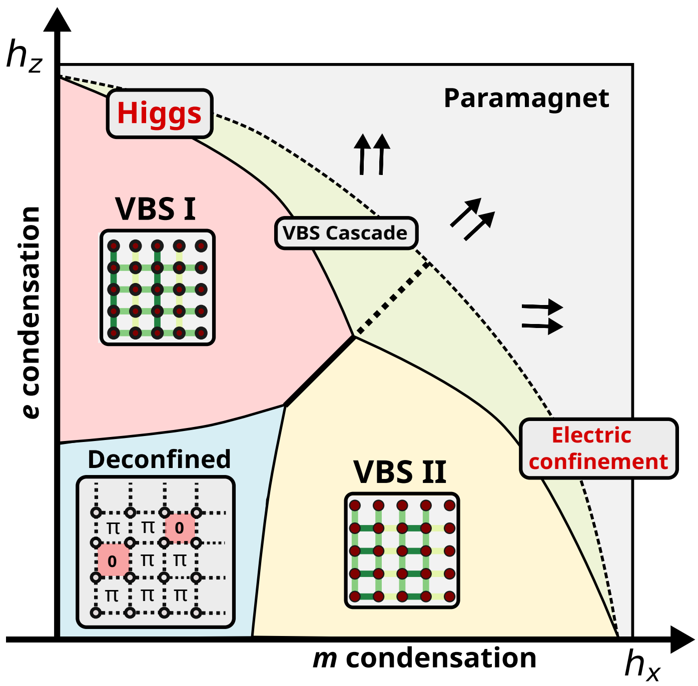

Fig 1. Phase diagram of the "Odd" Z_2 Fradkin-Shenker lattice gauge theory.

[1] U. Borla, A. De, S. Gazit, arXiv:2507.16523 (2025).
[2] E. Fradkin, S. H. Shenker, Phys. Rev. D 19, 3682 (1979).
[3] A. Kitaev, Annals of Physics 303 2–30 (2003).

P30

Topological characterization of magnon polaron bands and thermal Hall conductivity in a frustrated kagome antiferromagnet

Shreya Debnath, Kuntal Bhattacharyya and Saurabh Basu

Department of Physics Indian Institute of Technology Guwahati Guwahati-781039 Assam India

Spin-phonon coupling and its efficacy in inducing multiple topological phase transitions in a frustrated kagome antiferromagnet have been rare in literature. To this end, we study the ramifications of invoking optical phonons in such a system via two different coupling mechanisms, namely, a local and a non-local one, which are distinct in their microscopic origin. In case of the local spin-phonon coupling, a single phonon mode affects the magnetic interactions, whereas in the non-local case, two neighbouring phonon modes are involved in the energy renormalization, and it would be worthwhile to compare and contrast between the two. To tackle these phonons, we propose an analytic approach involving a canonical spin-Peierls transformation applied to magnons. The formalism renders a hybridization between the magnons and the phonon modes, yielding magnon-polaron quasiparticles. In both the coupling regimes, validations for the topological signatures are systematically derived from the bulk and edge spectral properties of the magnon-polaron bands that are characterized by their corresponding Chern numbers. Thereafter, we investigate transitions from one topological phase to another solely via tuning the spin-phonon coupling strength. Moreover, these transitions significantly impact the behavior of the thermal Hall conductivity that aids in discerning distinct topological phases. Additionally, the explicit dependencies on the temperature and the external magnetic field are explored in inducing topological phase transitions associated with the magnon-polaron bands. Thus, our work serves as an ideal platform to probe the interplay of frustrated magnetism and polaronic physics.

P31

Classifying Spin Liquids: PSG Approach and Energy Considerations

Rohit Deb[1], Sambuddha Sanyal[1]
[1] Indian Institute of Science Education and Research Tirupati

Spin liquids are exotic quantum phases that evade conventional symmetry breaking and exhibit fractionalized excitations due to long-range quantum entanglement. These phases are best understood using the parton construction, where spin degrees of freedom are decomposed into emergent fractionalized particles. In this work, we classify spin liquid states using the Projective Symmetry Group (PSG) approach, systematically identifying symmetry-allowed mean-field ansätze. To determine the most relevant physical states, we perform energy minimization within mean-field theory and in future we want to discuss the role of Gutzwiller projection in refining these approximations. Our results provide insights into the interplay between symmetry, fractionalization, and energetics in the realization of spin liquid phases in quantum materials.

References

[1] Chunxiao Liu, Gábor B. Halász, Leon Balents ,*Phys. Rev. B*, **104**, 054401 (2021).

[2] Krushna Chandra Sahu, Sambuddha Sanyal, *Phys. Rev. B*, **110**, 115144 (2024).

P32

Towards more efficient matrix product state representations of fermionic Gaussian states

Carlo C. Bellinati [1], **Eric C. Andrade** [1], **and Hong-Hao Tu** [2]

[1] *Instituto de Física, Universidade de São Paulo, 05315-970 São Paulo, SP, Brazil*
[2] *Faculty of Physics and Arnold Sommerfeld Center for Theoretical Physics, Ludwig-Maximilians-Universität München, 80333 Munich, Germany*

Both fermionic Gaussian states (FGS) and matrix product states (MPS) are classes of quantum states that have proven to be very powerful for studying quantum many-body systems, particularly in the context of quantum spin liquid (QSL) phases. In recent years, several methods have been proposed to represent FGS as MPS, such as the MPO-MPS algorithm [1-2] and algorithms that use the correlation matrix formalism of FGS [3-4]. As currently formulated, both strategies face limitations. The MPO-MPS method does not support infinite MPS (iMPS) calculations and struggles numerically for larger system sizes. The correlation-matrix algorithms circumvent these problems but require the computation of Slater determinants (for U(1)-FGS) or pfaffians (for BCS-like wavefunctions), which complicates the formalism and increases the computational cost.

In this work, we propose a new method that integrates the key ideas from both algorithms to overcome these challenges. By using the correlation matrix formalism and avoiding the computation of determinants or pfaffians, we have shown that our approach successfully converts FGS into both MPS and iMPS. We benchmarked our method by testing Gutzwiller-projected variational wavefunctions for the J_1-J_2 Heisenberg model on the triangular lattice, focusing on the QSL region of the phase diagram. By converting the Dirac Spin Liquid ansatz into an iMPS, we were able to compare our results with previous iDMRG results [5], which had relied on indirect evidence to confirm the QSL nature of the ground state.

Our method simplifies the FGS-to-MPS mapping and supports scalable, infinite-size simulations, offering a practical route to explore spin liquid physics within the tensor network framework.

[1] Y.-H. Wu, L. Wang, and H.-H. Tu, Phys. Rev. Lett. **124**, 246401 (2020).
[2] H.-K. Jin, H.-H. Tu, and Y. Zhou, Phys. Rev. B Condens. Matter **101**, 165135 (2020).
[3] H.-K. Jin, R.-Y. Sun, Y. Zhou, and H.-H. Tu, Phys. Rev. B **105**, L081101 (2022).
[4] T. Liu, Y.-H. Wu, H.-H. Tu, and T. Xiang, Quantum Science and Technology **10**, 035033 (2025).
[5] S. Hu, W. Zhu, S. Eggert, and Y.-C. He, Phys. Rev. Lett. **123**, 207203 (2019).

P33

Classification of locality preserving symmetries on spin chains

Alex Bols[1], Wojciech De Roeck[2], Michiel De Wilde[2], and Bruno de O. Carvalho[2],

[1]Institute for Theoretical Physics, ETH Zürich
[2]Instituut voor Theoretische Fysica, KU Leuven

We consider the action of a finite group G by locality preserving automorphisms (quantum cellular automata) on quantum spin chains. We refer to such group actions as "symmetries". The natural notion of equivalence for such symmetries is *stable equivalence*, which allows for stacking with factorized group actions. Stacking also endows the set of equivalence classes with a group structure. We prove that the anomaly of such symmetries provides an isomorphism between the group of stable equivalence classes of symmetries with the cohomology group $H^3(G, U(1))$, consistent with previous conjectures. This amounts to a complete classification of locality preserving symmetries on spin chains. We further show that a locality preserving symmetry is stably equivalent to one that can be presented by finite depth quantum circuits with covariant gates if and only if the slant product of its anomaly is trivial in $H^2(G, U(1)[G])$.

[1] Alex Bols, Wojciech De Roeck, Michiel De Wilde, and Bruno de O. Carvalho. Classification of locality preserving symmetries on spin chains, 2025. URL: https://arxiv.org/abs/2503.15088, arXiv:2503.15088.

P34

Chiral Gapless Spin Liquid in Hyperbolic Space

Felix Dusel[1,2,3], **Tobias Hofmann**[1], **Atanu Maity**[1], **Rémy Mosseri**[4], **Julien Vidal**[4,5], **Yasir Iqbal**[5], **Martin Greiter**[1], **and Ronny Thomale**[1,5]

[1] *Institut für Theoretische Physik und Astrophysik and Würzburg-Dresden Cluster of Excellence ct.qmat, Julius-Maximilians-Universität, 97074 Würzburg, Germany*

[2] *Department of Physics, Technical University of Munich, 85748 Garching, Germany*

[3] *Munich Quantum Valley, 80807 Munich, Germany*

[4] *Sorbonne Université, CNRS, Laboratoire de Physique Théorique de la Matière Condensée, LPTMC, F-75005 Paris, France*

[5] *Department of Physics and Quantum Center for Diamond and Emergent Materials (QuCenDiEM), Indian Institute of Technology Madras, Chennai 600036, India*

We study the Kitaev model in the hyperbolic plane by placing spin-1/2 degrees of freedom on the tricoordinated $\{9, 3\}$ lattice, a negatively curved analogue of the honeycomb lattice[1]. Numerical analysis of large finite systems reveals a novel gapless chiral $\mathbb{Z}_2$ spin liquid that spontaneously breaks time-reversal symmetry, characterized by a finite zero-energy density of states and unidirectional edge propagation. Using local Chern markers and wave-packet dynamics, we confirm the chiral character of this gapless regime. Owing to the noncommutative nature of hyperbolic translation groups, this system suggests the possibility of novel quasiparticles with no Euclidean counterpart. Our results broaden the landscape of quantum spin liquids by demonstrating how negative curvature and non-Euclidean symmetries enable new strongly correlated phases with potential implications for exotic quasiparticle statistics and future synthetic realizations.

[1] F. Dusel et al., Phys. Rev. Lett. **134**, 256604 (2025).

P35

Spin-liquid candidate based on S=1/2 Ti3+ ions with a langbeinite structure

Berna Esmer [1], **Ivica Zivkovic** [1]

[1] *École Polytechnique Fédérale de Lausanne, Laboratory for Quantum Magnetism*

A quantum spin-liquid (QSL) phase represents an ultimate goal for the strongly-correlated research in magnetism. The purported entangled ground state could lead to emergent excitations beyond those predicted by a semi-classical approach. Aside from a 1D S=1/2 antiferromagnetic chain, QSL candidates in D>1 rely on some sort of geometric frustration to prevent long-range order in the presence of magnetic interaction between magnetic moments. Known examples of geometrically-frustrated lattices are triangular and kagome in 2D and hyper-kagome and pyrochlore in 3D [1]. Recent investigation [2] has shown that a 3D network of spins forming two interconnected trillium lattices represents a new, so far unexplored avenue of research in geometrically-frustrated magnetism. Recently, we have managed to synthesize and characterize K2Ti2(PO4)3, which is comprised of a fully quantum S=1/2 spins residing on Ti3+ ions. Half of the metallic sites of the langbeinite structure are occupied by non-magnetic S=0 ions (Ti4+), with the distribution of charges and its influence on magnetic properties unknown at the moment. In an ideal case, this would represent an S=1/2 network on a trillium lattice, which is indicated to be insufficiently frustrated to prevent long-range order to set in [3]. The high-temperature regime exhibits a Curie-Weiss behavior, with a characteristic Weiss temperature of -25K. On the other hand, thermodynamic measurements down to 2K do not indicate any features characteristic of long-range order. Furthermore, muSR results performed down to 30mK show a highly dynamic ground-state, without wiggles associated with long-range magnetic order. We conclude that K2Ti2(PO4)3 represents a highly interesting compound, confirming that the langbeinite structure provides a rich environment for the discovery of new geometrically-frustrated systems.

[1] Y. Zhou et al., Rev. Mod. Phys. **89**, 025003 (2017).
[2] Zivkovic et al., PRL **127**, 157204 (2021).
[3] J. M. Hopkinson and H.-Y. Kee, Phys. Rev. B **74**, 224441 (2006).

P36

Transient localization from fractionalization in gapless quantum magnets

Shi Feng[1], **Penghao Zhu**[2], **Nandini Trivedi**[2], **Johannes Knolle**[1], **Michael Knap**[1]

[1] *Technical University of Munich, TUM School of Natural Sciences, Physics Department, 85748 Garching, Germany*

[2] *Department of Physics, The Ohio State University, Columbus, Ohio 43210, USA*

We report disorder-free localization in a quantum spin liquid over an observable timescale, where the quantum fluctuation of visons (i) localizes the Majorana fermions without quench disorder nor extrinsic dynamical disorder and (ii) simultaneously closes the fermion gap. Compelling evidence of its localization is provided by the negligible spreading of energy after a local quench on its ground state; a highly confined lightcone of correlation function; and a vanishing energy current response despite the gapless energy spectrum. The gap closing is confirmed by the numerically obtained gapless dynamical spin spectral function and energy-density fluctuation. We formulate an effective theory with quantum coherent vison disorder for the transient disorder-free localization, giving close agreement to the observed slow transport and gapless spin spectrum. It demonstrates that the disorder-free localization can occur near equilibrium in fractionalized phases of matter, and offers an explanation for the paradox in recent experiments where a linear specific heat coexists with vanishing residual thermal conductivity in candidates of neutral Fermi surfaces.

[1] P. Zhu†, **S. Feng**†, K. Wang, T. Xiang, N. Trivedi, Nature Communications **16**, 2420 (2025).
[2] K. Wang†, **S. Feng**†, P. Zhu, R. Chi, H.-J Liao, N. Trivedi, T. Xiang, Phys. Rev. B **111**, L100402, *Editor's Suggestion* (2025).
[3] **S. Feng**, A. Agarwala, S. Bhattacharjee, N. Trivedi, Phys. Rev. B **108**, 035149 (2023).
[4] **S. Feng**, P. Zhu, J. Knolle, M. Knap, unpublished (2025).

P37

Unconventional Spin Dynamics and Supersolid Excitations in the Triangular-Lattice XXZ Model

Rafael Flores-Calderón[1,2], **Roderich Moessner** [2], **and Frank Pollmann**[1]

[1] *Department of Physics, Technical University of Munich, 85748 Garching, Germany*
[2]*Max Planck Institute for the Physics of Complex Systems, Nöthnitzer Strasse 38, D-01187 Dresden, Germany*

Motivated by recent experiments, we investigate the spin-1/2 XXZ model on the triangular lattice with strong Ising anisotropy, combining large-scale numerical simulations and analytical methods to uncover unconventional spin dynamics at $T = 0$. First, we compute the dynamical spin structure factor using density matrix renormalization group (DMRG) simulations and find excellent agreement with inelastic neutron scattering data on the layered compound $K_2Co(SeO_3)_2$. The low-energy spectrum reveals a roton-like minimum at the M point—absent in linear spin-wave theory—accompanied by peak intensity and a broad continuum above it. Near the Γ point, we observe an approximately linear dispersion with vanishing spectral weight. Second, we compare two analytical frameworks that reproduce the observed features. The first is a hard-core boson approach, which includes: (i) an effective staggered boson model (ESBM) at zero magnetic field, (ii) perturbation theory applied to the one-third magnetization plateau, and (iii) a self-consistent mean-field Schwinger boson theory (SBT). The second framework is based on a variational supersolid quantum dimer model (QDM) ansatz, combined with a single-mode approximation. The SBT captures the broad continuum, the M-point minimum, and linear dispersion at Γ, whereas the QDM reproduces the roton minimum and linear dispersion at finite momentum near Γ. Remarkably, both the QDM wavefunction and the DMRG ground state exhibit nearly identical structure factors with pronounced transverse photon-like excitations. Together, our comprehensive theoretical and numerical analysis elucidates the microscopic origin of supersolid excitations in the XXZ triangular lattice model and their proximity to a spin liquid phase observed experimentally [1,2].

[1] M. Zhu, V. Romerio, N. Steiger, S. D. Nabi, N. Mu- rai, S. Ohira-Kawamura, K. Y. Povarov, Y. Skourski, R. Sibille, L. Keller, Z. Yan, S. Gvasaliya, and A. Zheludev, Continuum excitations in a spin supersolid on a triangular lattice, Phys. Rev. Lett. 133, 186704 (2024).

[2] T. Chen, A. Ghasemi, J. Zhang, L. Shi, Z. Tagay, Y. Chen, L. Chen, E.-S. Choi, M. Jaime, M. Lee, Y. Hao, H. Cao, B. Winn, A. A. Podlesnyak, D. M. Pajerowski, R. Zhong, X. Xu, N. P. Armitage, R. Cava, and C. Bro- holm, Phase Diagram and Spectroscopic Signatures of Supersolids in Quantum Ising Magnet K2Co(SeO3)2 (2024), arXiv:2402.15869 [cond-mat].

P38

The Frustration of Being Odd

Franchini Fabio[1]

[1](*Division of Theoretical Physics, Ruđer Bosković Institute, Bijenicka cesta 54, 10000 Zagreb, Croatia*

Geometrical frustration (GF) stems from a subtle interplay between local and global constraints. We consider the effects of combining periodic boundary conditions inducing GF with quantum interaction, a setting we call ”topological frustration” (TF). Already in 1D spin chains, with TF we observe the emergence of phenomenologies precursor of systems with massive amount of frustration. After an introduction to these concepts, we focus on their implications, especially regarding the complexity of these systems, their experimental realization, and the opportunities for technological applications..

[1] http://thphys.irb.hr/qteam/publication/qmbp/

P39

Topological Order in the Rydberg Blockade on the Kagome Lattice with Projected Entangled Pair States

<u>Anna Francuz</u>[1], Norbert Schuch[1,2], and Bram Vanhecke[1]

[1]*University of Vienna, Faculty of Physics, Boltzmanngasse 5, 1090 Wien, Austria*
[2]*2University of Vienna, Faculty of Mathematics, Oskar-Morgenstern-Platz 1, 1090 Wien, Austria*

Topological order is notoriously difficult to detect, both theoretically and experimentally, due to the absence of local observables capable of distinguishing it from other long-range entangled phases. This challenge has motivated a shift from real materials toward quantum simulation platforms, particularly programmable Rydberg atom arrays, which offer promising avenues for realizing topological order. A notable example is the Kagome lattice quantum simulator demonstrated in Ref. [1].

In this work, we employ two-dimensional Projected Entangled Pair States (PEPS) to variationally optimize the PXP model on the Kagome lattice. We focus on a simplified version of the original Fendley-Sengupta-Sachdev model restricted to nearest- and next-nearest-neighbor interactions. PXP models in both one and two dimensions exhibit a rich variety of phenomena, including quantum scars, lattice gauge theories, and topological order. Our study also serves as a benchmark for state-of-the-art tensor-network methods, including ground-state optimization with automatic differentiation (AD) [2] and the extraction of F-symbols and modular data from topologically ordered PEPS [3].

To this end, we use a gradient-based L-BFGS optimization algorithm, where the energy is computed via PEPS contraction with boundary MPS (using the VUMPS algorithm [4]) and differentiated through AD applied to the characteristic equation of VUMPS [5]. We determine the existence of a continuous phase transition from a trivial to a topologically ordered phase and calculate the F-symbols as well as the S and T matrices of that phase [3], unequivocally identifying it as the $\mathbf{Z}_2$ toric code.

[1] G. Semeghini, H. Levine, A. Keesling, S. Ebadi, T. T. Wang, D. Bluvstein, R. Verresen, H. Pichler, M. Kalinowski, R. Samajdar, A. Omran, S. Sachdev, A. Vishwanath, M. Greiner, V. Vuletic, and M. D. Lukin, Science **374**, 1242 (2021).

[2] A. Francuz, N. Schuch, B. Vanhecke, Phys. Rev. Research, **7**, 013237 (2025).

[3] A. Francuz, L. Lootens, F. Verstraete, J. Dziarmaga, Phys. Rev. B, **104**, 195152 (2021)

[4] V. Zauner-Stauber, L. Vanderstraeten, M. T. Fishman, F. Verstraete, and J. Haegeman, Phys. Rev. B, **97**, 045145 (2018)

[5] B. Vanhecke, A. Francuz, L. Burgelman, J. Haegeman, F. Verstraete, *in preparation*.

P40

Boundary-bulk maps of topological phases via gauging.

P41

Quantum geometry from fidelity expansion

P42

Adiabatic echo protocols for robust many-body state preparation

Z. Zeng[1,2], G. Giudici[1,2,3], A. Senoo[4], A. Baumgärtner[4], A. M. Kaufman[4], H. Pichler[1,2]

[1]Institute for Theoretical Physics, University of Innsbruck, Innsbruck, Austria

[2]Institute for Quantum Optics and Quantum Information, Innsbruck, Austria

[3]PlanQC GmbH, Garching, Germany

[4]JILA, University of Colorado Boulder, Colorado, USA

Accurate and coherent control of neutral atom arrays is crucial for realizing entangled many-body quantum states. We employ optimal control methods to design protocols that enable reliable manipulation of complex quantum dynamics. In particular, we introduce an adiabatic echo protocol that substantially improves the robustness of state preparation in strongly correlated regimes. We demonstrate its effectiveness in generating both Greenberger–Horne–Zeilinger states and quantum spin liquids in Rydberg atom arrays, and further show that the approach is broadly applicable to a wide class of interacting quantum systems.

References

[1] Z. Zeng*, G. Giudici*, A. Senoo, A. Baumgärtner, A. M. Kaufman, H. Pichler, arXiv:2506.12138

P43

Spin Liquids on the Tetratrillium Lattice

Matías G. Gonzalez[1] **and Johannes Reuther**[2,3]

[1]*Physikalisches Institut, University of Bonn, Germany*
[2]*Helmholtz-Zentrum Berlin für Materialien und Energie, Germany*
[3]*Dahlem Center for Complex Quantum Systems, Freie Universität Berlin, Germany*

The langbeinite $K_2Ni_2(SO_4)_3$ is composed of two $S = 1$ magnetic intertwined trillium lattices. This highly-frustrated material exhibits a weak phase transition that only releases a small part of the total entropy, and below which the system remains highly-fluctuating [1]. This is also evidenced by the static and dynamical spin structure factors obtained via inelastic neutron scattering experiments [2, 3], which show weak Bragg peaks on top of a dynamical background. For this reason, $K_2Ni_2(SO_4)_3$ has been proposed to lie close to a quantum critical point leading to a quantum disordered phase. This disordered region surrounds a special point in which only two couplings are relevant and from a tetratrillium lattice: a trillium lattice in which each triangle is completed with an extra spin to form tetrahedra [3].

Here, we show detailed results on the classical spin liquid properties of the tetratrillium lattice using classical Monte Carlo and large-N theory calculations. From large-N theory, we find that the system presents a spin gap between the flat bands at the bottom of the spectrum, falling under the category of fragile spin liquids with exponentially decaying correlations according to the most recent classical spin liquid classification schemes [4]. We verify this in the more physical Heisenberg and Ising limits by performing classical Monte Carlo calculations. In the Ising case, we are able to build a loop-update algorithm based on the Ising spin liquid on the parent trillium lattice. In both Ising and Heisenberg cases, we find that there is no finite-temperature phase transition and the system remains disordered down to zero temperature. Surprisingly, the spin structure factor obtained at low temperature in all three limits (large-N, Heisenberg, and Ising) is indistinguishable, indicating the presence of a fragile spin liquid in all cases.

Finally, we also provide insight into the quantum $S = 1/2$ Heisenberg limit by performing pseudo-Majorana functional renormalization group calculations at finite temperatures. This method allows us to obtain reliable values for the two-point correlators at temperatures above $T = J$ and reasonable results down to $T = 0.1J$. We do not find any evidence of a phase transition; instead, we obtain a spin structure factor with no dominating peaks, indicative of a disordered phase. Unfortunately, we cannot study the quantum ground state using this method; however, we discuss the possible phases that can arise due to the processes enabled by quantum fluctuations.

[1] Zivkovic, I., Favre, V. et. al., Magnetic Field Induced Quantum Spin Liquid in the Two Coupled Trillium Lattices of K2Ni2(SO4)3, Phys. Rev. Lett. **127**, 157204 (2021).

[2] Yao, W., Huang, Q. et. al., Continuous Spin Excitations in the Three-Dimensional Frustrated Magnet K2Ni2(SO4)3. Phys. Rev. Lett. **131**, 146701 (2023).

[3] Gonzalez, M.G., Noculak, V., Sharma, A. et al., Dynamics of K2Ni2(SO4)3 governed by proximity to a 3D spin liquid model. Nat Commun **15**, 7191 (2024).

[4] Yan, H., Benton, O. et. al., Classification of classical spin liquids: Detailed formalism and suite of examples. Phys. Rev. B **109**, 174421 (2024).

P44

Chiral spin liquid in external magnetic field: Phase diagram of the decorated-honeycomb Kitaev model

Sabastian Granberg Cauchi[1], **Matthias Vojta**[1]

[1] *Institut für Theoretische Physik and Würzburg-Dresden Cluster of Excellence ct.qmat, Technische Universität Dresden, 01062 Dresden, Germany*

Recent evidence suggesting that α-$RuCl_3$ enters a field-induced quantum-disordered state has spurred interest in exploring the effect of a magnetic field on Kitaev spin liquids. Here we analyze the antiferromagnetic Kitaev model on the triangle-decorated honeycomb lattice which is known to realize a zero-field chiral spin liquid. We utilize a Majorana-based parton mean-field theory to determine the phase diagram for general direction of magnetic field. We find a variety of field-induced spin liquids, different valence-bond-solid states, and semi-classical spin liquids at elevated fields. The spin-liquid phases display Majorana bands with non-zero Chern number.

P45

Emergent $SU(4)$ Symmetry and Gapless Spin-Orbital Liquid in α-$ZrCl_3$ inspired model

Manoj Gupta[1], **Basudeb Mondal**[2], **Arijit Haldar**[1], **Subhro Bhattacharjee**[2] **and Tanusri Saha Dasgupta**[1]

[1]*Department of Condensed Matter Physics and Materials Science, S. N. Bose National Centre for Basic Sciences, Kolkata 700098, India*
[2]*International Centre for Theoretical Sciences, Tata Institute of Fundamental Research, Bengaluru 560 089, India*

Quantum Spin Liquids (QSLs) are the exotic phases of matter characterized by fractionalised excitations and the absence of long-range magnetic order. One intriguing route to realizing a nontrivial QSL is by generalizing conventional $SU(2)$ spin systems to $SU(N)$ spin systems with $N > 2$ [1]. Recent theoretical studies[2] have suggested an emergent $SU(4)$ symmetry in honeycomb lattice α-ZrCl$_3$ by considering an indirect Zr-Zr hopping mechanism through the intermediate Cl p states. In contrast, our first-principles calculations[3] reveal dominance of direct metal-metal d-d hopping, which modifies the underlying model.

Building on this input, we derive an effective spin Hamiltonian for $J = 3/2$ quartets in the infinite SOC and strong-coupling limit $(U/t >> 1)$. Despite the breaking of explicit $SU(4)$ symmetry by hopping and SOC, a gauge transformation restores an effective $SU(4)$-symmetric Hubbard form. Further, using the fermionic mean-field approach, we compute the dynamical spin-structure factor revealing the gapless-fractionalized excitation. This results in spectral features that can be accessed via inelastic neutron scattering experiments allowing us to distiniguish QSLs arising from the indirect and direct hopping machanism.

[1] Philippe Corboz et. al. *Phy. Rev. X 2, 041013 (2012).*
[2] Masahiko G. Yamada et.al *Phy. Rev. Letter 121, 097201 (2018).*
[3] Manoj Gupta, Basudeb Mondal, Subhro Bhattacharjee, Tanusri Saha Dasgupta *Phy. Rev. Research 5, 043219 (2023).*
[4] Manoj Gupta, Arijit Haldar, Subhro Bhattacharjee, Tanusri Saha Dasgupta, Multiple Dirac Spin-Orbital Liquids for $SU(4)$ Heisenberg Antiferromagnets on Honeycomb Lattice: *To be submitted*

The talk is based on the works [3] and [4].

P46

Abstract for Advanced School and Conference on Quantum Matter

Jonas Habel[1,2], **Roderich Moessner**[3], **and Johannes Knolle**[1,2,4]

[1]*(Presenting author underlined) Technical University of Munich, Germany*
[2]*Munich Center for Quantum Science and Technology, Germany*
[3] *Max-Planck-Institut für Physik komplexer Systeme, Dresden, Germany*
[4] *Blackett Laboratory London, UK*

The precise values of the magnetic exchange couplings in α-$RuCl_3$ are of significant interest to understand the proposed Kitaev spin liquid phase. A common method for extracting them involves fully field-polarizing the magnetic moments, performing an inelastic neutron scattering (INS) experiment, and fitting a non-interacting (linear) spinwave theory to the data. However, due to magnetic frustration, magnon manybody interactions are strong in α-$RuCl_3$ and cannot be neglected, even at high fields. We present a procedure for fitting an interacting (nonlinear) spinwave theory to INS data, explicitly accounting for these manybody interactions. This reveals a significant renormalization of the exchange couplings compared to linear spinwave estimates.

P47

Controlled probing of localization effects in the non-Hermitian Aubry-André model via topolectrical circuits

Dipendu Halder[1] **and Saurabh Basu**[1]

[1]*Department of Physics, Indian Institute of Technology Guwahati-Guwahati, 781039 Assam, India*

Anderson localization [1] and the non-Hermitian skin effect [2] are two distinct confinement phenomena of the eigenfunctions that are driven, respectively, by disorder and nonreciprocity. Understanding their interplay within a unified framework offers valuable insights into the localization properties of low-dimensional systems. To this end, we investigate a non-Hermitian version of the celebrated Aubry-André model [3], which serves as an ideal platform due to its unique self-dual properties and ability to demonstrate a delocalization-localization transition in one dimension. Interestingly, in our setting, the competition between Anderson localization and the skin effect can be precisely controlled via the complex phase of the quasiperiodic disorder. Additionally, by analyzing the time evolution, we demonstrate that quantum jumps [4] between the skin states and the Anderson-localized states occur in the theoretical model. Further, to gain support for our theoretical predictions in an experimental platform, we propose a topolectrical circuit [5] featuring an interface that separates two distinct electrical circuit networks. The voltage profile of the circuit exhibits confinement at the interface, analogous to the skin effect, while the phenomenon of Anderson localization in the circuit can be perceived via a predicted localization behavior near the excitation node, rather than exhibiting sudden non-Hermitian jumps, as observed in the tight-binding framework. This interplay leads to a spatially tunable localization of the output voltage of the circuit. Our findings provide deeper insights into the controlled confinement of the eigenstates of the non-Hermitian Aubry-André model by designing analogous features in topolectrical circuits, opening avenues in the fabrication of advanced electronic systems such as highly sensitive sensors and efficient devices for information transfer and communication.

[1] P. W. Anderson, Absence of diffusion in certain random lattices, Phys. Rev. **109**, 1492 (1958).

[2] S. Yao and Z. Wang, Edge states and topological invariants of non-Hermitian systems, Phys. Rev. Lett. **121**, 086803 (2018).

[3] S. Aubry and G. André, Analyticity breaking and Anderson localization in incommensurate lattices, Ann. Isr. Phys. Soc. **3**, 133 (1980).

[4] A. Leventis, K. G. Makris, and E. N. Economou, Non-Hermitian jumps in disordered lattices, Phys. Rev. B **106**, 064205 (2022).

[5] C. H. Lee, S. Imhof, C. Berger, F. Bayer, J. Brehm, L. W. Molenkamp, T. Kiessling, and R. Thomale, Topolectrical circuits, Commun. Phys. **1**, 39 (2018).

[6] D. Halder and S. Basu, Controlled probing of localization effects in the non-Hermitian Aubry-André model via topolectrical circuits, Phys. Rev. B **111**, 235447 (2025).

P48

The Pseudo-Majorana Functional Renormalization Group: An efficient tool for treating frustrated systems

Abstract: In recent years an improvement upon the Pseudo-Fermion Functional Renormalization Group (pffrg) has been developed that was shown to be more accurate and more efficient at treating frustrated spin systems at non-zero temperatures: The so called Pseudo-Majorana Functional Renormalization Group (pmfrg) [1, 4]. In the pmfrg an SO(3) Majorana representation is utilized as opposed to an Abrikosov-Fermion representation of Spins that has the advantage over the pffrg of not introducing artificial unphysical states. The pmfrg so far has been successfully applied to the study of magnetic phases and transitions between them in Heisenberg systems. Most recently it has also been used to analyze the full phase diagram of the XXZ model on the pyrochlore lattice detecting amongst other things Quantum Spin Ice phases [3]. Realistic materials may however display more complex interactions, including off-diagonal ones [2]. To connect to realistic systems it is hence necessary to generalize the existing pmfrg method to arbitrary diagonal and off-diagonal interactions. This has been achieved and first benchmarks indicate its accuracy and applicability.

References

[1] Nils Niggemann, Björn Sbierski, and Johannes Reuther. "Frustrated quantum spins at finite temperature: Pseudo-Majorana functional renormalization group approach". In: *Physical Review B* 103.10 (2021), p. 104431.

[2] Kate A Ross et al. "Quantum excitations in quantum spin ice". In: *Physical Review X* 1.2 (2011), p. 021002.

[3] Yannik Schaden, Matías G Gonzalez, and Johannes Reuther. "Phase diagram of the XXZ pyrochlore model from pseudo-Majorana functional renormalization group". In: *Physical Review B* 111.13 (2025), p. 134442.

[4] Benedikt Schneider et al. "Temperature flow in pseudo-Majorana functional renormalization for quantum spins". In: *Physical Review B* 109.19 (2024), p. 195109.

P49

TeMFpy: a Python library for converting fermionic mean-field states into tensor networks

Simon H. Hille[1], **Attila Szabó** [1]

[1]*Department of Physics, University of Zurich, Zurich, Switzerland*

Fermionic mean-field (or Gaussian) states are a class of variational wave functions of central importance. All eigenstates of non-interacting fermionic Hamiltonians are Gaussian states; as such, they also form the starting point of such mean-field theories as Hartree–Fock theory and the BCS theory of superconductivity and, in fact, often provide an excellent account of strongly interacting quantum systems already.

As first noted in Ref. [1], Slater determinants can conveniently be converted to MPS form by noting that their Schmidt vectors are themselves Slater determinants and so entries of the canonical MPS tensors are overlaps of Slater determinants, which can efficiently be computed. Since then, this idea has been expanded to Pfaffian (or Boguliubov mean-field) states [2] and successfully used to study Gutzwiller projected mean-field states and as starting points to DMRG [3].

In this poster, I will introduce TeMFpy, a Python library for converting fermionic mean-field states into finite and infinite matrix product states. TeMFpy includes new, efficient, and easy-to-understand algorithms for constructing MPS representations of both Slater determinants and Pfaffians. Together with Gutzwiller projection, these also allow the user to build variational wave functions for various strongly correlated electron systems such as quantum spin liquids. TeMFpy is built on top of TeNPy [4] and, therefore, integrates seamlessly with existing MPS-based algorithms.

[1] G. Petrica, B.-X. Zheng, G. K.-L. Chan, and B. K. Clark, Phys. Rev. B **103**, 125161 (2021).
[2] H.-K. Jin, R.-Y. Sun, Y. Zhou, and H.-H. Tu, Phys. Rev. B **105**, L081101 (2022).
[3] H.-K. Jin, H.-H. Tu, and Y. Zhou, Phys. Rev. B **104**, L020409 (2021).
[4] J. Hauschild, F. Pollmann, SciPost Phys. Lect. Notes **5**, 5 (2018).

P50

Quantum manipulation of energy transfer in quantum materials

Fatemeh Jadidi Kouhbanani [1] , **Ali Asadian** [1]

[1] *Department of Physics, Institute for Advanced Studies in Basics Sciences (IASBS), Zanjan 45137- 66731, Iran*

Energy propagation in systems that must be described in terms of quantum mechanics has become a very important area of study in the field of quantum materials. This is because understanding how to control and efficiently distribute energy is important for the development of modern quantum technologies [1].

We investigate and control steady-state energy transfer in quantum materials. To this end, we first study energy transfer in two different models: a spin-chain network and a chain of coupled quantum harmonic oscillators. In both models, we analyze the energy transfer behavior and then combine these two systems to actively control the energy transfer path. Here, we focus on a simple one-dimensional model that can be extended to higher dimensions.

First, we investigate steady-state energy transfer in a chain of coupled spins connecting with its terminal sites coupled to heat baths of different temperatures. Through an analytic treatment we found that the current in this system is independent of the system size [2]. Since we needed a more flexible carrier for heat transfer, we replaced the spins with a chain of coherent oscillators. The main finding is that quantum coherence enables ballistic flow independent of the chain length, and in the final step, we added coupled spins as controllers of energy transfer to the oscillator. By coupling spins to the chain of oscillators, we have created an "interactive information sensing protocol." Designed to verify the generation of dynamical entanglement even under weak conditions, this protocol acts as a controller [3, 4]. This combined architecture allows us to actively manipulate and control the steady-state energy flow along the chain. In particular, we show how this control element enables the tuning of the energy transfer path. This work provides a new theoretical framework for achieving dynamic quantum control over energy diffusion in a non-equilibrium steady state. The results of this work pave the way for the design of quantum materials capable of precisely controlling the flow of stable energy.

[1] U.S. Department of Energy, *Advanced Thermoelectric Materials for Efficient Waste Heat Recovery in Process Industries* (2009).
[2] D. Manzano, M. Tiersch, A. Asadian, and H. J. Briegel, arXiv:1112.2839 [quant-ph] (2012).
[3] A. Asadian, D. Manzano, M. Tiersch, and H. J. Briegel, Phys. Rev. E 87, 012109 (2013).
[4] D. Carney, H. Müller, and J. M. Taylor, PRX Quantum 2, 030330 (2021).

P51

A New, Exact Perturbation Theory for Operators Related by the Baker-Campbell-Hausdorff identity

Applied to the Ising model on the Square, Cubic and Hypercubic Lattices

Joseph M. Jones[1], **Martin W. Long**[1]

[1]*Theoretical Physics Group, University of Birmingham, United Kingdom*

We have developed a new, exact mathematical technique that we call statistical physics perturbation theory [1]. Our method competes with the high-temperature series expansion and also with Monte Carlo simulations. Indeed, we do not require the assumption of a phase transition to predict one!

Our perturbation theory is for operators related by the Baker-Campbell-Hausdorff (BCH) identity, $\exp(C) = \exp(A)\exp(B)$ [2], rather than by addition, $C = A + B$, as in quantum mechanics. We use the transfer matrix approach to classical statistical mechanics [3] which leads directly to the BCH identity and we must find the operator C. Our perturbation theory is almost verbatim the quantum case, save that the denominators, $1/x$, are replaced by hyperbolic functions, $\coth(x)$, and corrections!

We present predictions for the correlation length as a function of temperature and the associated critical exponent for the Ising model on the square, cubic and hypercubic lattices. Surprisingly, for the square lattice, we find the exact correlation length at first order with all higher order contributions vanishing!

[1] J. M. Jones and M. W. Long, in preparation.
[2] J. C. Moodie and M. W. Long, 2021 J. Phys. A: Math. Theor. 54 015208.
[3] T. D. Schultz, D. C. Mattis and E. H. Lieb, Rev. Mod. Phys. 36, 85

P52

Stability of the Spin Polaron Solution in the J_1–J_2 Doped Quantum Spin Liquid

Stanislaw Kalinowski[1], **Ronny Thomale**[2], **Yasir Iqbal**[3], **Krzysztof Wohlfeld**[1]

[1]*Institute of Theoretical Physics, Faculty of Physics, University of Warsaw, Pasteura St. 5, 02-093 Warsaw, Poland*

[2]*Institut für Theoretische Physik und Astrophysik and Würzburg-Dresden Cluster of Excellence ct.qmat, Julius-Maximilians-Universität, 97074 Würzburg, Germany*

[3]*Department of Physics and Quantum Center for Diamond and Emergent Materials (QuCenDiEM), Indian Institute of Technology Madras, Chennai 600036, India*

Hole-doped quantum spin liquids (QSLs) have long played a central role in the theoretical study of strongly correlated electron systems [1]. The behavior of holes in *some* antiferromagnetic (AF) backgrounds is relatively well understood. In 1D AF systems which lack long-range order, added holes separate into independent holons and spinons [2], leading to spin-charge separation. In contrast, in *ordered* 2D AF systems, hole motion typically results in the formation of spin polarons——quasiparticles in which mobile holes are dressed by a cloud of spin excitations (magnons) [3].

Given that QSLs are characterized by the absence of conventional magnetic order and by the presence of fractionalized excitations, they were expected to behave similarly to 1D AF systems, exhibiting spin-charge separation [4]. However, this long-standing paradigm has recently been challenged by several studies. Notably, evidence for Nagaoka polarons has been found in the Kitaev spin liquid (KSL) [5], and spin-polaron quasiparticles have been observed to be stable at specific momenta in the QSL found in the frustrated J_1-J_2 AF Heisenberg model on the square lattice [6, 7].

These findings motivate a deeper investigation into the nature of hole dynamics in QSLs. Here we approach this problem using state-of-the-art self-consistent Born approximation techniques. Specifically, we focus on analyzing the magnon-holon vertex and studying the possible decay channels of spin-polaron quasiparticles. Additionally, we explore the competition between coherent holon propagation and polaronic-type motion, where the holon becomes dressed by the spin excitations.

[1] P. W Anderson, G. Baskaran, Z. Zou, T. Hsu, Phys. Rev. Lett. **58**, 2790-2793 (1987).
[2] E. H. Lieb and F. Y. Wu, Phys. Rev. Lett. **20**, 1445 (1968).
[3] S. Schmitt-Rink, C. M. Varma, and A. E. Ruckenstein, Phys. Rev. Lett. **60**, 2793 (1988).
[4] X.-G Wen, Phys. Rev. B **65**, 165113 (2002).
[5] H.-K. Jin, W. Kadow, M. Knap, J. Knolle, npj Quantum Materials **9**, 65 (2024).
[6] J. H. Nyhegn, K. K. Nielsen, G. M. Bruun, Phys. Rev. B **111**, 035142 (2025).
[7] J. H. Nyhegn, K. K. Nielsen, L Balents, G. M. Bruun, arXiv:2507.02508 [cond-mat.str-el].

P53

Majorana polarization in disordered heterostructures

Shubhanshu Karoliya [1], Sumanta Tewari [2], and Gargee Sharma [1]

[1] *School of Physical Sciences, Indian Institute of Technology Mandi, Mandi 175005, India*
[2] *Department of Physics and Astronomy, Clemson University, Clemson, South Carolina 29634, USA*

Majorana-bound states (MBS) are of great interest for topological quantum computation due to their non-Abelian statistics. Recent theoretical work suggests that Majorana polarization can serve as a diagnostic tool for detecting these exotic excitations. In this study, we analyze the behavior of Majorana polarization in two systems: a strictly one-dimensional semiconducting nanowire and a quasi-one-dimensional geometry, both incorporating Rashba spin-orbit coupling, proximity-induced superconductivity, and disorder. While the condition $P^*_{left} \cdot P_{right} \sim -1$ has been proposed to signify the presence of topological MBS, our results reveal that this criterion alone is insufficient. We identify instances where this polarization condition is met even by partially separated Andreev bound states (psABS) or quasi-Majorana modes, which do not support non-Abelian braiding. Our analysis emphasizes that reliable identification of topological MBS - especially in disordered systems-requires a combination of diagnostics, including energy spectra, wavefunction localization, and topological gap analysis. These results highlight the need for caution in interpreting polarization-based signatures and aim to clarify the role of diagnostics in advancing topological quantum computing platforms.

[1] D. Sticlet et al., PRL (2012).

[2] V. Kaladzhyan et al., SciPost Physics (2017).

[3] G. Sharma et al., PRB (2020).

[4] Chuanchang Zeng et al., PRB (2022).

[5] S. Karoliya et. al, ArXiv (2025).

Title: *Multitime Correlators and the Quantum Regression Theorem in the Ultrastrong Coupling Regime*

Abstract: In the framework of open quantum systems, we investigate the behavior of multitime correlation functions in the ultrastrong coupling (USC) regime between a system and its environment. A central focus is the validity of the Quantum Regression Theorem (QRT), which is widely used to compute multitime correlations in the weak coupling regime. We derive the governing equations for two-time correlators in the USC regime and benchmark the QRT against the numerically exact Hierarchical Equations of Motion (HEOM) method.

Our results show that under the strong Markov approximation, the QRT remains remarkably accurate, even at strong coupling. However, beyond this approximation, the QRT fails for certain classes of correlation functions. We address this breakdown by introducing correction terms to the standard QRT formalism, enabling accurate recovery of correlation dynamics in excellent agreement with HEOM results.

P55

Quantum Machine Learning for Quantum Phase Recognition in Many-Body Systems

Mehran Khosrojerdi[1], **Leonardo Banchi**[1,2], **Alessandro Cuccoli**[1,2]

[1] *1 Department of Physics and Astronomy, University of Florence, via G. Sansone 1, I-50019 Sesto Fiorentino (FI), Italy*

[2] *INFN Sezione di Firenze, via G. Sansone 1, I-50019 Sesto Fiorentino (FI), Italy*

This poster highlights three projects applying quantum machine learning to quantum many-body systems with a focus on phase recognition. We explore supervised learning using support vector machines and optimized datasets, unsupervised spectral clustering based on affinity matrices, and clustering techniques to map phase diagrams in specialized systems. Case studies include the Axial Next-Nearest-Neighbor Ising (ANNNI) model, the Cluster-Ising model, and the Anisotropic Haldane chain, demonstrating insights into symmetry-protected topological phases and interactions. These studies showcase the potential of quantum machine learning to advance the understanding of complex quantum matters such as spin glasses.

[1] Learning to Classify Quantum Phases of Matter with a Few Measurements (2024).
[2] Unsupervised Learning to Clustering Quantum Phases of Matter using Tensor Networks (2025).
[3] Quantum Phase Recognition from Reduced Subsystems (2025).
[4] Supervised Quantum Image Processing (2025).

P56

Spin-phonon coupling induced chiral phonons and their signature in Raman Circular Dichroism

Eduard Koller[1,2,3], **Swetlana Swarup**[4], **Johannes Knolle**[1,2,5], **and Natalia B. Perkins**[4,3]

[1]Technical University of Munich, TUM School of Natural Sciences, Physics Department, 85748 Garching, Germany

[2]Munich Center for Quantum Science and Technology (MCQST), Schellingstr. 4, 80799 München, Germany

[3]Institute for Advanced Study, Technical University of Munich, Lichtenbergstr. 2a, 85748 Garching, Germany

[4]School of Physics and Astronomy, University of Minnesota, Minneapolis, Minnesota 55455, USA

[5]Blackett Laboratory, Imperial College London, London SW7 2AZ, United Kingdom

Recent Raman experiments on the Kitaev material α-$RuCl_3$ have reported a finite Raman circular dichroism (RCD), revealing chiral phonon behavior not expected from lattice symmetry alone. To explain this observation, we develop a diagrammatic framework for the spin–phonon coupled Kitaev model. We demonstrate that bare phonons contribute no RCD, but coupling to the chiral Majorana continuum under an applied magnetic field renormalizes the phonon propagator, mixing real polarization eigenvectors into complex superpositions with finite angular momentum. This interaction-induced modification generates a nonzero RCD accompanied by characteristic Fano line shapes in the Raman response, reflecting interference between discrete phonons and the continuum. The resulting signal grows with magnetic field strength, consistent with experiment, and directly tracks the field-induced chirality of the Majorana sector. More broadly, our results establish RCD as a powerful probe of interaction-induced chiral phonons in correlated quantum materials.

P57

Understanding the limits of the linear spin wave theory

R. Komar[1], **D. Cabra**[2], **G. Rossini**[2], **T. Tohyama**[3], **Y. Iqbal**[4], **K. Wohlfeld**[1]

[1] *Faculty of Physics, University of Warsaw, Warsaw, Poland*
[2] *IFLySiB-CONICET and Departamento de Física, Universidad Nacional de La Plata, Argentina*
[3] *Department of Applied Physics, Tokyo University of Science, Katsushika, Tokyo 125-8585, Japan*
[4] *Department of Physics and Quantum Center for Diamond and Emergent Materials (QuCenDiEM), Indian Institute of Technology Madras, Chennai 600036, India*

Linear spin-wave (LSW) theory has established itself as one of the most valuable methods of calculating low-energy excitations of ordered magnets. A case in point is the archetypical 2D Heisenberg antiferromagnet (AF) on a square lattice. Interestingly, however, even recently the valididy of LSW in this 2D ordered AF has been discussed, *cf.* [1, 2, 3].

As a way to understand what are the limits of the LSW approximation in an intuitive manner, we delve into this well-known model, but with tunable magnon-magnon interactions. The latter is introduced by scaling the $\lambda n_i n_j$ magnon-magnon interaction term in the hardcore bosons formulation after sublattice-respecting spin rotation, which allows us to tune the model from the Heisenberg model ($\lambda = 1$) to the LSW limit ($\lambda = 0$). Probing of the magnon spectra with spin dynamical structure factors gives us insight into how magnons behave in both cases and how we can tune their dynamics with the parameter λ.

We calculate the spectra using three complementary methods: (i) exact diagonalization on Betts' clusters [4], (ii) mean-field defined in the Jordan-Wigner fermion language, and (iii) Density Matrix Renormalisation Group. The obtained results show in an unambiguous manner how including the interaction between magnons as well as the hard-core boson constraint influences the well-known LSW results.

[1] R. Verresen, F. Pollmann, and R. Moessner, Phys. Rev. B **98**, 155102 (2018).
[2] J. Bao, M. Gohlke, J. G. Rau, and N. Shannon, Physical Review Research, **7**, 1, L012053 (2025).
[3] N. E. Shaik *et al.*, arXiv preprint, arXiv:2503.14643 (2025).
[4] D. Betts, S. Masui, N. Vats, and G. Stewart, Can. J. Phys. **77**, 353 (1999).

P58

Symmetry Study of Elemental Rhenium

Márk Kondákor[1,2], Karlo Penc[2]

[1] *Institute of Physics, Budapest University of Technology and Economics, Hungary*
[2] *HUN-REN Wigner Research Centre for Physics, Budapest, Hungary*

Recent muon spin rotation (μSR) experiments on elementary rhenium have shown that its superconducting phase spontaneously breaks time-reversal symmetry [1]. Ab initio calculations further indicate that finite magnetic moments of opposite directions arise on the two atoms in the crystal's elementary cell, coexisting with the superconducting state [2]. The observed activated specific heat can be accounted for by a mixture of spin-singlet and spin-triplet Cooper pairs.

To elucidate these findings, we performed a comprehensive symmetry classification of all possible superconducting and magnetic order parameters in the nonsymmorphic crystal structure of rhenium.We employed double-group theory to classify the spin-orbit coupled electronic states. We identified the relevant symmetry channels for time-reversal symmetry breaking and determined the corresponding terms in effective interaction. Our results shed light on the interplay between spin and orbital degrees of freedom in rhenium and provide a theoretical framework for exploring magnetism and superconductivity in other nonsymmorphic materials.

[1] T. Shang et al., Phys. Rev. Lett. **121**, 257002 (2018).
[2] G. Csire et al., Phys. Rev. B **106**, L020501 (2022)

P59

Quasi-isotropic magnetic interaction in Yb and Ce compounds

Kotaro Shimizu [1], **Esteban Agustin Ghioldi** [2], **Cristian Daniel Batista** [3,4]

[1] *Dept. of Appl. Phys., The Univ. of Tokyo, Japan*
[2] *Los Alamos National Laboratory, USA*
[3] *Dept. of Phys. and Astron., The Univ. of Tennessee, USA*
[3] *Oak Ridge National Laboratory, USA*

Quantum spin liquids represent an exotic magnetic state in which interacting localized moments fail to exhibit symmetry breaking down to the lowest temperatures. In such states, strong quantum fluctuations can give rise to topological order and fractionalized, delocalized quasiparticles, making them attractive platforms for robust quantum functionalities such as fault-tolerant quantum computation. Since Anderson's proposal, intensive theoretical and experimental efforts have been devoted to searching for and designing candidate systems, particularly in geometrically or interactionally frustrated lattices such as triangular antiferromagnets and Kitaev magnets. Rare-earth compounds, which have recently attracted significant attention as promising platforms for realizing such unconventional magnetic states, host strongly spin-orbit-entangled Kramers doublets arising from strong spin-orbit coupling and various crystal field structures. Although anisotropic interactions are naturally expected in these systems, triangular-lattice spin liquids based on nearly isotropic interactions have also been proposed, particularly in Yb-based compounds [1,2]. This highlights the importance of establishing clear design principles grounded in microscopic interactions.

In this work, we focus on Yb- and Ce-based compounds and investigate the relation between their microscopic material parameters and effective magnetic interactions. Starting from a multi-orbital Hubbard model, we perform a degenerate perturbation analysis to systematically enumerate and classify the hopping processes that contribute to either isotropic or anisotropic exchange [2,3]. We then discuss the conditions on the Kramers doublet ground states that suppress anisotropic terms and stabilize dominant isotropic Heisenberg exchange. Finally, we compare the condition we found with experimental reports for various isotropic and anisotropic Yb and Ce compounds, offering insights into the design of rare-earth-based quantum magnets.

[1] Y. Li *et al*. Sci. Rep. **5**, 16419 (2015); Y. Li *et al*., Phys. Rev. Lett. **118**, 107202 (2017); M. M. Bordelon *et al*., Nat. Phys. **15**, 1058 (2019); A. O. Scheie et al., Phys. Rev. B **109**, 014425 (2024).
[2] J. G. Rau and M. J. P. Gingras, Phys. Rev. B **98**, 054408 (2018).
[3] E. A. Ghioldi *et al*., Phys. Rev. B **110**, 195123 (2024).

P60

SU(2) symmetric Hamiltonian for the four-color states on the pyrochlore lattice

Péter Kránitz[1,2,3], **Yasir Iqbal**[2], **and Karlo Penc**[1,2]

[1]*Institute for Solid State Physics and Optics, Wigner Research Centre for Physics, H-1525 Budapest, P.O. Box 49, Hungary*
[2]*Department of Physics, Indian Institute of Technology Madras, Chennai 600036, India*
[3]*Department of Theoretical Physics, Institute of Physics, Budapest University of Technology and Economics, Műegyetem rakpart 3, H-1111 Budapest, Hungary*

Frustrated Heisenberg models are known to host numerous competing phases, making precise numerical identification of their ground states particularly challenging. Exactly solvable models play a crucial role in this context, providing reference points for exploring complex phase diagrams. Prominent examples include the Majumdar-Ghosh [1] and Affleck-Kennedy-Lieb-Tasaki (AKLT) [2] Hamiltonians, which can be expressed as sums of noncommuting projectors whose eigenstates naturally yield the ground state wavefunctions. Recently, a macroscopically degenerate XXZ model was identified for the spin-1/2 kagome quantum antiferromagnet, featuring a three-coloring product state as its exact ground state [3].

In this work, we introduce a chiral, SU(2)-symmetric spin-1 Hamiltonian defined on the pyrochlore lattice, expanding the class of known exactly solvable models. Its ground states form a product state over tetrahedra, with each tetrahedron hosting four spin-coherent states

$$|\psi\rangle = \prod_{\text{tetrahedra}} \otimes|\mathbf{n}_1\rangle \otimes |\mathbf{n}_2\rangle \otimes |\mathbf{n}_3\rangle \otimes |\mathbf{n}_4\rangle, \tag{1}$$

where $|\mathbf{n}_i\rangle$, $i = 1, 2, 3, 4$, are the spin coherent state pointing in four directions $\mathbf{n}$ on the Bloch-sphere and obey the four color rule on each tetrahedron (termed tetrahedratic states). A representative configuration, defined up to a global O(3) rotation, is given by:

$$\mathbf{n}_1 = (111),\ \mathbf{n}_2 = (\bar{1}\bar{1}1),\ \mathbf{n}_3 = (1\bar{1}\bar{1}),\ \mathbf{n}_4 = (\bar{1}1\bar{1}), \tag{2}$$

Twelve distinct configurations arise from even permutations of Eq. (2) [4], and these configurations with the global O(3) rotation span exactly 65 linearly independent states within the 81-dimensional Hilbert space (3^4) of each tetrahedron. We construct the Hamiltonian $\mathcal{H}_\alpha$ on each tetrahedron explicitly:

$$\mathcal{H}_\alpha = \sqrt{3}J\sum_{ijk}\mathbf{S}_i(\mathbf{S}_j \times \mathbf{S}_k) - J\sum_{i<j}\mathbf{S}_i\mathbf{S}_j + J\sum_{(ij)(kl)}(\mathbf{S}_i\mathbf{S}_j)(\mathbf{S}_k\mathbf{S}_l), \tag{3}$$

where in the first sum $ijk = 123, 142, 134, 243$ and the last sum is over $(ij)(kl) = (12)(34), (13)(24)$, and $(14)(23)$. Summing $\mathcal{H}_\alpha$ over all tetrahedra gives the full Hamiltonian $\mathcal{H} = \sum_\alpha \mathcal{H}_\alpha$, whose ground-state manifold is precisely spanned by these four-color product states, Eq. (1).

[1] C. K. Majumdar and D. K. Ghosh, J. Math. Phys. **10**, 1338 (1969)
[2] I. Affleck, T. Kennedy, E. H. Lieb and H. Tashaki, Phys. Rev. Lett. **59**, 799 (1987)
[3] H. J. Changlani *et al.*, Phys.Rev.Lett. **120**, 117202 (2018).
[4] D. Lozano-Gómez, Y. Iqbal and M. Vojta, Nat. Commun. **15**, 10162 (2024).

P61

Pseudocriticality in antiferromagnetic spin chains

Sankalp Kumar[1], Sumiran Pujari[1], and Jonathan D'Emidio[2]

[1]*Department of Physics, Indian Institute of Technology Bombay, Mumbai, MH 400076, India*
[2]*Department of Physics and Astronomy, University of Tennessee, Knoxville, TN 37996, USA*

Weak first-order pseudocriticality with approximate scale invariance has been observed in a variety of settings, including the intriguing case of deconfined criticality in 2+1 dimensions. Recently, this has been interpreted as extremely slow flows ("walking behavior") for real-valued couplings in proximity to a *bona fide* critical point with complex-valued couplings, described by a complex conformal field theory (CFT)[1,2]. Here we study an SU(N) generalization of the the Heisenberg antiferromagnet, which is a familiar model for deconfined criticality in 2+1 dimensions. We show that in 1+1 dimensions the model is located near a complex CFT, whose proximity can be tuned as a function of N. We employ state-of-the-art quantum Monte Carlo simulations for *continuous* N along with an improved loop estimator for the Rényi entanglement entropy based on a nonequilibrium work protocol. These techniques allow us to track the central charge of this model in detail as a function of N, where we observe excellent agreement with CFT predictions. Notably, this includes the region $N > 2$, where the CFT moves into the complex plane and pseudocritical drifts enable us to recover the real part of the complex central charge with remarkable accuracy. Since the present model with $N = 3$ is also equivalent to the spin-1 biquadratic model, our work sheds new light on the dimerized phase of the spin-1 chain, demonstrating that it is pseudocritical and proximate to a complex CFT.

[1] H. Ma and Y.-C. He, Phys. Rev. B **99**, 195130 (2019)
[2] Victor Gorbenko, Slava Rychkovb, and Bernardo Zanb, JHEP, **108** (2018).

P62

Thermal quenches in spin 3 ice

Arnab Seth[a 1] Souvik Kundu[a 2 †] Sthitadhi Roy [2 ‡] Subhro Bhattacharjee [2 §] and Roderich Moessner[3 ¶]

[1] *School of Physics Georgia Institute of Technology Atlanta Georgia 30332 USA.*

[2] *International Centre for Theoretical Sciences Tata Institute of Fundamental Research Bengaluru 560089 India*

[3] *Max Planck Institute for the Physics of Complex Systems*

Nöthnitzer Strasse 38 01187 Dresden Germany

(Dated: July 31, 2025)

We study a class of pyrochlore magnets where two low-lying crystal-field doublets give rise to a family of spin-3 2 generalizations of spin ice. These systems exhibit a topological Coulomb liquid phase with an enhanced ground-state degeneracy. Perturbations around this phase lead to a novel branch of ultra-localized dipole excitations. We investigate the thermal quench dynamics in di erent regimes of the phase diagram.

aseth65@gatech.edu

† souvik.kundu@icts.res.in;

[a] The authors contributed equally. Arnab Seth was at ICTS Bangalore when a large part of this work was was done.

‡ sthitadhi.roy@icts.res.in

§ subhro@icts.res.in

¶ moessner@pks.mpg.de

P63

Emergent topological phases and coexistence of gapless and spectral-localized Floquet quantum spin Hall states via electron-phonon interaction

Srijata Lahiri, Kuntal Bhattacharyya and Saurabh Basu

Department of Physics, Indian Institute of Technology Guwahati, Guwahati-781039, Assam, India

In this work, a thorough exploration has been carried out to unravel the role of electron-phonon interaction (EPI) in a Bernevig-Hughes-Zhang (BHZ) quantum spin Hall (QSH) insulator subjected to a time-periodic step drive. It is observed that upon inclusion of the EPI, the system demonstrates emergent Floquet QSH (FQSH) phases and several topological phase transitions thereof, mediated solely by the interaction strength. Quite intriguingly, we observe the emergence of phases hosting a topological zero (π) energy gap while its π (zero) energy sector is gapless. With other invariants being found to be deficient in characterizing such coexistent phases, a spectral localizer ($\mathcal{SL}$) is employed, which distinctly ascertains the nature of the (zero or π) edge modes obtained within the corresponding topological gap. Following the $\mathcal{SL}$ prescription, a real-space Chern marker computed by us further provides support to such *gapless* Floquet topological scenario. Our results may be realized in optical setups that may underscore the importance of EPI-induced Floquet features.

P64

Dissipative quantum spin ice

Afonso Ribeiro[1], Paul McClarty[1], Pedro Ribeiro[2,3] and Manuel Weber[4]

[1] *Laboratoire Léon Brillouin, CEA, CNRS, Université Paris-Saclay, CEA Saclay, 91191 Gif-sur-Yvette, France*
[2] *CeFEMA-LaPMET, Departamento de Física, Instituto Superior Técnico, Universidade de Lisboa, Av. Rovisco Pais, 1049-001 Lisboa, Portugal*
[3] *Beijing Computational Science Research Center, Beijing 100193, China*
[4] *Institut für Theoretische Physik and Würzburg-Dresden Cluster of Excellence ct.qmat, Technische Universität Dresden, 01062 Dresden, Germany*

Coupling of a many-body system to external degrees of freedom can drastically alter the nature of the phase diagram. Motivated by recent works on the effect of dissipation on quantum liquid phases [1, 2], we study the stability of quantum spin ice against environment-induced dissipation.

For this purpose, we develop a quantum Monte-Carlo method in the continuous-time path-integral formalism with worm update scheme. The use of the recently introduced wormhole updates [3] allow us to simulate quantum systems where each site is locally coupled to one or more bosonic bath. In this work, we simulate the XXZ model on the pyrochlore lattice where, on each site, a U(1)-symmetric two-bath couples to the system spin operators. We map the phase diagram of the dissipative XXZ model for the ohmic and sub-ohmic bath cases. This is done by inspecting the structure factors $\langle S^z(k)S^z(-k)\rangle$ and $\langle S^x_\mu(k)S^y_\mu(-k)\rangle$ and the finite-size XY correlation length estimator as a function of bath coupling. We conclude that quantum spin ice is stable to the environment up to finite bath coupling. For higher couplings, the bath induces a transition into the 3D XY ordered phase.

To understand the numeric results, we look into the effect of the bath-induced terms in the 4D compact QED description of quantum spin ice. Using the usual Villain approximation, we find that the bath simply renormalizes the coupling in the Coulomb gas dual action. The quantum spin ice to 3D XY ordered transition is then driven by the same deconfinement-confinement transition of the topological charges as in the usual XXZ model on the pyrochlore.

Finally, we analyse the stability of classical spin ice as a function of the bath exponent and relate our results to the two-bath spin-boson model.

[1] A. L. Ribeiro, P. McClarty, P. Ribeiro, and M. Weber, Dissipation-induced long-range order in the one-dimensional bose-hubbard model, Physical Review B **110**, 115145 (2024).
[2] M. Weber, D. J. Luitz, and F. F. Assaad, Dissipation-induced order: the s= 1/2 quantum spin chain coupled to an ohmic bath, Physical Review Letters **129**, 056402 (2022).
[3] M. Weber, Quantum Monte Carlo simulation of spin-boson models using wormhole updates, Phys. Rev. B **105**, 165129 (2022).
[4] B. Bruognolo, A. Weichselbaum, C. Guo, J. von Delft, I. Schneider, and M. Vojta, Two-bath spin-boson model: Phase diagram and critical properties, Physical Review B **90**, 245130 (2014)

P65

Probing Spinon Interactions in the Bilinear-Biquadratic Spin-1 Chain

Yonatan Lin [1], **Anna Keselman** [1,2], **and Oleg A. Starykh** [2]

[1] *Physics Department, Technion, 32000 Haifa, Israel*
[2] *Department of Physics and Astronomy, University of Utah, Salt Lake City, Utah 84112, USA*

The bilinear-biquadratic spin-1 antiferromagnetic chain is a paradigmatic model in the study of topological phases and fractionalized excitations. When the strength of the biquadratic coupling equals that of the bilinear term, known as Uimin-Lai-Sutherland (ULS) point, the system undergoes a quantum phase transition from the topological Haldane phase to an extended critical phase characterized by deconfined, fractionalized spinons [1,2].
In this poster, I will present our studies of the dynamical spin and quadrupolar correlations of the system in the vicinity of the ULS point in the presence of a magnetic field. Using a hydrodynamic approach [3], we show that probing the system's response at small momenta provides direct access to the strength of interactions between spinons in the effective low-energy description. Our theoretical predictions are supported by numerical matrix-product-state (MPS)-based calculations on the microscopic model.

[1] F. D. M. Haldane, Physics letters a 93, 464 (1983)
[2] C. Itoi and M.-H. Kato, Physical Review B 55, 8295 (1997)
[3] R.-B. Wang, A. Keselman, and O. A. Starykh, Physical Review B 105, 184429 (2022)

P66

Superconductivity in the repulsive Hubbard model on different geometries induced by density-assisted hopping

Franco T. Lisandrini[1], **Edmond Orignac**[2], **Roberta Citro**[3], **Ameneh Sheikhan**[1], **and Corinna Kollath**[1]

[1]*(Presenting author underlined) Physikalisches Institut, University of Bonn, Nussallee 12, 53115 Bonn, Germany*

[2]*ENSL, CNRS, Laboratoire de Physique, F-69342 Lyon, France*

[3]*Physics Department "E. R. Caianiello" and CNR-SPIN, Universitá degli Studi di Salerno, INFN, Gruppo Collegato di Salerno, 84084-Fisciano (Sa), Italy*

We study the effect of density-assisted hopping on different dimerized lattice geometries, such as bilayers and ladder structures. We show analytically that the density-assisted hopping induces an attractive interaction in the lower (bonding) band of the dimer structure and a repulsion in the upper (anti-bonding) band. Overcoming the onsite repulsion, this can lead to the appearance of superconductivity. The superconductivity depends strongly on the filling, and present a pairing structure more complex than s-wave pairing. Combining numerical and analytical methods such as the matrix product states ansatz, bosonization and perturbative calculations we map out the phase diagram of the two-leg ladder system and identify its superconducting phase. We characterize the transition from the non-density-assisted repulsive regime to the spin-gapped superconducting regime as a Berezinskii-Kosterlitz-Thouless transition.

P67

Highly Entangled Stationary States from Strong Symmetries

Yahui Li[1,2], **Frank Pollmann**[1,2], **, Nicholas Read**[3,4], **and Pablo Sala**[5,6]

[1] *Technical University of Munich, TUM School of Natural Sciences, Physics Department, Lichtenbergstrasse 4, 85748 Garching, Germany*

[2] *Munich Center for Quantum Science and Technology (MCQST), Schellingstrasse 4, 80799 München, Germany*

[3] *Department of Physics, Yale University, P.O. Box 208120, New Haven, Connecticut 06520-8120, USA*

[4] *Department of Applied Physics, Yale University, P.O. Box 208284, New Haven, Connecticut 06520-8284, USA*

[5] *Department of Physics and Institute for Quantum Information and Matter, California Institute of Technology, Pasadena, California 91125, USA*

[6] *Walter Burke Institute for Theoretical Physics, California Institute of Technology, Pasadena, California 91125, USA*

We find that the presence of strong non-Abelian symmetries can lead to highly entangled stationary states even for unital quantum channels [1]. We derive exact expressions for the bipartite logarithmic negativity, Rényi negativities, and operator space entanglement for stationary states restricted to one symmetric subspace, with focus on the trivial subspace. We prove that these apply to open quantum evolutions whose commutants, characterizing all strongly conserved quantities, correspond to either the universal enveloping algebra of a Lie algebra or the Read-Saleur commutants. The latter provides an example of quantum fragmentation, whose dimension is exponentially large in system size. We find a general upper bound for all these quantities given by the logarithm of the dimension of the commutant on the smaller bipartition of the chain. As Abelian examples, we show that strong $\mathrm{U}(1)$ symmetries and classical fragmentation lead to separable stationary states in any symmetric subspace. In contrast, for non-Abelian $\mathrm{SU}(N)$ symmetries, both logarithmic and Rényi negativities scale logarithmically with system size. Finally, we prove that, while Rényi negativities with $n > 2$ scale logarithmically with system size, the logarithmic negativity (as well as generalized Rényi negativities with $n < 2$) exhibits a volume-law scaling for the Read-Saleur commutants. Our derivations rely on the commutant possessing a Hopf algebra structure in the limit of infinitely large systems and, hence, also apply to finite groups and quantum groups.

[1] Y. Li, F. Pollmann, N. Read, and P. Sala, Highly entangled stationary states from strong symmetries, Phys. Rev. X 15, 011068 (2025).

P68

An Atlas of Classical Pyrochlore Spin Liquids

Daniel Lozano-Gómez[1,2], Owen Benton[3], Michel J. P. Gingras[2], Han Yan[4]

[1] *Institut für Theoretische Physik and Würzburg-Dresden Cluster of Excellence ct.qmat, Technische Universität Dresden, 01062 Dresden, Germany*

[2] *Department of Physics and Astronomy, University of Waterloo, Waterloo, Ontario, N2L 3G1, Canada*

[3] *School of Physical and Chemical Sciences, Queen Mary University of London, London, E1 4NS, United Kingdom*

[4] *Institute for Solid State Physics, The University of Tokyo, Kashiwa, Chiba 277-8581, Japan*

The pyrochlore lattice magnet has been one of the most fruitful platforms for the experimental and theoretical search for spin liquids. Besides the canonical case of spin ice, works in recent years have identified a variety of new quantum and classical spin liquids from the generic nearest-neighbor anisotropic spin Hamiltonian on the pyrochlore lattice. However, a general framework for the thorough classification and characterization of these exotic states of matter has been lacking and so is an *exhaustive* list of all possible spin liquids that this model can support and what is the corresponding structure of their emergent field theory. In this work, we develop such a theoretical framework to allocate interaction parameters stabilizing different classical spin liquids and derive their corresponding effective generalized emerging Gauss's laws at low temperatures. Combining this with Monte Carlo simulations, we systematically identify all classical spin liquids for the general nearest-neighbor anisotropic spin Hamiltonian on the pyrochlore lattice. We uncover new spin liquid models with exotic forms of generalized Gauss's law and multipole conservation laws. Furthermore, we present an atlas of all spin liquid regimes in the phase diagram which illuminates the global picture of how different classical spin liquids are connected in parameter space and transition into each other. Our work serves as a treasure map for the theoretical study of classical and quantum spin liquids, as well as for the experimental search and rationalization of exotic pyrochlore lattice magnets.

P69

Fermionic parton theory of Rydberg $\mathbb{Z}_2$ quantum spin liquids

Atanu Maity[1], **Yasir Iqbal**[2] **and Rhine Samajdar**[3,4]

[1] *Institut für Theoretische Physik und Astrophysik and Würzburg-Dresden Cluster of Excellence ct.qmat, Julius-Maximilians-Universität Würzburg, Am Hubland Campus Süd, Würzburg 97074, Germany*

[2] *Department of Physics and Quantum Centers in Diamond and Emerging Materials (QuCenDiEM) group, Indian Institute of Technology Madras, Chennai 600036, India*

[3] *Department of Physics, Princeton University, Princeton, NJ 08544, USA*

[4] *Princeton Center for Theoretical Science, Princeton University, Princeton, NJ 08544, USA*

Quantum spin liquids are novel highly entangled phases of matter that evade long-range order, even at absolute zero temperature. Experimentally, unambiguously identifying such an intricate quantum liquid state in solid-state materials is challenging. However, in recent years, programmable arrays of Rydberg atoms have emerged as a powerful tool for simulating strongly interacting quantum spin systems. For example, recent experiments on such a neutral-atom quantum simulator have demonstrated the realization of a $\mathbb{Z}_2$ spin liquid phase on a ruby lattice [1]. This raises an important question about the precise microscopic nature of the phase realized on this quantum simulator.

Wen's projective symmetry group (PSG) framework provides an effective tool for characterizing such phases based on the parton representation of spins and the emergent gauge structure. In this study, we employ PSG classification to analyze fermionic parton mean-field states with a $\mathbb{Z}_2$ low-energy gauge group on the ruby lattice. Considering a symmetry group that includes the full lattice space group and time-reversal symmetry, we identify 64 algebraic PSG solutions. However, when restricting interactions to third-nearest neighbors, only 50 of these solutions exhibit a low-energy $\mathbb{Z}_2$ gauge group. By systematically comparing the static structure factors of *all* possible mean-field *Ansätze* against density-matrix renormalization group calculations, we identify a promising candidate for the precise $\mathbb{Z}_2$ QSL realized microscopically. We also present detailed analyses of the dynamical structure factors as a reference for future experiments and showcase how these spin correlations can differentiate between varied QSL *Ansätze*.

[1] Semeghini, G. et al. Probing topological spin liquids on a programmable quantum simulator. Science 374, 1242-1247 (2021).
[2] Atanu Maity, Yasir Iqbal, Rhine Samajdar, arXiv:2409.17219 (2024).

P70

Thermal Hall response of an abelian chiral spin liquid at finite temperatures

Avijit Maity[1], **Haoyu Guo**[2], **Subir Sachdev**[3] **and Vikram Tripathi**[1]

[1]*Department of Theoretical Physics, Tata Institute of Fundamental Research, Homi Bhabha Road, Colaba, Mumbai 400005, India.*

[2]*Laboratory of Atomic and Solid State Physics, Cornell University, 142 Sciences Drive, Ithaca, New York 14853-2501, USA*

[3]*Department of Physics, Harvard University, Cambridge, Massachusetts 02138, USA*

Thermal Hall transport has emerged as a valuable tool for probing the fractionalized excitations in chiral quantum spin liquids. Observing quantized thermal Hall response, expected at temperatures below the spectral gap, has been challenging and controversial. The finite temperature behavior, especially in the quantum critical regime above the spectral gap, can provide useful signatures of the underlying topological order. In this context, we study the spin-1/2 Heisenberg antiferromagnet on a kagome lattice that is believed to be a U(1) Dirac spin liquid over a wide intermediate energy range. Scalar spin chirality perturbations turn this into a gapped abelian chiral spin liquid (CSL) with semionic topological order. Using a recently developed large-N technique [Guo *et al.*, Phys. Rev. B **101**, 195126 (2020)], we obtain explicit expressions for the thermal Hall conductivity κ_{xy} at finite temperatures taking into account both matter and gauge fluctuations. At low temperatures below the spectral gap, the quantized thermal Hall response agrees with that expected from conformal field theory and gravitational anomaly arguments. Our main finding is that in a large temperature window spanning the spectral gap and the Curie temperature scales where quantum critical fluctuations dominate, κ_{xy}/T obeys a power-law with logarithmic corrections. Our analysis also provides a route to understanding the thermal Hall response at higher temperatures in the quantum critical regime.

[1] Avijit Maity, Haoyu Guo, Subir Sachdev, and Vikram Tripathi, Thermal Hall response of an Abelian chiral spin liquid at finite temperatures, Phys. Rev. B **111**, 205119 (2025).

Dynamical signatures of fractionalization in spin-1/2 1d Kitaev chain

Ritwika Majumder[1,2], **Subhajyoti Pal**[1,2], **Anamitra Mukherjee**[1,2], **and Nandini Trivedi**[3], **Jean-Sébastien Caux**[4]

[1]*School of Physical Sciences, National Institute of Science Education and Research, Jatni 752050, India*
[2]*Homi Bhabha National Institute, Training School Complex, Anushaktinagar, Mumbai 400094, India*
[3]*Department of Physics, Ohio State University, Columbus, OH 43210, USA*
[3]*Institute for Theoretical Physics, Universiteit van Amsterdam, PO Box 94485, NL-1090 GL Amsterdam, The Netherlands*

We investigate the dynamical properties of the one-dimensional spin-1/2 Kitaev chain by analyzing the one and two-spin dynamical structure factors. Using a combination of density matrix renormalization group (DMRG) and Exact Diagonalization (ED) we map out one and two-spin response for the Kitaev chain over the Brillouin zone at zero and finite magnetic fields. Exploiting the exact solvability of the Kitaev chain we provide analytic understanding of the observed spectral features and spectral weight transfers with magnetic fields. We also compute specific two-spin correlations as predictions Resonant inelastic X-ray spectroscopy.

[1] M. Mourigal, M. Enderle, A. Kl¨opperpieper, J.-S. Caux, A. Stunault, and H. M. Rønnow, Nature Physics, vol. 9, no. 7, pp. 435–441, 2013.

P72

Extraordinary-log phase in the Heisenberg spin chain

Grigorios Makris[1], Francesco Parisen Toldin [1], and Stefan Wessel[1]

[1] *Institute for Theoretical Solid State Physics, RWTH Aachen University, Germany*

We examine the ground state correlations emerging in a spin-1/2 Heisenberg chain upon coupling it to a quantum critical two-dimensional bilayer Heisenberg system. Based on the quantum-to-classical mapping and recent findings of unconventional surface criticality of three-dimensional classical Heisenberg models [1] [2], extraordinary-log criticality is expected to become accessible within this setup along the coupled chain. The coupled chain is viewed as a line defect that corresponds, through the quantum-to-classical mapping, to a classical planar defect which also exhibits extraordinary-log criticality [2]. Part of the inspiration for this setup comes from experiments demonstrating that spin chains can be assembled on material surfaces [3]. We used large-scale quantum Monte Carlo simulations to systematically explore this scenario, based on measurements of correlations and the spin stiffness, using the stochastic series expansion methods.

[1] Max A Metlitski, SciPost Phys. **12**, 131 (2022).
[2] Francesco P. Toldin, Abijith Krishnan, Max A Metlitski, Phys. Rev. Research **7**, 023052 (2025).
[3] R. Toskovic, R. van den Berg, A. Spinelli,*et al*, Nature Physics volume **12**, pages 656–660 (2016)

P73

Cold quantum gases of many flavors

Abstract

We investigate the dynamics of a three-dimensional gas consisting of n_f flavors of fermions. In the $n_f \to \infty,\ p_F \to 0$ limit with the total density $\propto n_f p_F^3$ held fixed, we identify a new superfluid-like mode arising from the collective density fluctuations of the fermions. For $p < p_F$, the system behaves as a Fermi liquid, and the superconducting instability is suppressed. As $p_F \to 0$, the wavefunction becomes identical to that of distinguishable bosons, which we use to write down an effective field theory for the gas. We discuss applications to neutron stars, non-Fermi liquids, and cold atom simulators.

P74

Extrinsic contribution to bosonic thermal Hall transport

<u>Léo Mangeolle</u> [1,2] , Johannes Knolle [1,2,3]

[1] *Technical University of Munich, TUM School of Natural Sciences,*

[2] *Munich Center for Quantum Science and Technology (MCQST)*

[3] *Blackett Laboratory, Imperial College London*

Bosonic excitations like phonons and magnons dominate the low-temperature transport of magnetic insulators. Similar to electronic Hall responses, the thermal Hall effect (THE) of charge neutral bosons has been proposed as a powerful tool for probing topological properties of their wavefunctions. For example, the intrinsic contribution of the THE of a perfectly clean system is directly governed by the distribution of Berry curvature, and many experiments on topological magnon and phonon insulators have been interpreted in this way. However, disorder is inevitably present in any material and its contribution to the THE has remained poorly understood. Here we develop a rigorous kinetic theory of the extrinsic side-jump contribution to the THE of bosons. We show that the extrinsic THE can be of the same order as the intrinsic one but sensitively depends on the type of local imperfection. We study different types of impurities and show that a THE can even arise as a pure impurity-induced effect in a system with a vanishing intrinsic contribution. As a side product, we also generalize existing results for the electronic AHE to general types of impurities beyond the standard assumption of local potential scattering. We discuss the importance of our results for the correct interpretation of THE measurements and provide a ready-to-use formula for comparison to experimental data.

P75

Exotic Gapless Mott Insulator with Tile-invariant Symmetry

Dan Mao, Department of Physics, University of Zurich, Winterthurerstrasse 190, 8057 Zurich, Switzerland
T: +41 784413789, dan.mao@physik.uzh.ch

The interplay between the finite dimension of the local Hilbert space and local energetic constraints enforces a novel *exact* emergent global symmetry, which we call “tile-invariant symmetry”. By mapping the states in low-energy Hilbert space to tiling patterns, we prove the exactness of the tile-invariant symmetry utilizing the boundary invariant proposed by Conway and Lagarias. The spontaneous breaking of the tile-invariant symmetry provides a robust mechanism towards an exotic gapless Mott insulator, with a gapless charge neutral Goldstone mode but a vanishing order parameter and zero off-diagonal long-range correlation function measured on the lattice.

P76

Quantum Spin Liquids in Spin Ice Pyrochlores Stabilized by Disorder

Marcus Marinho[1], **Eric C. Andrade**[1]

[1]*Instituto de Física, Universidade de São Paulo, 05315-970 São Paulo, SP, Brazil*

Quantum spin liquids (QSLs) are exotic phases of matter characterized by long-range entanglement, emergent gauge structures and non-local excitations. Recent theoretical proposals suggest that in non-Kramers spin ice materials, the disorder can drive the formation of a Coulomb quantum spin liquid (CQSL). In particular, the presence of structural disorder in these systems can transform high-entropy classical spin ice into an entangled CQSL. We then have an unusual mechanism where defects stabilize a spin-liquid phase. Naturally, this scenario brings into question the stability of the CQSL with respect to the disorder itself. In particular, if the disorder is high enough, one can expect the CQSL to give room to a paramagnet. Interestingly, an intermediate Griffiths Coulomb quantum spin liquid (GCQSL) phase, akin to the well-known Mott glass phase, is expected to separate both. Mapping this problem to a random transverse field Ising model, we numerically investigate the effects of disorder on CQSL stability and identify regions in the parameter space where GCQSL emerges. Specifically, we explore the disorder-induced condensation of spinons, an exotic non-local excitation of the CQSL, to determine the complete phase diagram of the model. Our results provide quantitative insights into the conditions under which disorder supports or destabilizes the CQSL state, with direct implications for the candidate material $\mathrm{Pr_2Zr_2O_7}$.

[1] L. Savary, L. Balents, Phys. Rev. Lett. **118**, 087203 (2017).
[2] O. Benton, Phys. Rev. Lett. **121**, 037203 (2018).

P77

Single-site entanglement unveils superconducting transition in a correlated fermionic system

Marina Sanino[1], Irene D'Amico[2], Vivian V. França[1] and Isaac M. Carvalho[1].

[1]*Institute of Chemistry, São Paulo State University, 14800-090, Araraquara, São Paulo, Brazil.*

[2]*School of Physics, Engineering and Technology, University of York, York YO10 5DD, United Kingdom.*

Single-site entanglement is notable for its versatility in identifying quantum phase transitions in correlated fermionic systems. In contrast to conventional order parameters, it is inherently related to nonlocal correlations, rooted in the superposition principle of quantum theory, quantifying the entanglement between a single site and the remaining sites of a quantum system. Its limitation in predicting superconducting transitions, which are associated with off-site long-range order, has been widely recognized. Yet, this conclusion was drawn from studies on small system sizes that fail to properly capture higher-order transitions, whose anomalies become discernible only in larger systems [1, 2, 3]. In this work, we apply density matrix renormalization group (DMRG) techniques to investigate the superconducting transition probed by single-site entanglement in a larger fermionic system. We show that it exhibits a well-defined local minimum marking the transition. Contrary to previous understanding, our results reveal that single-site entanglement can reflect transitions related to off-site order through its dependence on quantum fluctuations—specifically, charge and spin variances at the site. We also demonstrate that entanglement can be directly obtained from these fluctuations, which are experimentally accessible through spectroscopy-based measurements.

[1] SJ Gu, SS Deng, YQ Li, HQ Lin, Phys. Rev. Lett. **93**, 086402 (2004).
[2] SQ Su, JL Song, SJ Gu, Phys. Rev. A **74**, 032308 (2006).
[3] Ö Legeza, J Sólyom, Phys. Rev. Lett. **96**, 116401 (2006).

P78

Quantum Fisher Information, Dynamical Susceptibility, and Topological Non-Fermi Liquids in the interacting SSH chain

Sepide Mohamadi, Jahanfar Abouie

Department of Physics, Institute for Advanced Studies in Basic Sciences (IASBS), Zanjan 45137-66731, Iran

We investigate the interplay between topology, interactions, and entanglement in the Su-Schrieffer-Heeger (SSH) chain with long-range interactions, governed by the constrained Hatsugai-Kohmoto interaction [3]. Our study reveals the emergence of a topological non-Fermi liquid (TNFL) phase [1, 2]. We characterize this phase using a combination of the Zak phase, Luttinger integral, and polarization, highlighting its strongly correlated and gapless nature.

We then focus on the system's response to external magnetic fields through the lens of dynamical spin and charge susceptibilities. Using exact diagonalization, we analyze how these susceptibilities evolve across different fillings. Our results demonstrate that dynamical susceptibility successfully captures the transition between trivial and topological phases as the filling changes. Notably, the susceptibility vanishes in the trivial insulating phase at $n = 1$ and becomes finite in the topological phase at $n = 2$, marking a clear distinction in low-energy excitations.

In parallel, we explore the entanglement structure encoded in the ground state via the quantum Fisher information (QFI). At $n = 1$, where the system is insulating and topologically trivial and non-trivial, the stored quantum information is negligible. In contrast, at $n = 2$, the QFI reaches a maximum in the topological phase, indicating robust multipartite entanglement. Although the TNFL phase is entangled, the QFI derived solely from spin-spin and charge-charge correlations may not fully resolve the transition between TNFL and trivial non-Fermi liquid regimes, suggesting the need for refined entanglement probes.

Our results offer insight into how dynamical and entanglement-based quantities can characterize exotic phases in interacting topological systems.

[1] Su, W. P., Schrieffer, J. R., Heeger, A. J. (1980). Soliton excitations in polyacetylene. Physical Review B,22, 4, 2099.

[2] Mohamadi, S., Abouie, J. (2025). Emergence of topological non-Fermi liquid phases in a modified Su-Schrieffer-Heeger chain with long-range interactions. Physical Review B, 111, 16, 165129.

[3] Hatsugai, Y., Kohmoto, M. (1992). Exactly solvable model of correlated lattice electrons in any dimensions. Journal of the Physical Society of Japan, 61, 6, 2056-2069.

P79

Phase diagram of the hard-core bosonic Hubbard model for frustrated dipolar bosons using Neural Network Quantum States (NQS)

P80

Controlling Chaos in Sachdev-Ye-Kitaev Model

Arkaprava Mukherjee[1], **Vatsal**[2], **Sumilan Banerjee**[3] , **Sandip P. Trivedi**[2] **and Nandini Trivedi**[1]

[1]*Department of Physics, The Ohio State University, Columbus, OH 43210, USA*
[2]*Department of Theoretical Physics, Tata Institute of Fundamental Research, Colaba, Mumbai 400 005, India*
[3]*Centre for Condensed Matter Theory, Department of Physics, Indian Institute of Science, Bangalore 560012, India*

We study a generalized Sachdev-Ye-Kitaev (SYK) model of complex fermions with all-to-all random interactions drawn from a Gaussian distribution with a non-zero mean [1]. Using exact diagonalization for up to $N = 26$ sites, we show that while the model remains a fast scrambler, it is no longer maximally chaotic. Despite this reduction in chaos, it retains a finite residual entropy and exhibits chaotic spectral correlations at intermediate and long times. We observe that the ground-state compressibility increases, whereas the entanglement entropy decreases and becomes more localized within charge sectors. Additionally, a finite spectral gap appears in the many-body density of states at higher energies. These findings demonstrate how introducing a non-zero mean qualitatively modifies the thermodynamic and chaotic properties of the SYK model.

We also investigate the extreme limit of the model in which all couplings are identical, resulting in a clean, translationally invariant version of the SYK model. This non-chaotic variant lacks an analytical solution. Using similar techniques, we find that chaotic behavior breaks down at all timescales in this limit [2].

[1] Arkaprava Mukherjee, Vatsal, Sumilan Banerjee, Sandip P. Trivedi, Nandini Trivedi; “Controlling Chaos in SYK Model”, In Preparation .

[2] Arkaprava Mukherjee, Vatsal, Sumilan Banerjee, Sandip P. Trivedi, Nandini Trivedi; “Does Chaos in SYK model survive Without disorder” , In Preparation.

P81

SU(2) Gauge Theory for Fluctuating Stripes in the Pseudogap Regime

Henrik Müller-Groeling[1], **Pietro M. Bonetti**[2], **Paulo Forni**[1], **and Walter Metzner**[1]

[1]*Max Planck Institute for Solid State Research, D-70569 Stuttgart, Germany*
[2]*Department of Physics, Harvard University, Cambridge MA 02138, USA*

We investigate the role of charge order in a pseudogap described by an SU(2) gauge theory of fluctuating magnetic order.
The theory is based on a fractionalization of electrons into a fermionic chargon pseudospinor and a bosonic spinon, which leads to an emergent SU(2) pseudospin symmetry. In the mean-field solution of the 2D Hubbard model, which we use to describe the electrons in the copper-oxygen planes, Néel, spiral, or stripe order were observed below a density dependent transition temperature T^* [1].
Fluctuations of the spin orientation are described by a non-linear sigma model obtained from a gradient expansion of the spinon action. The spin stiffnesses are computed from a random phase approximation for the chargon susceptibility. The spinon fluctuations prevent magnetic long-range order of the electrons at any finite temperature. The phase with magnetic chargon order exhibits the most salient features characterizing the pseudogap regime in high-T_c cuprates: a strong reduction of charge carrier density, a spin gap, and Fermi arcs [2], and we set out to observe the effects of charge order in this context.

[1] R. Scholle, P. M. Bonetti, D. Vilardi, W. Metzner, PRB **108** 035139 (2023);
[2] P. M. Bonetti, W. Metzner, PRB **106**, 205152 (2022).

P82

rojectively implemented altermagnetism in an exactly solvable quantum spin liquid

Avedis Neehus [1 2] Achim Rosch [3] Johannes Knolle [1 2 4] and Urban F. P. Seifert[3]

Technical University of Munich, TUM School of Natural Sciences, Physics Department, 85748 Garching, Germany
[2]*Munich Center for Quantum Science and Technology MCQST), Schellingstr. 4, 80799 München, Germany*
[3]*Institute for Theoretical Physics, University of Cologne, 50937 Cologne, Germany*
[4]*Blackett Laboratory, Imperial College London, London SW7 2AZ, United Kingdom*

(Dated: April 16, 2025)

Altermagnets are a new class of symmetry-compensated magnets with large spin splittings. Here, we show that the notion of altermagnetism extends beyond the realm of Landau-type order: we study exactly solvable $_2$ quantum spin(-orbital) liquids (QSL), which simultaneously support magnetic long-range order as well as fractionalization and $_2$ topological order. Our symmetry analysis reveals that in this model three distinct types of "fractionalized altermagnets (AM) may emerge, which can be distinguished by their residual symmetries. Importantly, the fractionalized excitations of these states carry an emergent $_2$ gauge charge, which implies that they transform *projectively* under symmetry operations. Consequently, we show that "altermagnetic spin splittings are now encoded in a momentum-dependent particle-hole asymmetry of the fermionic parton bands. We discuss consequences for experimental observables such as dynamical spin structure factors and (nonlinear) thermal and spin transport.

P83

Phases and phase transitions in a dimerized spin-1/2 XXZ chain

P84

Generalized Dimer Physics in Multi-Level Rydberg Atom Arrays

José M. Cruz[1,2], **Ciarán Hickey**[1,2]

[1]*School of Physics, University College Dublin, Belfied, Dublin 4, Ireland*
[2]*C-QuEST, University College Dublin, Dublin 4, Ireland*

Many physical systems with local constraints can effectively be described using a dimer model approach. The active degrees of freedom are represented by dimers that live on links connecting sites and the local constraints translate to dimer constraints that limit the number of dimers touching each site. This implies that, unlike say regular quantum spin models, the total Hilbert space cannot be written as a tensor product state of local Hilbert spaces. One platform in which dimer models have been proposed to be relevant is Rydberg atom arrays. Rydberg atoms interact predominantly via a dipole-dipole coupling which, in certain regimes, leads to the Rydberg blockade effect [1]. As a result of this effect, two atoms near one another cannot simultaneously occupy a Rydberg excited state. It is then straightforward to make a connection between Rydberg atom arrays and dimer models. Each atom can be interpreted as a dimer and the blockade effect generates the dimer constraints.

Beyond the conventional setup, there are also three-level Rydberg atom arrays [2], and dual species platforms [3], which motivate the study of generalized dimer models, the focus of this work. An extra "color" degree of freedom can be associated with each dimer allowing for a connection with the generalized Rydberg atom arrays. Here, we study a simple toy 2-color dimer model on a 1D ladder lattice, including the possibility of Ising-like color interactions between parallel dimers. Using a mix of exact diagonalization and DMRG numerical methods the full phase diagram of this toy model was obtained in terms of the dimer potential V and Ising coupling Jz. The limiting behaviours of the model were compared with the results of perturbation theory. For the ferromagnetic case (Jz=-1) two phases were found, and the model effectively reduces to the conventional (single color) dimer model [4]. For the antiferromagnetic case (Jz=+1) four phases were found. For large negative V the theory can be mapped to the 1D spin-1/2 XXZ model. For large positive V we find non-trivial antiferromagnetic order driven by interactions generated at fourth-order in perturbation theory. In addition, two intermediate phases were discovered. One is likely to be connected to a decoupled plaquette phase, while the other may be continuously connected to the phase at large negative V.

To make this toy model more realistic the next steps will be to include a more realistic van der Waals interaction[1]. An extension to quasi two-dimensional lattices is also planned, to explore the impact of lattice geometry and frustration.

[1] Browaeys, A. & Lahaye, T. Many-body physics with individually controlled Rydberg atoms. Nat. Phys. 16, 132–142 (2020).
[2] Liu, V. S. et al. Supersolidity and Simplex Phases in Spin-1 Rydberg Atom Arrays. Preprint at http://arxiv.org/abs/2407.17554 (2024).
[3] Anand, S. et al. A dual-species Rydberg array. Nat. Phys. 20, 1744–1750 (2024).
[4] Chepiga, N. & Mila, F. DMRG investigation of constrained models: from quantum dimer and quantum loop ladders to hard-boson and Fibonacci anyon chains. SciPost Phys. 6, 033 (2019).

P85

Lattice local integrable regularization of the Sine-Gordon model.

A.A.Ovchinnikov

Institute for Nuclear Research, RAS, Moscow

Abstract

We study the local lattice integrable regularization of the Sine-Gordon model written down in terms of the lattice Bose- operators. We show that the local spin Hamiltonian obtained from the six-vertex model with alternating inhomogeneities in fact leads to the Sine-Gordon in the low-energy limit. We show that the Bethe Ansatz results for this model lead to the correct general relations for different critical exponents of the coupling constant.

1. Introduction

It is interesting and important to study various integrable lattice regularizations of the integrable quantum field theory models in two dimensions. Among them the lattice regularizations connected with the vertex models associated with the trigonometric S-matrix are especially interesting. In particular for the Sine-Gordon (SG) model the so called Light Cone lattice approach was proposed [1]. The main shortcoming of this lattice Hamiltonian is its non-locality. The local version of this Hamiltonian was proposed in [2] and later its Fermionic version was studied in Ref.[3]. However to reduce the Lagrangian to the Lagrangian of the SG- model, the naive Bosonization of the lattice strongly-interacting Fermionic operators was used, so that even the parameter β in terms of the parameters of the six-vertex model was not calculated directly.

In the present Letter we use directly the Bosonic version of the approaches [2],[3] which allows one to deal with the original (bosonic) six-vertex model with the alternating inhomogeneity parameters. We reduce the original lattice problem to the system of two weakly coupled XXZ- spin chains and perform the Bosonization rigorously, which allows us to obtain the Hamiltonian of the SG- model directly without any reference to the Massive Thirring Model. In particular we calculate the constant β - directly from the well defined Bosonization procedure.

We write down the lattice Hamiltonian and the Bethe Ansatz (BA) equations in Section 2. We perform the Bosonization of this Hamiltonian using the well known formulas for the spin operators in the XXZ- spin chain in Section 3. Finally in Section 4 we check the general relations for the critical exponents in the expansion of the physical quantities in the coupling constant.

2. Lattice Hamiltonian.

To write down the Hamiltonian let us first introduce the well known trigonometric S- matrix. It can be represented as a 4×4 matrix of the form

$$S_{12}(t_1 - t_2) = \begin{pmatrix} a & 0 & 0 & 0 \\ 0 & c & b & 0 \\ 0 & b & c & 0 \\ 0 & 0 & 0 & a \end{pmatrix}_{12} (t), \quad t = t_1 - t_2,$$

in the standard notations, where the operator entries are

$$a(t) = \mathrm{sh}(t + i\eta), \quad c(t) = \mathrm{sh}(t), \quad b(t) = \mathrm{sh}(i\eta).$$

This S- matrix obeys the Yang-Baxter equation $S_{12}S_{13}S_{23} = S_{23}S_{13}S_{12}$. The transfer matrix $Z(t)$ acting in the quantum space $(1, \ldots L)$ has the form:

$$Z(t) = Z(t; \xi_1, \ldots \xi_L) = Tr_0 \left(S_{10}S_{20} \ldots S_{L0} \right), \tag{1}$$

where the inhomogeneity parameter ξ_i corresponds to each site i. We choose the alternating values of the parameters $\xi_{2k+1} = 0$, $\xi_{2k} = \theta$, $k \in Z$. The local Hamiltonian corresponding to the SG- model equals

$$H = H(0) + H(\theta) = \frac{\mathrm{sh}(i\eta)}{2} \left(Z^{-1}(0)\dot{Z}(0) + Z^{-1}(\theta)\dot{Z}(\theta) \right), \tag{2}$$

where the dots stand for the derivatives. Substituting the transfer matrix (1) into the equation (2) we obtain the following local Hamiltonian:

$$H = \sum_i \left(S^{-1}_{i+1,i+2}P_{i,i+2}\dot{S}_{i,i+2}S_{i+1,i+2} + \mathrm{sh}(i\eta)S^{-1}_{i+1,i+2}\dot{S}_{i+1,i+2} \right), \tag{3}$$

where the periodic boundary conditions are implied and P_{ij} is the permutation operator. The Hamiltonian (3) is correct both for even and odd i provided the corresponding inhomogeneity parameter is the spectral parameter for each site. We consider the Hamiltonian (3) at large θ and expand it in powers of $e^{-\theta}$. At $e^{-\theta} = 0$ we get two coupled XXZ- spin chains:

$$H_0 = \frac{1}{2}b_1^+ b_3 e^{i2\eta(n_2-1/2)} + h.c. + \Delta n_1 n_3 + \frac{1}{2}b_2^+ b_4 e^{-i2\eta(n_3-1/2)} + h.c. + \Delta n_2 n_4 + \ldots, \Delta = \cos(\eta), \tag{4}$$

where the dots stand for the next terms of the odd and even spin chains and the hard-core bosons b_i^+, b_i, $n_i = b_i^+ b_i$ are introduced to describe the state at the site i in such a way that $n_i = 1$ ($n_i = 0$) corresponds to the spin-up (spin-down) state and b_i^+ (b_i) change the direction of spin. Now we can remove the interaction between two chains performing the transformation

$$\tilde{b}^+_{1x} = b^+_{1x} e^{i2\eta\Delta N_2(x)}, \quad \tilde{b}^+_{2x} = b^+_{2x} e^{-i2\eta\Delta N_1(x)}, \tag{5}$$

where the notations $b^+_{1x} = b^+_{2x-1}$, $b^+_{2x} = b^+_{2x}$, $x = 1, 2, \ldots L/2$ are used and $\Delta N_1(x) = \sum_{i<x}(n_{1i} - 1/2)$, $\Delta N_2(x) = \sum_{i<x}(n_{2i} - 1/2)$. In terms of the new operators $\tilde{b}^+_{1x}$, $\tilde{b}^+_{2x}$ (5) the Hamiltonian (4) takes the form of two independent XXZ- spin chains and one can use the known results for the spin chain to study the Hamiltonian (3). Note that this substitution leads to the kind of the twisted boundary conditions which enter the effective low-energy theory through the well defined quantum number $\Delta N_1 + \Delta N_2 = M - L/2$ which show which boundary conditions for the field $\phi(x) \sim (\phi(L/2) - \phi(0))$ in the Lagrangian (12) below are actually implied (see Section 3). The Bethe Ansatz equations (see eq.(13) below) will take care about these twists automatically. Now we calculate the interaction of the two spin chains of order $e^{-\theta}$. The explicit form of the Hamiltonian (3) is rather complicated. The task is simplified if one is extracting the terms which lead to the relevant interaction $\sim \cos(\beta\phi)$. This operator has the scaling dimension $d = \beta^2/4\pi$ and is relevant at the interval $0 < \beta^2 < 8\pi$ which corresponds exactly to the interval $\eta \in (0; \pi)$ where the spectrum of the single XXZ- spin chain is gapless. For example, the terms which contain the factor $(n_i - 1/2) \sim \partial_x \phi(x)|_{x=i}$, where $\phi(x)$- is some Bose field, lead to the irrelevant operators and can be omitted. Analogously the factors n_i in front the operators b_i^+, b_i can be substituted as $n_i \to 1/2$. The result of the calculations has the form:

$$\hat{V} = 2(\sin(\eta))^2 e^{-\theta} \left(\sum_x (b^+_{1x} b_{2x} + h.c.) + \sum_x (b^+_{1(x+1)} b_{2x} + h.c.) \right). \tag{6}$$

From the point of view of application of the Bosonization procedure the two terms in eq.(6) are very similar and the factor 2 comes from the two different terms in eq.(3). Below we will use (6) to derive the SG model.

3. Bosonization.

We have seen that up to the order $\sim e^{-\theta}$ the Hamiltonian has the form of two coupled XXZ- spin chains. The low-energy effective theory for an XXZ- spin chain is well known: it is the Luttinger liquid (for example, see [4],[5]) with the parameter $\xi = 2(\pi - \eta)/\pi$, which after rescaling of x and t is equivalent to the free massless Bose field. For the two chains we have to such fields. Now we consider the interaction of two chains and seek for the operators which are *relevant* and neglect the operators which are irrelevant in the low-energy limit. To do it we perform the Bosonization of the Hamiltonian (3). The analysis performed in the previous Section shows that the only relevant interaction term has the form (6) which can be further simplified to

$$\hat{V} = hC \sum_x b^+_{1x} b_{2x} + h.c., \tag{7}$$

where now C is some unimportant constant (see eq.(6)) and where the coupling constant $h = e^{-\theta}$. To express this interaction in term of the scalar Bose fields one can use the well known Bosonization formulas for the XXZ- spin chain. We have up to the constant:

$$\tilde{b}^+_{1x} \simeq (-1)^x e^{-i\pi\sqrt{\xi}(\hat{N}_1 - \hat{N}_2)^{(1)}(x)}, \quad \tilde{b}_{2x} \simeq (-1)^x e^{i\pi\sqrt{\xi}(\hat{N}_1 - \hat{N}_2)^{(2)}(x)}, \tag{8}$$

where the operators $\hat{N}^{(i)}_{1,2}(x)$ for the two chains $i = 1, 2$ are expressed through the initial Fermi-operators of the Luttinger model $a_{1,2}(k)$ as

$$\hat{N}_1 - \hat{N}_2 = (1/\sqrt{\xi})(N_1 - N_2), \quad \hat{N}_1 + \hat{N}_2 = \sqrt{\xi}(N_1 + N_2),$$

where ξ- is the standard Luttinger liquid parameteter and

$$N_{1,2}(x) = \frac{i}{L'} \sum_{p \neq 0} \frac{\rho_{1,2}(p)}{p} e^{-ipx}, \quad \rho_{1,2}(p) = \sum_k a^+_{1,2}(k+p) a_{1,2}(k).$$

where $L' = L/2$. The standard Bose fields $\phi_1(x)$, $\phi_2(x)$ are connected with the fields $\hat{N}^{(i)}_{1,2}(x)$ in the following way:

$$(\hat{N}^{(i)}_1 + \hat{N}^{(i)}_2)(x) = (1/\sqrt{\pi})\phi_i(x), \quad (\hat{N}^{(i)}_1 - \hat{N}^{(i)}_2)(x) = (1/\sqrt{\pi})\tilde{\phi}_i(x), \quad i = 1, 2,$$

where the dual fields $\tilde{\phi}_i(x)$ are defined according to the equations

$$\tilde{\phi}_i(x) = \int^x dy \pi_i(y), \quad \pi_i(x) = \dot{\phi}_i(x), \quad i = 1, 2,$$

where $\pi_i(x)$- are the conjugated momenta. Now from the equations (5) one can see that the operator b^+_{1x} take the following form:

$$b^+_{1x} \simeq \exp\left(-i\pi\sqrt{\xi}(\hat{N}_1 - \hat{N}_2)^{(1)}(x) + i(2\pi - 2\eta)\frac{1}{\sqrt{\xi}}(\hat{N}_1 + \hat{N}_2)^{(2)}(x) \right) = e^{i\sqrt{\pi}\sqrt{\xi}(-\tilde{\phi}_1(x) + \phi_2(x))}, \tag{9}$$

where the value $\xi = 2(\pi - \eta)/\pi$ was substituted. Analogously for the operator b_{2x} we obtain the expression

$$b_{2x} \simeq \exp\left(i\pi\sqrt{\xi}(\hat{N}_1 - \hat{N}_2)^{(2)}(x) + i(2\pi - 2\eta)\frac{1}{\sqrt{\xi}}(\hat{N}_1 + \hat{N}_2)^{(1)}(x) \right) = e^{i\sqrt{\pi}\sqrt{\xi}(\tilde{\phi}_2(x) + \phi_1(x))}. \tag{10}$$

Note that in the process of the derivation of (9), (10) we have inserted the additional factors equal to unity of the form $\prod_{i<x} e^{i2\pi n_i} = (-1)^x \prod_{i<x} e^{i2\pi(n_i-1/2)}$ which cancels the factors $(-1)^x$ in the equations (8). Combining the equations (9) and (10) we get for the interaction density the expression:

$$b_{1x}^{+} b_{2x} \simeq e^{i\sqrt{\pi}\sqrt{\xi}(-\tilde{\phi}_1(x)+\tilde{\phi}_2(x)+\phi_1(x)+\phi_2(x))} = e^{i2\sqrt{\pi}\sqrt{\xi}\phi(x)}, \tag{11}$$

where we have introduced two new fields $\phi(x)$ and $\chi(x)$ defined according to the equations

$$\phi(x) = \sqrt{\pi}(\hat{N}_2^{(1)} + \hat{N}_1^{(2)})(x), \quad \chi(x) = \sqrt{\pi}(\hat{N}_1^{(1)} + \hat{N}_2^{(2)})(x),$$

or in terms of the dual fields

$$\phi(x) + \chi(x) = \phi_1(x) + \phi_2(x), \qquad \phi(x) - \chi(x) = -\tilde{\phi}_1(x) + \tilde{\phi}_2(x).$$

In terms of this new fields we get exactly the Lagrangian of the SG- model:

$$L = \frac{1}{2}(\partial_\mu \phi)^2 + \frac{1}{2}(\partial_\mu \chi)^2 + C\mu^\xi h \cos(\beta\phi) \tag{12}$$

with the correct value of the constant $\beta = 2\sqrt{\pi}\sqrt{\xi}$ or $\beta^2 = 8(\pi - \eta)$. In the equation (12) μ is the normalization point and the dimensionless constant C before the term $\cos(\beta\phi)$ was found in [6] but cannot be fixed exactly in the framework of our approach because of the contribution of the operators $e^{\pm i2\eta N^{(1,2)}(x)}$ to the interaction term. The dimension of μ is equal to unity, while the dimension of the coupling constant h is $2 - \xi = 2\eta/\pi$ so that the dimension of the factor $\mu^\xi h$ in eq.(12) is exactly equal to the $(mass)^2$ (see the expression for the physical mass M which by definition has the dimension of mass in Section 4). Note that the constants in front of the operators (9),(10) depend on the normalization point μ in such a way that the lattice correlator does not depends on μ. The auxiliary field $\chi(x)$ decouples from the SG- model. The direct evaluation of the constant β is the main result of the present Letter. One can see from eq.(11) that as it should be, the effective low-energy theory at $M \neq L/2$ depends on the total number of Bosons M in such a way that it leads to a twist boundary conditions for the field $\phi(x)$ of order $\Delta M = (M - L/2)$. In fact one should shift both the dual fields $\tilde{\phi}_{1,2}(x)$ (as can be seen from the Luttinger liquid relation for a system with twist) and the fields $\phi_{1,2}(x)$ in such a way that the boundary conditions for the Sine-Gordon model become $\beta(\phi(L) - \phi(0)) = 2\pi\Delta M$ which corresponds exactly to the boundary conditions for ΔM solitons.

4. Critical behaviour.

Let us calculate the physical mass of the soliton (dressed particle or hole) and the vacuum energy and compare the behaviour of this quantities as a functions of the coupling constant $h = e^{-\theta}$ with the general predictions of the perturbation theory in h. The

Bethe Ansatz equations for the parameters t_α, $\alpha = 1, \dots M$, which determine the common eigenstates of the transfer matrix (1) and the Hamiltonian (2) have the standard form:

$$\left(\frac{\mathrm{sh}(t_\alpha - i\eta/2)}{\mathrm{sh}(t_\alpha + i\eta/2)}\right)^{L/2} \left(\frac{\mathrm{sh}(t_\alpha - \theta - i\eta/2)}{\mathrm{sh}(t_\alpha - \theta + i\eta/2)}\right)^{L/2} = \prod_{\gamma \neq \alpha} \frac{\mathrm{sh}(t_\alpha - t_\gamma - i\eta)}{\mathrm{sh}(t_\alpha - t_\gamma + i\eta)} \tag{13}$$

The solution of the equations (13) is similar to the solution of the corresponding equations for the XXZ- spin chain. In terms of the parameters $t_1, \dots t_M$ the energy and the momentum of the eigenstates of the operator (3) are

$$E = (\sin(\eta)/2) \sum_\alpha (\phi'(t_\alpha) + \phi'(t_\alpha - \theta)), \quad P = \sum_\alpha (\phi(t_\alpha) + \phi(t_\alpha - \theta)), \tag{14}$$

where the function $\phi(t) = (1/i)\ln(-\mathrm{sh}(t - i\eta/2)/\mathrm{sh}(t + i\eta/2))$. For the ground state the roots t_α are real and the corresponding density of roots $R(t)$ equals

$$R(t) = \frac{1}{2}(R_0(t) + R_0(t - \theta)), \quad R_0(t) = \frac{1}{2\eta \mathrm{ch}(\pi t/\eta)}. \tag{15}$$

The calculation of the energy and the momentum of the single hole is quite standard and the result is analogous to that for the XXZ- spin chain:

$$\epsilon(t) = (\sin(\eta)/2)2\pi(R_0(t) + R_0(t - \theta)), \quad p'(t) = 2\pi(R_0(t) + R_0(t - \theta)), \tag{16}$$

where t is the rapidity of the hole and the prime means the derivative over t. From the equation (16) in the limit $\theta \to \infty$ one can easily obtain the relativistic dispersion relation for the soliton:

$$\epsilon(t) = M\mathrm{ch}(\pi t/\eta), \quad p(t) = M\mathrm{sh}(\pi t/\eta), \quad M = 4\sqrt{v}e^{-\pi\theta/2\eta}. \tag{17}$$

The physical mass equals $M = 4\sqrt{v}e^{-\pi\theta/2\eta}$ where $v = (\sin(\eta)/\eta)(\pi/2)$ - is the sound velocity of the single XXZ- spin chain. It appears in eq.(17) because as was shown in the previous section, the relativistic form of the Lagrangian (12) was obtained only after the corresponding rescaling of the space coordinate and time. Thus the physical mass M is calculated. Note that once the physical mass is evaluated it also fix the canonical dimensions of all dimensional parameters in the Lagrangian written down in the continuous space and time (see Section 3). Now the energy of the ground state $E_0(h)$ for the Hamiltonian (3) can be easily calculated. It is given by the following Fourier integral:

$$E_0(h) = \frac{1}{2}\left(\frac{\sin(\eta)}{2}\right) \int d\omega e^{i\omega\theta} \frac{\mathrm{sh}(\omega(\pi - \eta)/2)}{\mathrm{sh}(\omega\pi/2)\mathrm{ch}(\omega\eta/2)}. \tag{18}$$

The vacuum energy (18) is divergent which means that $E_0(h)$ contains the terms of order $\sim h^2$ which is parametrically much larger than the constant term $\sim e^{-\pi\theta/\eta}$, and which should be subtracted to express (18) in terms of the physical mass M. This is equivalent to the evaluation of the contribution of the pole of the factor $1/\mathrm{ch}(\omega\eta/2)$ in the integrand. Thus in terms of the soliton mass M the expression for the energy takes the form (one should take into account that our SG- model is defined at the interval $(0, L/2)$)

$$E_0(h) = \frac{1}{4} M^2 \mathrm{ctg}\left(\frac{\pi^2}{2\eta}\right) \tag{19}$$

in agreement with [7],[8].

Now we confirm our expression for β and the critical behaviour of the mass gap and the ground state energy found from the exact solution. Consider the system of free massless Bose field (H_0) perturbed by the relevant operator $V = h\sum_x V_x$. The perturbation theory in the coupling constant h has the infrared divergences. To take them into account one has to sum up the whole perturbation theory series. In general for the ground and excited states we have the expression of the type

$$E(h) = V\frac{1}{E_0 - H_0}V\left(1 + U + U^2 + \ldots\right), \quad U = \frac{1}{E_0 - H_0}V\frac{1}{E_0 - H_0}V.$$

To estimate the first term we write

$$\langle V\frac{1}{E_0 - H_0}V\rangle \sim h^2\frac{1}{(1/L)}\sum_{i,j}\langle V_i V_j\rangle \simeq L^2 h^2 \sum_x \frac{1}{x^d} \sim h^2 L^{3-2d},$$

where d- is the scaling dimension of the operator V_x. Analogously we obtain $U \sim h^2 L^{4-2d}$. We see that the operator V is relevant provided $d < 2$. Thus the ground state energy has the form $E_0(h) = h^2 L^{3-2d} f(h^2 L^{4-2d})$ with some unknown function $f(y)$. From the condition $E_0 \sim L$ one can find the behaviour of $f(y)$ at large y. Thus we obtain the result:

$$E_0(h) \sim h^{\frac{2}{2-d}}. \tag{20}$$

Analogously for the mass gap we find:

$$M \sim h^{\frac{1}{2-d}}. \tag{21}$$

The equations (20), (21) are known also from the conformal line of arguments [9]. In our case the scaling dimension $d = \beta^2/4\pi = \xi$ and we see that the equations (20), (21) are in agreement with the predictions (17), (19) (in our case $h \sim e^{-\theta}$ and $1/(2-d) = 1/(2-\xi) = \pi/2\eta$). Thus the complete agreement of the perturbation theory estimates with the exact results (17),(19) is established. Note that using the BA results (17),(19) one can predict the correct value of the constant β using the renormalization group arguments [3]. In our case it is interesting that the renormalization group arguments correctly fix the canonical dimension of the interaction term in the Lagrangian (12) (the anomalous dimension of the operator $\cos(\beta\phi)$ equals $\beta^2/4\pi = \xi$).

5. Conclusion.

In the present paper we have shown that the six-vertex model with alternating inhomogeneity parameters can be used to construct the local lattice integrable regularization of the Sine-Gordon model. We have shown *directly* that the system is equivalent to the two weakly coupled XXZ- spin chains and up to the irrelevant operators the interaction gives exactly the Sine-Gordon Lagrangian with the correct value of the parameter β. We compare the soliton mass and the vacuum energy obtained in the framework of the Bethe Ansatz with the general predictions of the perturbation theory for their power-law behaviour in the coupling constant. The direct Bosonization proposed in the present paper can be useful for study of the other integrable models of relativistic quantum field theory.

References

[1] C.Destri, H.J.de Vega, Nucl.Phys.B 290 (1987) 363.

[2] N.Yu.Reshetikhin, H.Saleur, Nucl.Phys.B 419 (1994) 507.

[3] C.Destri, T.Segalini, Nucl.Phys.B 455 (1995) 759.

[4] A.Luther, I.Peschel, Phys.Rev.B9 (1974) 2911.

[5] F.D.M.Haldane, Phys.Rev.Lett.47 (1981) 1840; J.Phys.C 14 (1981) 2585.

[6] Al.B.Zamolodchikov, Int.J.Mod.Phys.A 10 (1995) 1125.

[7] C.Destri, H.J.de Vega, Nucl.Phys.B 358 (1991) 251.

[8] S.Lukyanov, A.Zamolodchikov, Nucl.Phys.B 493 (1997) 571.

[9] A.O.Gogolin, A.A.Nersesyan, A.M.Tsvelik, “Bosonizations and Strongly Correlated Systems”, Cambridge University Press, Cambridge, 1998.

P86

Symmetry protected topological wire in a topological vacuum

Subrata Pachhal[1,*] and Adhip Agarwala[1,†]

[1] *Department of Physics, Indian Institute of Technology Kanpur, Kalyanpur, UP 208016, India*

Symmetry-protected topological phases host gapless modes at their boundary with a featureless environment of the same dimension or a trivial vacuum. In this study [1], we explore their behavior in a higher-dimensional environment, which itself is non-trivial - a *topological vacuum*. In particular, we embed a one-dimensional topological wire within a two-dimensional Chern insulator, allowing the zero-dimensional edge modes of the wire to interplay with the surrounding chiral boundary states created by the environment. In contrast to a trivial vacuum, we show that depending on the nature of low-energy modes, the topology of the environment selectively influences the topological phase transitions of the wire. Interestingly, such selectivity leads to scenarios where the environment trivializes the wire and even induces topological character in an otherwise trivial phase - an example of 'proximity-induced topology'. Using both numerical and analytical approaches, we establish the general framework of such embedding and uncover the role of symmetries in shaping the fate of low-energy theories. Our findings will provide a deeper understanding of heterostructural topological systems, paving the way for their experimental exploration.

[1] S. Pachhal and A. Agarwala, Symmetry protected topological wire in a topological vacuum (2025), arXiv:2504.02745 [cond-mat.mes-hall].

* pachhal@iitk.ac.in

† adhip@iitk.ac.in

P87

Topological finite-size effects in magnetic topological insulators

P88

Magnetic superconductors in Metal-Organic framework hybrids with flat-bands

Sudeshna Pal[1], **Madhuparna Karmakar**[2], **and Rajesh Narayanan**[1]

[1] *Indian Institute of Technology Madras (IITM),* [2] *SRM Institute of Science and Technology.*

e-mail: sudeshnapal.702@gmail.com

Crafting synthetic two-dimensional (2D) functional materials with novel quantum characteristics is a key focus of contemporary condensed matter physics. The adaptability to manipulate both the lattice arrangements and electronic band configurations of these artificially designed materials presents a distinct opportunity to control their properties externally. Among these, the Metal-Organic Framework (MOF) and Covalent Organic Framework (COF) have attracted substantial attention due to their potential applications in organic electronics, spintronics, and topological materials [1]. Characterized by a pair of dispersive bands, a Fermi level-linked flat energy band, and a Dirac cone at the M-point, the Lieb lattice [3] design has been experimentally realized recently in sp^2C-COF and sp^2N-COF [2]. In addition to the topologically nontrivial band structures, this lattice model exhibits flat bands, which could give rise to exotic strongly correlated electron states even for relatively weak interaction strength [3].

Our investigation explores the distinct quantum phases that result from the interplay of the electronic and spin degrees of freedom in the Lieb lattice. Our approach involves coupling an s-wave superconductor to a lattice of localized magnetic spins using Kondo interactions. This interplay creates a "*Magnetic Superconductor*" characterized by the coexistence of magnetic and superconducting orders. Using a comprehensive model that unifies a 2D attractive Hubbard framework with Kondo interactions, we harness the spectroscopic signatures to explore the evolution of the Fermi surface across distinct parameter regimes. By analyzing the ground state phase diagram with precision, we observe the emergence and coexistence of gapped and gapless superconducting states with anti-ferromagnetic and non-collinear magnetic orders, as well as the transition from anti-ferromagnetic to non-collinear magnetic phases. Here we discover that the superconducting order parameter has a non-monotonic dependence on the number density, which is a significant feature of flat band superconductivity. At half filling, the superconductivity is solely contributed by the geometric weight of the quantum metric, as the conventional contribution of dispersive bands become insignificant.

References

[1] Xiaojuan Ni, Huaqing Huang, Chemistry of Materials **10**, 1021 (2022).

[2] Bin Cui, Xingwen Zheng, Nature Communications **11**, 66 (2020).

[3] C. Weeks , M. Franz, Phys. Rev. B. **82**, 085310 (Aug 2010).

P89

Topology, anomaly, and 2d criticality at strong randomness

Yasamin Panahi*[1], Naren Manjunath*[1], Subhayan Sahu*[1], and Chong Wang[1]

*These authors contributed equally to this work.

[1] *Perimeter Institute for Theoretical Physics, Waterloo, Ontario N2L 2Y5, Canada*

We study a two-dimensional free-fermion model that realizes a topological phase transition between a disordered average symmetry-protected topological (ASPT) phase and a trivial phase. In the ASPT phase, the protecting symmetry holds only on average across disorder realizations [1, 2]. By computing a disorder-averaged topological invariant and the minimum spectral gap over samples, we find evidence that this transition is a critical point and identify an anomaly that shapes its physics. Through a strong-disorder renormalization group analysis [3] of a simpler microscopic model that captures the critical behavior of this topological transition, we show that it flows to a strong-randomness fixed point [4] and exhibits distinctive properties in the correlation functions, which are manifestations of the anomaly.

[1] R. Ma and C. Wang, Phys. Rev. X **13**, 031016 (2023).
[2] R. Ma, J.-H. Zhang, Z. Bi, M. Cheng, and C. Wang, Phys. Rev. X **15**, 021062 (2025).
[3] S.-k. Ma, C. Dasgupta, and C.-k. Hu, Phys. Rev. Lett. **43**, 1434 (1979).
[4] D. S. Fisher, Phys. Rev. B **50**, 3799 (1994).

P90

Flux-fractionalization in two dimensional non-bipartite lattices

Jay Pandey[1], **Souvik Kundu**[2], **and Kedar Damle**[1]

[1]*Tata Institute Of Fundamental Research, 1 Homi Bhabha Road, Mumbai 400005, India*
[2]*International Centre for Theoretical Sciences, Tata Institute of Fundamental Research, Bengaluru 560089, India*

We show that the low-temperature (T) behavior of a class of anisotropic spin-1 antiferromagnets on corner-sharing fully-frustrated squares forming a kagome lattice (corner-sharing fully-frustrated hexagons forming a triangular lattice) at a field-induced 1/2-magnetization (2/3-magnetization) plateau can be described by a model of fully packed dimers and loops on the kagome (triangular) lattice, with a temperature-dependent relative fugacity $w(T)$ for the dimers. The constraint is that each site is touched either by a nontrivial loop or a dimer. We study this model as a function of the relative fugacity of dimers w, which bridges between two well-studied limits of this model: The fully-packed $O(1)$ loop model (at $w = 0$) and the fully-packed dimer model (at $w = \infty$). Our findings reveal a continuous phase transition between two disordered phases at a nonzero finite w on both lattices, with distinct characteristics of the two phases. The $w > w_c$ phase has short loops and dimers, whereas the $w < w_c$ phase is dominated by large loops with the loop size distribution governed by that of the six-vertex model. It being a non-bipartite lattice, fluxes are not well defined, but one can still define winding numbers, $\phi(x), \phi(y)$, along the two principal directions. They are equal to the sum of the number of dimers and trivial loops crossing it with a weight of 1(1/2) given to dimers(non trivial loops).

The phase transition at w_c is characterized by an emergent winding number-fractionalization mechanism: Fractional winding numbers existing in the $w < w_c$ phase, while they are bound to only integer values in the $w > w_c$ phase. Surprisingly the transition is very similar to the flux-fractionalization transition hosted by its bipartite counterparts in spite of the absence of any well defined fluxes in the non-bipartite model. It is a second order phase transition between two short range correlated phases, purely topological in character.

P91

Reallocation of Nonlocal Entanglement in Incommensurate Cold Atom Arrays

Jemin Park[1], **Junmo Jeon**[1], **and Sungbin Lee**[1]

[1]*Korea Advanced Institute of Science and Technology*

Cold atom arrays in optical lattices offer a highly tunable platform for exploring complex quantum phenomena that are difficult to realize in conventional materials. Here, we investigate the emergence of controllable longrange quantum correlations in a simulated twisted bilayer structure with fermionic cold atoms. By exploiting the incommensurate nature of the twisted bilayer, we observe a significant enhancement of long-range susceptibility, suggesting the formation of stable entangled states between spatially distant localized spins. We further show that the tunability of the interlayer coupling in terms of driving fields enables us to manipulate these entangled states without deformation of lattice structure and extra doping. Our findings provide a pathway for overcoming challenges in establishing strong correlations across distant sites, highlighting the potential of optical lattices as a versatile platform for advanced quantum technologies.

P92

Physica A 582 (2021) 126239

Contents lists available at ScienceDirect

Physica A

journal homepage: www.elsevier.com/locate/physa

Thermal coherence of the Heisenberg model with Dzyaloshinsky–Moriya interactions in an inhomogenous external field

Manikandan Parthasarathy [a], Segar Jambulingam [a], Tim Byrnes [b,c,d,e,f], Chandrashekar Radhakrishnan [g,b,d,*]

[a] Department of Physics, Ramakrishna Mission Vivekananda College, Mylapore, Chennai 600 004, India
[b] New York University Shanghai, 1555 Century Avenue, Pudong, Shanghai 200122, China
[c] State Key Laboratory of Precision Spectroscopy, School of Physical and Material Sciences, East China Normal University, Shanghai 200062, China
[d] NYU-ECNU Institute of Physics at NYU Shanghai, 3663 Zhongshan Road North, Shanghai, 200062, China
[e] National Institute of Informatics, 2-1-2 Hitotsubashi, Chiyoda-ku, Tokyo 101-8430, Japan
[f] Department of Physics, New York University, New York, NY 100003, USA
[g] Laboratoire Systèmes Complexes et Information Quantify, ESSIE Group, 9 Rue Vèsale, Paris 75005, France

ARTICLE INFO

Article history:
Received 16 January 2021
Available online 4 July 2021

Keywords:
Anisotropic spin model
DM interaction
Quantum coherence

ABSTRACT

The quantum coherence of the two-site XYZ model with Dzyaloshinsky–Moriya (DM) interactions in an external inhomogenous magnetic field is studied. The DM interaction, the magnetic field and the measurement basis can be along different directions, and we examine the quantum coherence at finite temperature. With respect to the spin–spin interaction parameter, we find that the quantum coherence decreases when the direction of measurement basis is the same as that of the spin–spin interaction. When the spin–lattice interaction is varied, the coherence always increases irrespective of the relation between its direction and the measurement basis. Similar analysis of quantum coherence based on the variation of the external inhomogenous magnetic field is also carried out, where we find that the coherence decreases when the direction of the measurement basis is the same as that of the external field.

1. Introduction

Quantum coherence has been a central concept in the theory of quantum mechanics since its earliest days. In the context of quantum optics, coherence was investigated using phase space distributions and higher order correlation functions [1,2]. It was only recently that a rigorous quantum information theoretic framework for measuring coherence was developed, in the seminal paper by Baumgratz, Cramer and Plenio [3]. The work introduced a set of axioms which are necessary for a mathematical function to be a proper quantifier of quantum coherence. In Ref. [3], two measures of quantum coherence were introduced based on these axioms, namely the relative entropy measure of coherence and the ℓ_1-norm based quantum coherence. The fundamental properties of quantum coherence have been investigated [4–12] and also their applications in different quantum phenomena [13–17] have been studied. These investigations also gave rise to the resource theory framework of quantum coherence [12,18–24].

* Corresponding author at: Laboratoire Systèmes Complexes et Information Quantify, ESSIE Group, 9 Rue Vèsale, Paris 75005, France.
E-mail address: chandrashekar10@gmail.com (C. Radhakrishnan).

https://doi.org/10.1016/j.physa.2021.126239

Quantum coherence has been investigated with regards to search algorithms [13,14], quantum thermodynamics [17,25] and quantum metrology [16]. Previous studies have established applications of quantum coherence in quantum information processing tasks like quantum dense coding and teleportation [26]. Another important application of quantum coherence is in the characterization of quantum states. Multipartite systems have a large number of degrees of freedom, and it is of interest to understand what type of coherences a given state possesses. Such a scheme was introduced in Ref. [24], where coherence could be subdivided into its constituent parts. Quantum simulation [27] is a prime example of where this can be applied, since the naturally arising states of a condensed matter system can show strikingly different properties depending upon the physical parameters driving phase transitions in the system. In the field of condensed matter physics, the measurement and properties of quantum coherence has been studied in various models [28–31]. Heisenberg spin models [32–37] are one of the important class of models in which coherence has been investigated [38–41], where one of the main themes has been the investigation of quantum phase transition [39–42]. In the Heisenberg XYZ model, the spins have a direct interaction between nearby sites. In addition, they can also have a spin–lattice interaction generally referred to as the Dzyaloshinsky–Moriya (DM) interaction [43,44]. Spins are usually aligned parallel or anti-parallel to each other depending on whether it is in the ferromagnetic phase or antiferromagnetic phase. Due to the spin–lattice interaction the spins are tilted at an angle to the parallel, a feature known as spin-canting. This spin-canting usually leads to weak ferromagnetic behavior even in an antiferromagnetic system. In addition to these inherent properties, it is also possible to apply an external magnetic field to the spin system to control and modify its quantum properties.

A minimal example of the DM model is the two-site model which has been studied to understand the overall dependence of quantities such as entanglement [45–50], quantum discord [51–53], and coherence [54] as a function of the various parameters of the system. In Ref. [54], a detailed investigation of quantum coherence in two-spin models were carried out. In this paper, we extend the investigations carried out in Ref. [54] and investigate two-spin models with DM interactions in the presence of an external field. A detailed analysis of the dependence of the quantum coherence on various parameters such as the spin–spin interaction, the spin–orbit interaction, DM interaction, and external magnetic field is carried out. As quantum coherence is a basis dependent quantity, in our work we choose different orientations of the DM interaction parameter and the external fields keeping the measurement direction in the σ_z basis for all cases. This will help us to understand the basis-dependent nature of coherence with respect to the internal parameters such as spin–spin interaction, as well as the DM interaction parameter. Finally, the relation between quantum coherence and the external driving forces such as the homogeneous component and the inhomogenous component of the magnetic field will be explored.

The article is structured as follows: In Section 3 we discuss the quantum coherence dependence in the two-spin XYZ model with DM interactions and external field in the same direction. The features of quantum coherence where the two-site XYZ model with the DM interaction and external field in different directions is discussed in Section 4. Section 5 gives the simultaneous variation of the quantum coherence with spin–spin interaction and any one of the other parameters such as DM interaction, homogeneous component, or the inhomogenous component of the external field. Finally, we present our conclusions in Section 6.

2. The Heisenberg model with DM interaction and the coherence measure

The Heisenberg spin model consists of a collection of interacting spins arranged periodically on a lattice. The Hamiltonian of the Heisenberg spin chain is written as

$$H = \sum_n J_x \sigma_n^x \sigma_{n+1}^x + J_y \sigma_n^y \sigma_{n+1}^y + J_z \sigma_n^z \sigma_{n+1}^z, \tag{1}$$

where $\sigma_n^{x,y,z}$ are the Pauli spin matrices at the site n and $J_{x,y,z}$ are the spin–spin interaction terms in the x, y and z directions. For $J_x \neq J_y \neq J_z$, the spin model is referred to as XYZ model. The model is antiferromagnetic when $J_i > 0$ $(i = x, y, x)$ and ferromagnetic for $J_i < 0$. Along with the spin–spin interaction we may also have a spin–lattice interaction which are known as the Dzyaloshinsky–Moriya (DM) interaction. The Hamiltonian of the XYZ spin chain with the DM interaction is

$$H = \sum_n J_x \sigma_n^x \sigma_{n+1}^x + J_y \sigma_n^y \sigma_{n+1}^y + J_z \sigma_n^z \sigma_{n+1}^z + \vec{D}.(\vec{\sigma}_n \times \vec{\sigma}_{n+1}) \tag{2}$$

The antisymmetric spin–lattice interaction is accounted for by the DM interaction coefficient $\vec{D}$.

In our work we further consider an inhomogenous external magnetic field. The Hamiltonian of a two-spin system with DM interaction in an external inhomogenous field is

$$H = J_x \sigma_1^x \sigma_2^x + J_y \sigma_1^y \sigma_2^y + J_z \sigma_1^z \sigma_2^z + \vec{D} \cdot (\vec{\sigma}_1 \times \vec{\sigma}_2) + (\vec{B} + \vec{b}) \cdot \vec{\sigma}_1^j + (\vec{B} - \vec{b}) \cdot \vec{\sigma}_2^j. \tag{3}$$

This field can be written as two fields of the form $\vec{B} + \vec{b}$ acting on the first qubit and the field $\vec{B} - \vec{b}$ acting on the second qubit, where B is the homogeneous and b is the inhomogenous component of the external magnetic field.

From the Hamiltonian of this model, the quantum properties can be studied by examining its eigenstates. In our work, we investigate the quantum coherence of the system at finite (non-zero) temperature. Quantum coherence is measured as the distance between the density matrix ρ and the decohered density matrix ρ_d. The decohered density matrix is defined according to the matrix elements

$$\langle\sigma_1\sigma_2|\rho_d|\sigma_1'\sigma_2'\rangle = \langle\sigma_1\sigma_2|\rho|\sigma_1'\sigma_2'\rangle\delta_{\sigma_1,\sigma_1'}\delta_{\sigma_2,\sigma_2'}. \tag{4}$$

In Ref. [3], two different measures of coherence namely the relative entropy measure belonging to the entropic class and the ℓ_1-norm of coherence which is a geometric measure were introduced. Another measure based on the quantum version of the Jensen–Shannon divergence [55–57] was introduced in Ref. [24]

$$\mathcal{D}(\rho,\sigma) \equiv \sqrt{J(\rho,\sigma)} = \sqrt{S\left(\frac{\rho+\sigma}{2}\right) - \frac{S(\rho)}{2} - \frac{S(\sigma)}{2}}. \tag{5}$$

Here ρ, σ are arbitrary density matrices and $S = -\mathrm{Tr}\rho\log\rho$ is the von Neumann entropy. This measure has the advantage that it has both geometric and entropic properties and is also a metric satisfying triangle inequality. The coherence is then defined in our case as

$$\mathcal{C}(\rho) = \mathcal{D}(\rho, \rho_d). \tag{6}$$

The coherence of the two-spin XYZ model in Eq. (3) at finite temperature is discussed in the rest of the paper. Since quantum coherence is a basis-dependent quantity we examine the spin model in two different cases namely: (*i*) when the control parameters and measurement basis are in the same direction; (*ii*) when the control parameters like DM interaction and the external field are orthogonal to the measurement basis.

3. DM interaction and the external magnetic field along the same direction

3.1. $\vec{D} \propto \vec{x}, \vec{B} \propto \vec{x}$ case

For the case where both the DM interaction and the external magnetic field are in the x direction, the Hamiltonian reads

$$H = J_x\sigma_1^x\sigma_2^x + J_y\sigma_1^y\sigma_2^y + J_z\sigma_1^z\sigma_2^z + D_x(\sigma_1^y\sigma_2^z - \sigma_1^z\sigma_2^y) + (B_x + b_x)\sigma_1^x + (B_x - b_x)\sigma_2^x, \tag{7}$$

where D_x is the DM interaction in the x-direction, and B_x is the average magnetic field and b_x is the inhomogenous magnetic field in the x-direction. The matrix representation of the Hamiltonian in the σ_z-basis is

$$H = \begin{pmatrix} J_z & G_2 & G_3 & J_- \\ G_4 & -J_z & J_+ & G_1 \\ G_1 & J_+ & -J_z & G_4 \\ J_- & G_3 & G_2 & J_z \end{pmatrix}, \tag{8}$$

where $G_{1,2} = iD_x + B_x \pm b_x$, $G_{3,4} = G_{1,2}^*$ and $J_\pm = J_x \pm J_y$. The eigenvalues of the Hamiltonian are

$$E_{1,2} = J_x \pm \omega_1, \qquad E_{3,4} = -J_x \pm \omega_2, \tag{9}$$

and their corresponding eigenvectors are

$$|\psi_{1,2}\rangle = \frac{1}{\sqrt{2}}(\sin\varphi_{1,2}|00\rangle + \cos\varphi_{1,2}|01\rangle + \cos\varphi_{1,2}|10\rangle + \sin\varphi_{1,2}|11\rangle) \tag{10}$$

$$|\psi_{3,4}\rangle = \frac{1}{\sqrt{2}}(\sin\varphi_{3,4}|00\rangle + \chi\cos\varphi_{3,4}|01\rangle - \chi\cos\varphi_{3,4}|10\rangle - \sin\varphi_{3,4}|11\rangle) \tag{11}$$

where the various factors used are

$$\chi = \frac{-iD_x - b_x}{\sqrt{b_x^2 + D_x^2}}, \quad \omega_1 = \sqrt{4B_x^2 + (J_y - J_z)^2}, \quad \omega_2 = \sqrt{4b_x^2 + 4D_x^2 + (J_y + J_z)^2}$$
$$\varphi_{1,2} = \arctan\left(\frac{2B_x}{J_y - J_z \pm \omega_1}\right), \quad \varphi_{3,4} = \arctan\left(\frac{2\sqrt{b_x^2 + D_x^2}}{-J_y - J_z \pm \omega_2}\right). \tag{12}$$

The state of the two-spin spin system at thermal equilibrium is given by the thermal density matrix $\rho(T) = \exp(-\beta H)/Z$ where $Z = \mathrm{Tr}[\exp(-\beta H)]$ is the partition function of the system and $\beta = 1/k_BT$, and k_B and T are the Boltzmann constant and temperature respectively. For the sake of convenience we assume $k_B = 1$ throughout our discussion. The matrix form of the thermal density matrix in the σ_z-basis is

$$\rho(T) = \begin{pmatrix} u_1 & q_1^* & q_2^* & u_2 \\ q_1 & v_1 & v_2 & q_2 \\ q_2 & v_2 & v_1 & q_1 \\ u_2 & q_2^* & q_1^* & u_1 \end{pmatrix}. \tag{13}$$

The elements of the thermal density matrix (13) are

$$u_{1,2} = \frac{1}{2Z}\left[e^{-\frac{J_x+\omega_1}{T}}\sin^2\varphi_1 + e^{-\frac{J_x-\omega_1}{T}}\sin^2\varphi_2 \pm e^{\frac{J_x-\omega_2}{T}}\sin^2\varphi_3 \pm e^{\frac{J_x+\omega_2}{T}}\sin^2\varphi_4\right], \tag{14}$$

$$v_{1,2} = \frac{1}{2Z}\left[e^{-\frac{J_x+\omega_1}{T}}\cos^2\varphi_1 + e^{-\frac{J_x-\omega_1}{T}}\cos^2\varphi_2 \pm e^{\frac{J_x-\omega_2}{T}}\cos^2\varphi_3 \pm e^{\frac{J_x+\omega_2}{T}}\cos^2\varphi_4\right], \tag{15}$$

$$q_{1,2} = \frac{1}{2Z}\Big[e^{-\frac{J_x+\omega_1}{T}}\sin\varphi_1\cos\varphi_1 + e^{-\frac{J_x-\omega_1}{T}}\sin\varphi_2\cos\varphi_2 \pm e^{\frac{J_x-\omega_2}{T}}\chi\sin\varphi_3\cos\varphi_3 \pm e^{\frac{J_x+\omega_2}{T}}\chi\sin\varphi_4\cos\varphi_4\Big]. \tag{16}$$

where the partition function is

$$Z = 2\left[e^{-\frac{J_x}{T}}\cosh\left(\frac{\omega_1}{T}\right) + e^{\frac{J_x}{T}}\cosh\left(\frac{\omega_2}{T}\right)\right]. \tag{17}$$

From the density matrix $\rho(T)$, we can write down the decohered density matrix ρ_d using which we can measure coherence introduced through Eq. (6).

The behavior of quantum coherence is shown in Fig. 1. Since quantum coherence is a basis dependent quantity, the choice of measurement basis plays an important role. In the Hamiltonian of Eq. (7), the DM interaction and the field are in the x-direction, and the measurement is carried out in the z-direction. This behavior of coherence is very similar to the entanglement results reported in Ref. [47]. In Fig. 1(a) the variation of coherence with temperature is shown and we find that coherence decreases with temperature. This can be explained by the thermal fluctuations inducing decoherence in the quantum system, thereby decreasing coherence. The rate of decrease of coherence is lower for higher values of the DM interaction parameter. This is because the DM interaction creates an extra spin–lattice coupling apart from the existing spin–spin coupling. This additional spin lattice coupling gives rise to additional coherence in the quantum system. The variation of quantum coherence with the DM interaction parameter is shown in Fig. 1(b) for different values of temperature. We find that for lower values of temperature ($T = 0.5, T = 1.0$), the coherence decreases initially, reaches a minimum value and then increases to reach a saturation value. Initially at $D_x = 0$, the spin–spin interaction is dominant and when it is increased the spin–lattice interaction is slowly introduced. The initial decrease in the spin–lattice interaction might be due to the competing effects of the spin–spin and spin–lattice interaction. The increase later on can be attributed to the co-operation between the spin–spin and spin–lattice interaction. At higher values of temperature ($T = 1.5$), the coherence increases gradually to a saturation value.

The variation of the quantum coherence is investigated as a function of the external magnetic field in Fig. 1(c) and 1(d). We now examine the role played by the external inhomogenous field. In Fig. 1(c) we show the variation of quantum coherence with the field B_x and we find that for the lower values of temperature, the coherence initially decreases and reaches a minimum value and then increases to attain a saturation value. For the higher values of temperature, the coherence increases with the homogeneous field B_x. The overall behavior of the quantum coherence with the inhomogenous field b_x resembles the variation of coherence with the field B_x as we can see from a comparison between Figs. 1(c) and 1(d). On comparison with the earlier works Ref. [47] we find that quantum coherence exhibits behavior very similar to entanglement. From concurrence measurements one can see that entanglement also increases with the DM interaction. The main reason is that the entire coherence comes from the two-spin correlation in a manner similar to entanglement.

3.2. $\vec{D} \propto \vec{z}, \vec{B} \propto \vec{z}$ case

For the case where the DM interaction and the external magnetic field along the z-direction, the Hamiltonian reads

$$H = J_x\sigma_1^x\sigma_2^x + J_y\sigma_1^y\sigma_2^y + J_z\sigma_1^z\sigma_2^z + D_z(\sigma_1^x\sigma_2^y - \sigma_1^y\sigma_2^x) + (B_z + b_z)\sigma_1^z + (B_z - b_z)\sigma_2^z. \tag{18}$$

Here, B_z is the average external magnetic field in the z direction and b_z is the degree of inhomogeneity of the field in the z-direction. In the standard measurement basis (σ_z basis) the Hamiltonian can be written in matrix form as

$$H = \begin{pmatrix} 2B_z + J_z & 0 & 0 & J_x - J_y \\ 0 & 2b_z - J_z & 2iD_z + J_x + J_y & 0 \\ 0 & -2iD_z + J_x + J_y & -2b_z - J_z & 0 \\ J_x - J_y & 0 & 0 & -2B_z + J_z \end{pmatrix}. \tag{19}$$

The eigenvalues and eigenvectors corresponding to the Hamiltonian are

$$E_{1,2} = J_z + \omega_1 \qquad |\psi_{1,2}\rangle = \sin\theta_{1,2}|00\rangle + \cos\theta_{1,2}|11\rangle, \tag{20}$$

$$E_{3,4} = -J_z + \omega_2 \qquad |\psi_{3,4}\rangle = \sin\theta_{3,4}|01\rangle + \chi\cos\theta_{3,4}|10\rangle, \tag{21}$$

where the factors ω_1 and ω_2 are

$$\omega_1 = \sqrt{4B_z^2 + (J_x - J_y)^2}, \qquad \omega_2 = \sqrt{4b_z^2 + 4D_z^2 + (J_x + J_y)^2}. \tag{22}$$

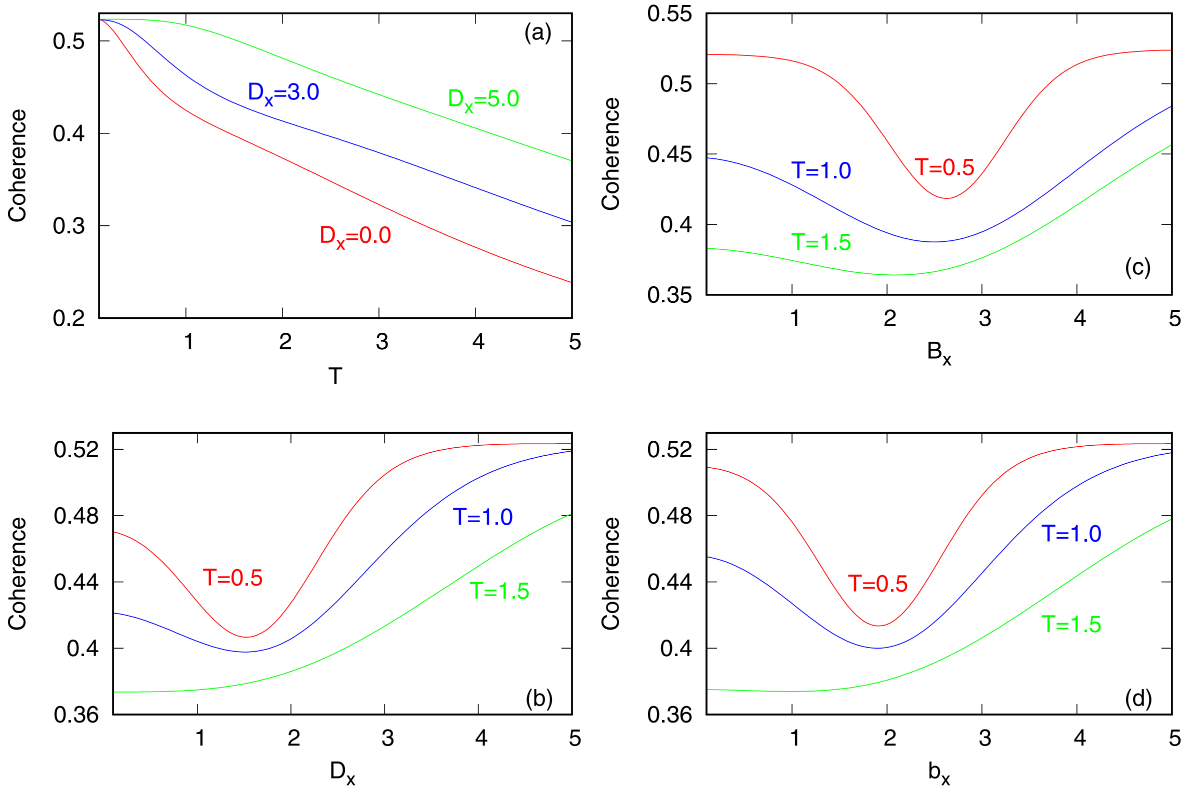

Fig. 1. Quantum coherence measurement in σ_z basis in the XYZ model with DM interactions in the x-direction and the external magnetic field in the x-direction. (a) Quantum coherence versus temperature T for different D_x, for $B_x = 3.0$, $b_x = 1.5$, $J_x = 0.8$, $J_y = 0.5$ and $J_z = 0.2$. (b) Quantum coherence versus D_x for different temperatures T, for $B_x = 3.0$, $b_x = 1.5$, $J_x = 0.8$, $J_y = 0.5$ and $J_z = 0.2$. (c) Quantum coherence versus B_x for different temperatures T, for $D_x = 1.0$, $b_x = 1.5$, $J_x = 0.8$, $J_y = 0.5$ and $J_z = 0.2$. (d) Quantum coherence versus b_x for different temperatures T, for $D_x = 1.0$, $B_x = 3.0$, $J_x = 0.8$, $J_y = 0.5$ and $J_z = 0.2$.

In the expression for the eigenvectors the parameters used are

$$\theta_{1,2} = \arctan\left(\frac{J_x - J_y}{\pm\omega_1 - 2B_z}\right), \qquad \theta_{3,4} = \arctan\left(\frac{\sqrt{(J_x + J_y)^2 + D_z^2}}{\pm\omega_2 - 2b_z}\right) \tag{23}$$

and $\chi = \frac{J_x + J_y - 2iD_z}{\sqrt{(J_x+J_y)^2 + 4D_z^2}}$. The thermal density matrix $\rho(T)$ in the σ_z-basis is

$$\rho(T) = \frac{1}{2Z}\begin{pmatrix} m_1 & 0 & 0 & m_3 \\ 0 & n_1 & n_3 & 0 \\ 0 & n_4 & n_2 & 0 \\ m_3 & 0 & 0 & m_2 \end{pmatrix}. \tag{24}$$

The matrix elements of the thermal density matrix (24) are

$$m_{1,2} = \mp e^{\frac{-J_z}{T}}\left[\cosh\left(\frac{\mu}{T}\right) \mp \frac{B_z}{\mu}\sinh\left(\frac{\mu}{T}\right)\right] \tag{25}$$

$$m_3 = -e^{\frac{-J_z}{T}}\left[\frac{J_-}{\mu}\sinh\left(\frac{\mu}{T}\right)\right] \tag{26}$$

$$n_{1,2} = e^{\frac{J_z}{T}}\left[\cosh\left(\frac{\nu}{T}\right) \mp \frac{b_z}{\nu}\sinh\left(\frac{\nu}{T}\right)\right] \tag{27}$$

$$n_{3,4} = -e^{\frac{-J_z}{T}}\left[\frac{J_+ \pm iD_z}{\nu}\sinh\left(\frac{\nu}{T}\right)\right] \tag{28}$$

where the partition function

$$Z = 2\left[e^{-\frac{J_z}{T}}\cosh\left(\frac{\mu}{T}\right) + e^{\frac{J_z}{T}}\cosh\left(\frac{\nu}{T}\right)\right]. \tag{29}$$

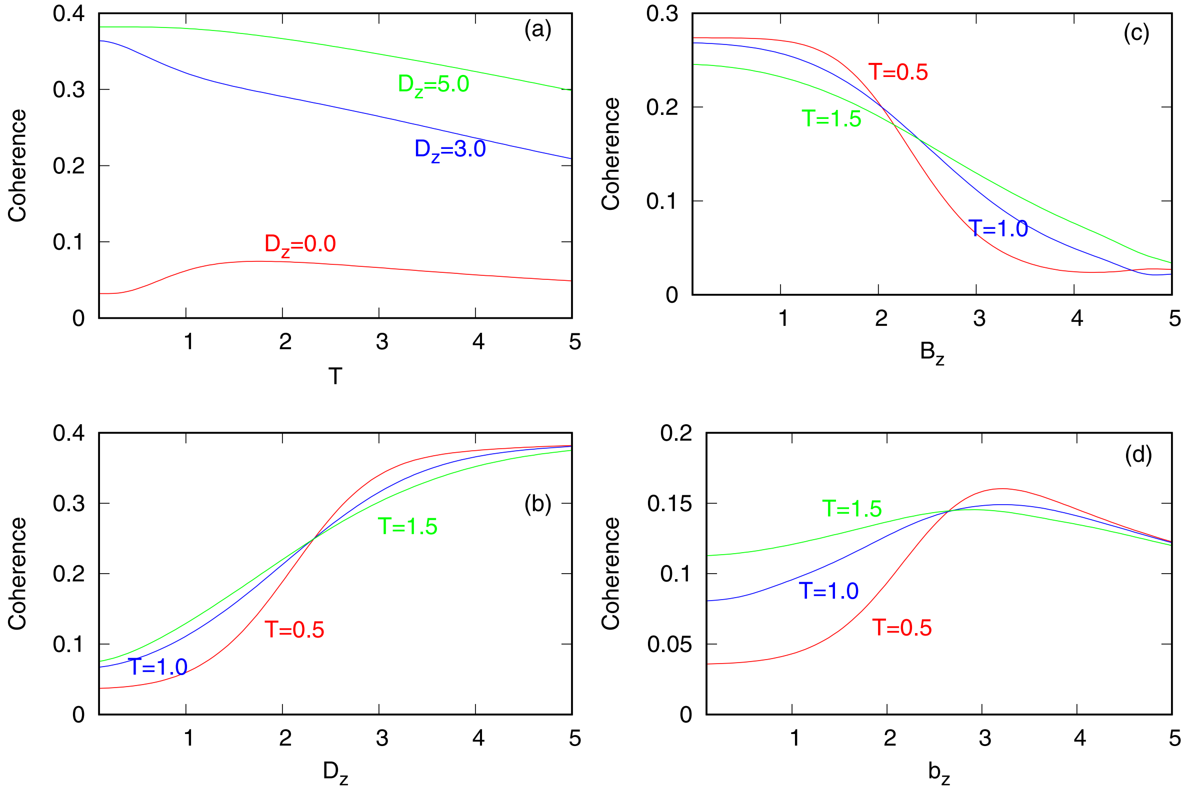

Fig. 2. Measurement of coherence in the σ_z basis in the two-spin XYZ model with DM interactions in the z-direction and the external magnetic field in the z-direction. (a) Quantum coherence versus temperature T for different D_z, for $B_z = 3.0$, $b_z = 1.5$, $J_x = 0.8$, $J_y = 0.5$ and $J_z = 0.2$. (b) Quantum coherence versus D_z for different temperatures T, for $B_z = 3.0$, $b_z = 1.5$, $J_x = 0.8$, $J_y = 0.5$ and $J_z = 0.2$. (c) Quantum coherence versus B_z for different temperatures T, for $D_z = 1.0$, $b_z = 1.5$, $J_x = 0.8$, $J_y = 0.5$ and $J_z = 0.2$. (d) Quantum coherence versus b_z for different temperatures T, for $D_z = 1.0$, $B_z = 3.0$, $J_x = 0.8$, $J_y = 0.5$ and $J_z = 0.2$.

The variation of quantum coherence as a function of the DM interaction and external field in the σ_z basis is described through the plots in Fig. 2. The change of coherence with temperature is shown in Fig. 2(a) for different values of the DM interaction parameter. For larger values of the DM interaction parameter ($D_x = 3.0, 5.0$), we find that the quantum coherence decreases with temperature. This is in line with the observation in Ref. [47] and the well known effect of thermal decoherence on quantum systems. For $D_z = 0$, the coherence decreases but there is an initial increase. Through Fig. 2(b) we show the evolution of coherence with DM interaction. Quantum coherence increases with D_z and this occurs for all values of temperature. The influence of magnetic field on quantum coherence is given in Figs. 2(c) and 2(d) for the homogeneous part and the inhomogenous part of the field respectively. In Fig. 2(c) we see that the quantum coherence decreases with the average homogeneous magnetic field B_z. From Fig. 2(d) we see that the coherence initially increases with the homogeneous field b_z, attains a maximum and then decreases to a saturation value.

In summary, in this section we considered the situation where the DM interaction and the external magnetic field are along the same direction. In both the cases the quantum coherence shows a decrease with temperature. When we look into the variation of quantum coherence with the DM interaction parameter, the average homogeneous magnetic field B, and the inhomogenous magnetic field b we find that the measurement basis has a definite outcome on the value of quantum coherence. Hence the qualitative behavior of quantum coherence is quite different for the situations described in Sections 3.1 and 3.2 and this is a unique feature of quantum coherence which does not have an analog in entanglement measurements.

4. DM interaction and the external field in different directions

In this section we consider the two-site XYZ model in which the spin–lattice interaction and the external field are in different directions. Under these conditions we have three different cases as follows: (*i*) The DM interaction is along the measurement basis; (*ii*) the external inhomogenous field is along the measurement basis and; (*iii*) both DM interaction and the external field are in different directions and orthogonal to the measurement basis. The coherence of all these cases are examined in the discussion below.

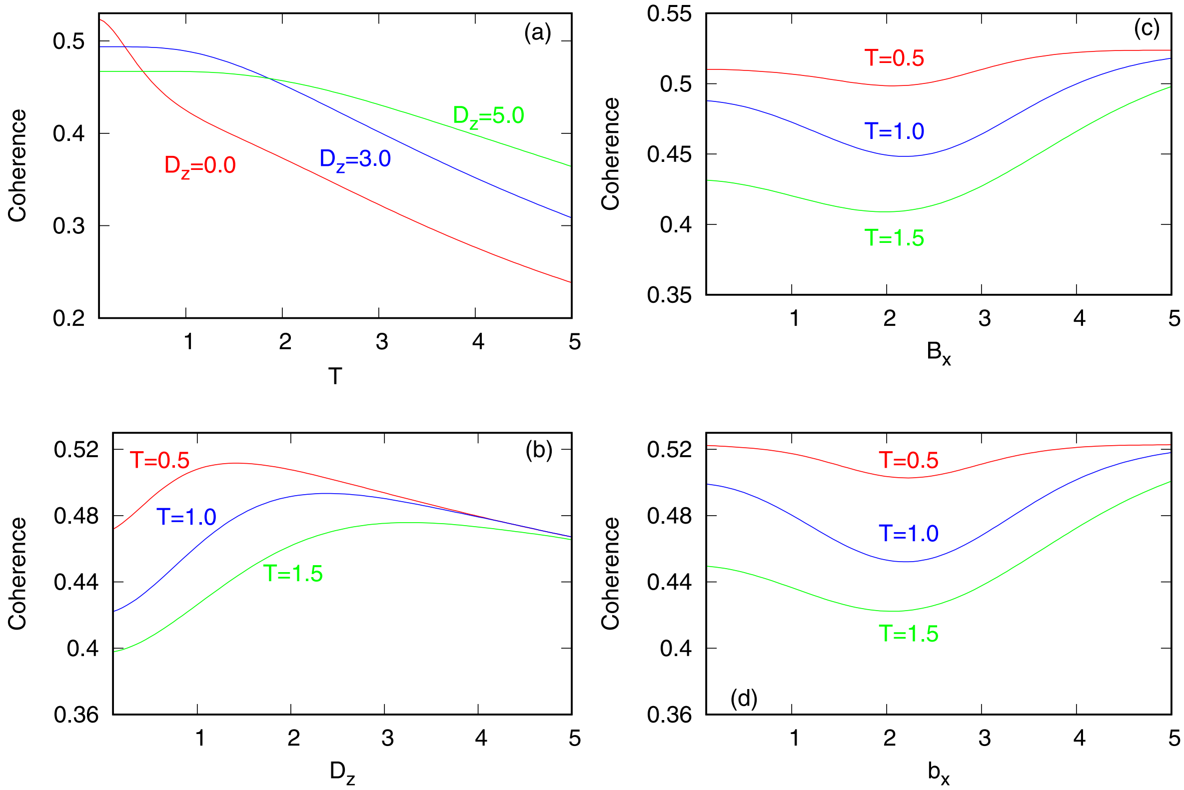

Fig. 3. The change in coherence measured in the σ_z basis for the two-site XYZ model with DM interactions in the z-direction and the external field in the x-direction. (a) Quantum coherence versus temperature T for different D_z for $B_x = 3$, $b_x = 1.5$, $J_x = 0.8$, $J_y = 0.5$ and $J_z = 0.2$. (b) Quantum coherence versus D_z, for different temperatures T, for $B_x = 3.0$, $b_x = 1.5$, $J_x = 0.8$, $J_y = 0.5$ and $J_z = 0.2$. (c) Quantum coherence versus B_x for different temperatures T, for $D_z = 1.0$, $b_x = 1.5$, $J_x = 0.8$, $J_y = 0.5$ and $J_z = 0.2$. (d) Quantum coherence versus b_x for different temperatures T, for $D_z = 1.0$, $B_x = 3.0$, $J_x = 0.8$, $J_y = 0.5$ and $J_z = 0.2$.

4.1. $\vec{D} \propto \vec{z}, \vec{B} \propto \vec{x}$ case

For the case with the DM interaction along the z-axis and the inhomogenous magnetic field along the x-axis, we have the Hamiltonian

$$H = J_x\sigma_1^x\sigma_2^x + J_y\sigma_1^y\sigma_2^y + J_z\sigma_1^z\sigma_2^z + D_z(\sigma_1^x\sigma_2^y - \sigma_1^y\sigma_2^x) + (B_x + b_x)\sigma_1^x + (B_x - b_x)\sigma_2^x. \tag{30}$$

In the σ^z-basis the matrix form of the Hamiltonian is

$$H = \begin{pmatrix} J_z & -b_x + B_x & b_x + B_x & J_x - J_y \\ -b_x + B_x & -J_z & 2iD_z + J_x + J_y & b_x + B_x \\ b_x + B_x & -2iD_z + J_x + J_y & -J_z & -b_x + B_x \\ J_x - J_y & b_x + B_x & -b_x + B_x & J_z \end{pmatrix}. \tag{31}$$

From the Hamiltonian, one can calculate the density matrix $\rho(T)$ at thermal equilibrium. Using the thermal density matrix we can write down the diagonal form of the density matrix ρ_d and using Eq. (6) we can calculate coherence in the system.

For this model, the variation of quantum coherence with the different parameters is shown in Fig. 3 with the measurement being carried out in the σ_z basis. Thermal decoherence causes a loss of coherence due to increase in temperature and this is being observed in Fig. 3(a) for different strengths of the DM interaction. With respect to the DM interaction parameter, the coherence increases initially to attain a maximum value and then decreases. This behavior is shown in Fig. 3(b) for different temperatures. When the average homogeneous magnetic field B_z is varied, the coherence decreases slightly to reach the minimum value and then increases back to a saturation value as shown in Fig. 3(c). A similar behavior is observed for the variation of the inhomogenous component of the field b_z as seen in Fig. 3(d).

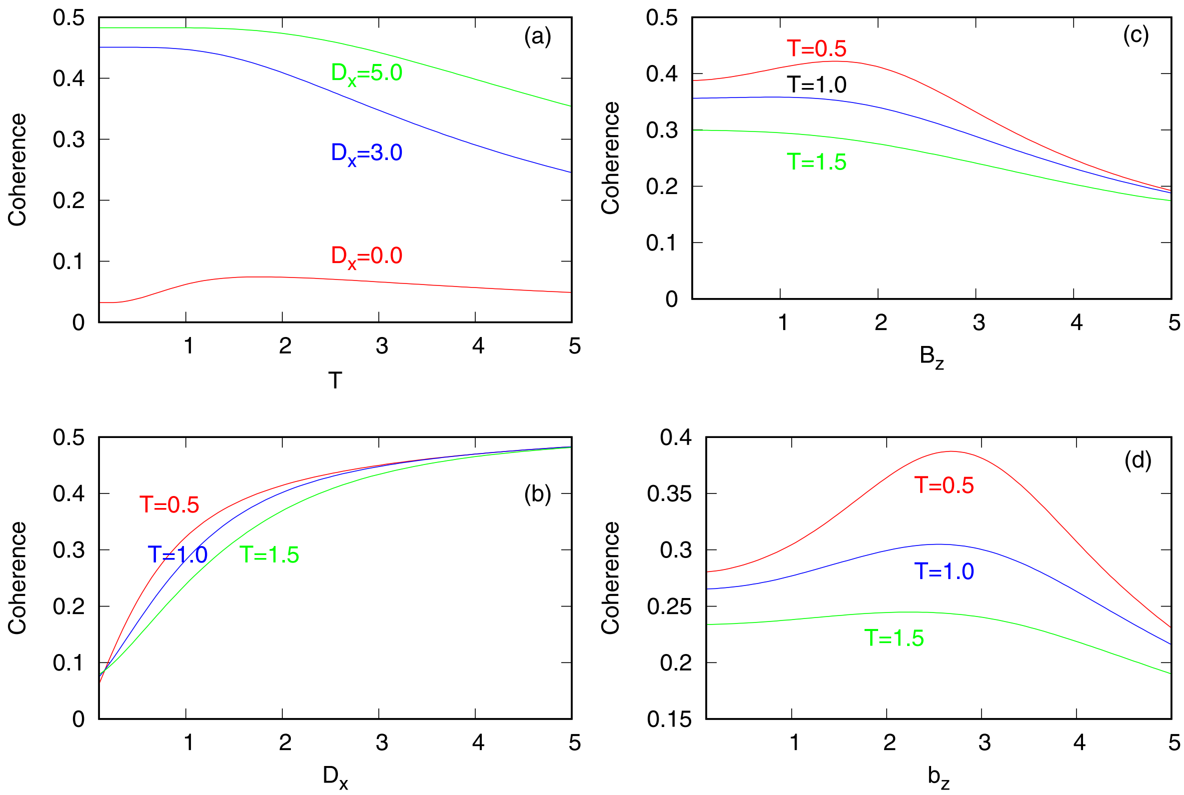

Fig. 4. The variation in coherence is measured in the σ_z basis for the two-spin XYZ model with DM interactions in the x-direction and the external magnetic field in the z-direction. (a) Quantum coherence versus temperatures T for different D_x for $B_z = 3$, $b_z = 1.5$, $J_x = 0.8$, $J_y = 0.5$ and $J_z = 0.2$. (b) Quantum coherence versus D_x, for different temperatures T, for $B_z = 3.0$, $b_z = 1.5$, $J_x = 0.8$, $J_y = 0.5$ and $J_z = 0.2$. (c) Quantum coherence versus B_z for different temperatures T, for $D_x = 1.0$, $b_z = 1.5$, $J_x = 0.8$, $J_y = 0.5$ and $J_z = 0.2$. (d) Quantum coherence versus b_z for different temperatures T, for $D_x = 1.0$, $B_z = 3.0$, $J_x = 0.8$, $J_y = 0.5$ and $J_z = 0.2$.

4.2. $\vec{D} \propto \vec{x}, \vec{B} \propto \vec{z}$ case

When the magnetic field is oriented along the z-axis and the DM interaction is along the x-axis, the Hamiltonian of the system reads:

$$H = J_x\sigma_1^x\sigma_2^x + J_y\sigma_1^y\sigma_2^y + J_z\sigma_1^z\sigma_2^z + D_x(\sigma_1^y\sigma_2^z - \sigma_1^z\sigma_2^y) + (B_z + b_z)\sigma_1^z + (B_z - b_z)\sigma_2^z. \tag{32}$$

The matrix form in the σ^z basis is

$$H = \begin{pmatrix} 2B_z + J_z & iD_x & -iD_x & J_x - J_y \\ -iD_x & 2b_z - J_z & J_x + J_y & iD_x \\ iD_x & J_x + J_y & -2b_z - J_z & -iD_x \\ J_x - J_y & -iD_x & iD_x & -2B_z + J_z \end{pmatrix}. \tag{33}$$

The thermal density matrix $\rho(T)$ can be calculated from the Hamiltonian (33) using which we can find the quantum coherence of the system from Eq. (6).

The dependence of quantum coherence with temperature is shown in Fig. 4(a). As before, we find that the coherence decreases with temperature as expected due to thermal effects removing coherence. With increase in the value of the DM interaction parameter, we find that quantum coherence increases monotonically as seen in Fig. 4(b). From Fig. 4(c) we can see that coherence decreases with the average homogeneous field B_z. While this is uniform for higher temperatures, for lower values of temperature the coherence increases to a peak value and then decreases. The same behavior is also replicated when we look into the variation of coherence with the inhomogenous field b_z as seen in Fig. 4(d).

4.3. $\vec{D} \propto \vec{x}, \vec{B} \propto \vec{y}$ case

An interesting situation arises when the DM interaction and the external field are perpendicular to each other and neither of them are oriented along the measurement basis. The Hamiltonian in this case is

$$H = J_x\sigma_1^x\sigma_2^x + J_y\sigma_1^y\sigma_2^y + J_z\sigma_1^z\sigma_2^z + D_x(\sigma_1^y\sigma_2^z - \sigma_1^z\sigma_2^y) + (B_y + b_y)\sigma_1^y + (B_y - b_y)\sigma_2^y. \tag{34}$$

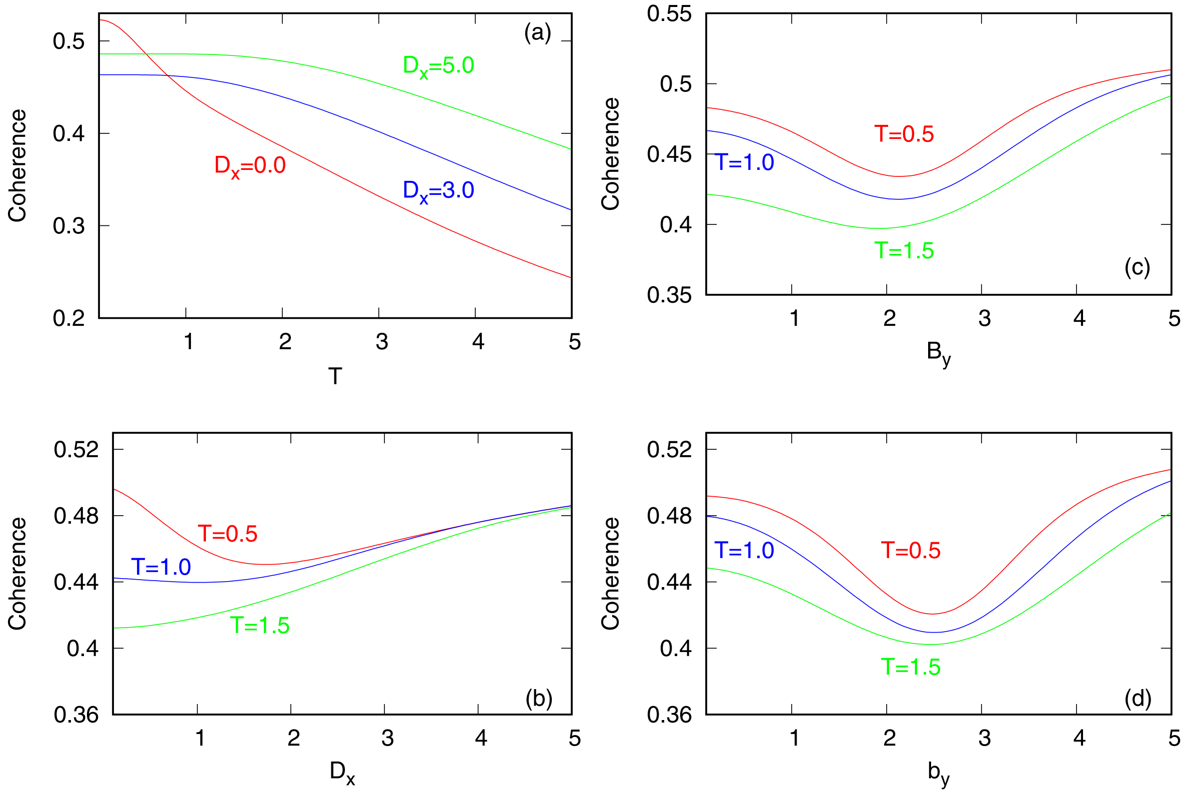

Fig. 5. The coherence variation measured in the σ_z basis for the XYZ model with DM interactions in the x-direction and the external field in the y-direction. (a) Quantum coherence versus temperature T for different D_x for $B_y = 3$, $b_y = 1.5$, $J_x = 0.8$, $J_y = 0.5$ and $J_z = 0.2$. (b) Quantum coherence versus D_x, for different temperatures T, for $B_y = 3.0$, $b_y = 1.5$, $J_x = 0.8$, $J_y = 0.5$ and $J_z = 0.2$. (c) Quantum coherence versus B_y for different temperatures T, for $D_x = 1.0$, $b_y = 1.5$, $J_x = 0.8$, $J_y = 0.5$ and $J_z = 0.2$. (d) Quantum coherence versus b_y for different temperatures T, for $D_x = 1.0$, $B_y = 3.0$, $J_x = 0.8$, $J_y = 0.5$ and $J_z = 0.2$.

From the knowledge of the Hamiltonian we can calculate $\rho(T)$ the thermal density matrix of the system and calculate the coherence using Eq. (6). Our results are shown in Figs. 5(a)–(d).

The quantum coherence decreases with temperature as seen in Fig. 5(a), as before due to thermal decoherence. The qualitative behavior of coherence with respect to change in the DM interaction parameter, the external homogeneous field B_z, and the inhomogenous field b_z is shown in Figs. 5(b), (c) and (d) respectively. The presence of spin–lattice interaction gives rise to new or enhanced contributions to off-diagonal elements and hence the overall effect is to increase the quantum coherence in the system. However in the XYZ model with both DM interaction and field in the x-direction, there is initially a decrease in coherence. After reaching the minimum the coherence again starts to increase. This dip occurs because the coherence arises due to two different interactions namely the spin–spin and the spin–lattice interaction. While the amount of coherence due to the spin–spin interaction decreases, the coherence due to the spin–lattice increases with the DM parameter D_x. There is a mismatch between the two rates of change leading to the formation of a dip in the amount of coherence. For higher values of temperature no dip is observed. In the case of the other two cases described in Sections 4.1 and 4.3 the coherence increases with D_x for higher values of temperature. For lower values of temperature, the coherence decreases with DM parameter. This special behavior is also due to the competing rates of change of coherence of the spin–spin and spin–lattice interactions. Hence, overall we can conclude that coherence increases with the DM interaction, even if the effect may not be so easily observed.

In summary, when an external field is applied on a spin system, the field changes the quantum properties by influencing the spins. In our work, we study the effect of an inhomogenous external field. The external field can be divided into an homogeneous component B and an inhomogenous component b. The strength and the direction of the homogeneous component B of the field is the same for the spins at both the lattice sites. In the case of the homogeneous component b, the strength of the field acting on both the spins is the same, but their direction is different. From Figs. 1–5 we observe that the quantum coherence decreases when the direction of the homogeneous field B is the same as the measurement basis. On the other hand, the coherence increases when the measurement basis and the external field are orthogonal to each other. In the case of the inhomogenous component of the field, the coherence mostly increases except for the isolated case of XYZ model with DM interaction along the x-direction and the field b is along the z-direction.

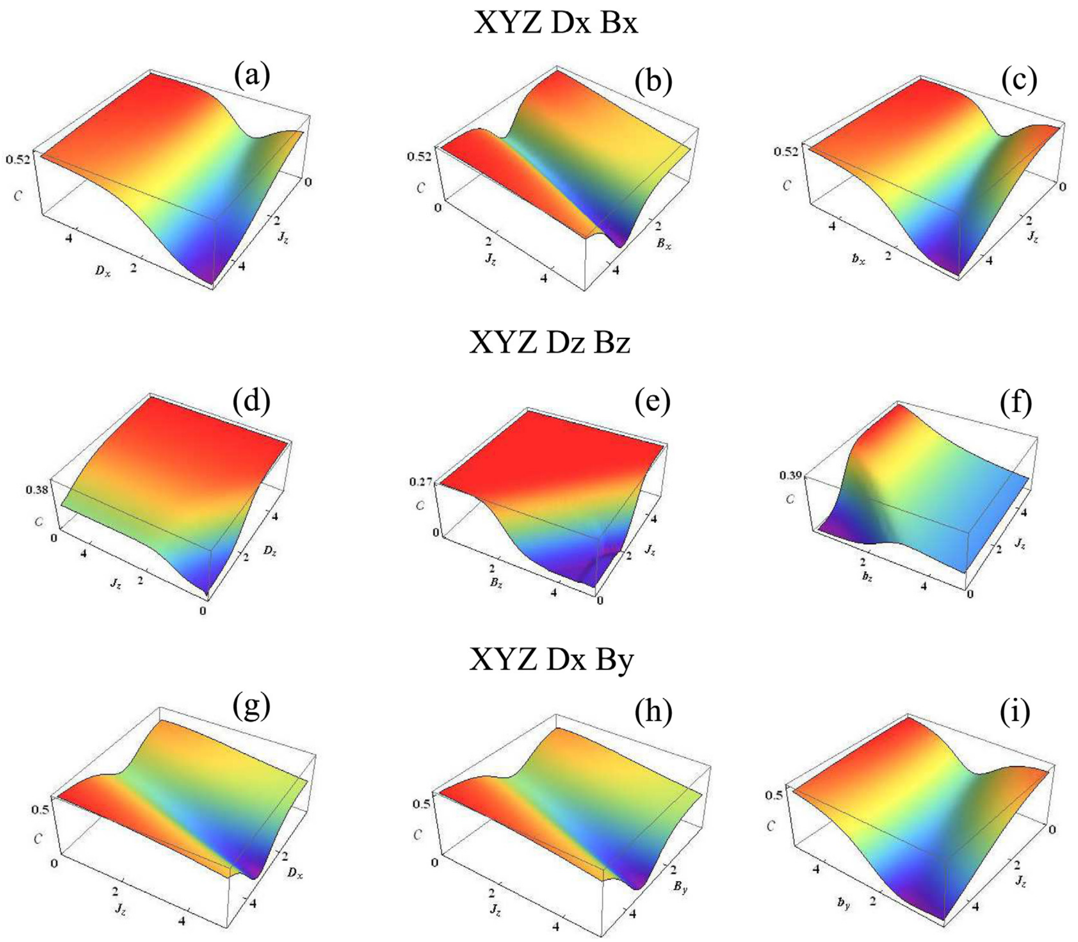

Fig. 6. The variation of coherence in the XYZ model with DM interaction and external field along the x-axis is shown through the first row of plots as follows: (a) coherence Vs J_z Vs D_x (b) coherence Vs J_z Vs B_x (c) coherence Vs J_z Vs b_x. The fixed values are $D_x = 1.0$, $B_x = 3.0$, $b_x = 1.5$, $J_x = 0.8$, $J_y = 0.5$ and $T = 0.5$. In the second row, the XYZ model with DM interaction and the field in the z-direction is given as follows: (d) coherence Vs J_z Vs D_z (e) coherence Vs J_z Vs B_z (f) coherence Vs J_z Vs b_z. The fixed values are $D_z = 1.0$, $B_z = 3.0$, $b_z = 1.5$, $J_x = 0.8$, $J_y = 0.5$ and $T = 0.5$. The final row describes the XYZ model with DM interaction in the x-direction and the field along the y-direction as follows: (d) coherence Vs J_z Vs D_x (e) coherence Vs J_z Vs B_y (f) coherence Vs J_z Vs b_y. The fixed values are $D_x = 1.0$, $B_y = 3.0$, $b_y = 1.5$, $J_x = 0.8$, $J_y = 0.5$ and $T = 0.5$. All the measurements are made uniformly in the σ_z basis.

5. Coherence variation under two control parameters

Up to this point we have not considered the dependence of the spin–spin interaction J_i, which has been considered a constant. In this section, we examine the variation of coherence with respect to the simultaneous variation of the spin–spin interaction parameter and one of the other control parameters such as the DM parameter or the external field.

The quantum coherence in the two-spin XYZ model with DM interaction and the external field along the x-direction is described in the first row of plots in Figs. 6(a)–(c). Fig. 6(a) shows the variation of coherence with respect to the spin–spin interaction parameter J_z and the DM interaction parameter D_x. From the plot we observe that for a given a constant temperature, the amount of quantum coherence decreases with the spin–spin interaction parameter J_z. Contrarily on increasing D_x the amount of coherence increases. This implies that the spin–spin interaction and the spin–lattice interaction have counteracting effects on the amount of coherence in the system. Fig. 6(b) shows the quantum coherence variation with respect to the parameters J_z and B_x (homogeneous component of the external field). Again we find that the coherence decreases with J_z, but increases with the external field. The external field B_x tries to align the spins in a uniform direction and hence we observe an increase in the amount of quantum coherence. Fig. 6(c) shows coherence as a function of the spin–spin interaction J_z and the inhomogenous component of the field b_x. This plot exhibits the features where we find that coherence decreases with J_z, whereas it increases with b_x. These observations are identical to the results obtained in Figs. 6(a)–(b)

In Figs. 6(d)–(f) the quantum coherence features of the two-site anisotropic model with DM interaction and the field in the z-direction is shown. We choose the measurement basis also to be in the σ_z basis and consider a constant temperature

Table 1
The variation of the coherences for the different parameters is summarized below. Here $+$ means coherence increases with the variable and $-$ means coherence decrease with the variable. The measurement basis is always in the z-direction.

Parameters	$\vec{D} \propto \vec{x}$ $\vec{B} \propto \vec{x}$	$\vec{D} \propto \vec{z}$ $\vec{B} \propto \vec{z}$	$\vec{D} \propto \vec{z}$ $\vec{B} \propto \vec{x}$	$\vec{D} \propto \vec{x}$ $\vec{B} \propto \vec{z}$	$\vec{D} \propto \vec{x}$ $\vec{B} \propto \vec{y}$
Temperature T	$-$	$-$	$-$	$-$	$-$
DM interaction D	$+$	$+$	$+$	$+$	$+$
Homogeneous magnetic field B	$+$	$-$	$+$	$-$	$+$
Homogeneous magnetic field b	$+$	$+$	$+$	$-$	$+$

T. From Fig. 6(d) we find that the coherence increases with J_z as well as D_z. In this situation, there is no counteracting influence between the spin–spin and spin–lattice interactions. Rather they exhibit a co-operative nature and enhances the coherence in the system with increase in these parameters. In Fig. 6(e) we notice that coherence decreases with increase in B_z and it increases with J_z. Finally in Fig. 6(f) we observe that coherence increases with the inhomogeneity of the external field b_z as well with the increase of the spin–spin interaction parameter J_z.

Finally, in Figs. 6(g)–(i) we look into the coherence dependence of the model with the spin lattice interaction in the x-direction and measurement along the σ_z basis. The external inhomogenous field is along the y-direction. When the spin–spin interaction J is increased, the coherence decreases. But when the spin lattice interaction is increased, the coherence increases. These results are shown in Fig. 6(g). Also through the plots Figs. 6(h)–(i) we find that coherence decreases with increase in the spin–spin interaction J_z. On increasing the homogeneous component B_y and inhomogenous component b_y we observe that the coherence increases.

In Table 1, based on the two dimensional plots, we summarize the variation of quantum coherence with different parameters for all the models. Using this in conjunction with Fig. 6 we arrive at the following conclusions. We find that when the direction of the DM interaction and external field is orthogonal to the measurement, the coherence in the system decreases with the spin–spin coupling J value. Similarly, the coherence increases with the spin–lattice interaction parameter D. Also in this situation both the homogeneous and inhomogenous fields helps to increase the coherence in the system. Under the conditions when the direction of measurement basis is same as the direction of the spin–lattice, the spin–spin interaction and the DM interaction increases the quantum coherence in the system. With respect to the external field, the coherence decreases with increase in the homogeneous component of the field B and it increases with the inhomogenous component of the field b.

6. Conclusions

The finite temperature quantum coherence of the two-spin XYZ Heisenberg model with Dzyaloshinsky–Moriya (DM) interaction subjected to an external inhomogenous magnetic field was investigated. In the investigation of these two-site models we consider two major cases namely: (i) the DM interaction and the external magnetic field are in the same direction; (ii) when the DM interaction and the external field are not in the same direction. Since quantum coherence is a basis-dependent quantity, these two classes are further divided based on the relation between the measurement basis and the direction of the DM parameter and the field. We first confirm that quantum coherence always decreases with temperature, due to the commonly observed effect that quantum coherence is destroyed by thermal decoherence. Next we find that the quantum coherence always increases with the strength of the DM interaction parameter irrespective of the relation between the spin–lattice interaction and the measurement basis. This result is similar to the one obtained for entanglement measured using concurrence. The quantum coherence decreases when the direction of the measurement basis is the same as that of the spin–spin interaction. A similar behavior of quantum coherence is observed when the external field is varied.

A spin chain always contains a spin–spin interaction apart from the DM interaction and the external field as described in our work. We investigated the change in coherence when the spin–spin interaction is simultaneously varied with the DM interaction parameter or the external fields. From the observations we find that the spin–spin interaction and the spin–lattice interaction have counteracting effects on the quantum coherence of the system when the direction of the measurement is orthogonal to the direction of the spin–lattice interaction. We note that this study could be further extended to larger systems, and studying spin models with staggered DM interactions [58,59] and random field interactions [60,61].

The amount and distribution of quantum coherence is connected to quantum information processing tasks like dense coding and quantum teleportation [26]. For example, the optimal dense coding capacity of a bipartite system is inversely related to the amount of local coherence in the system [26]. Similarly, there is an inverse relation between the teleportation fidelity and the local coherence in a system [26]. From our earlier studies [24] we know that coherence can exist localized within a qubit or as correlations between the qubits. Hence a small amount of local coherence must imply a higher amount of global coherence, which naturally means strongly correlated quantum systems help in tasks such as dense coding and quantum teleportation. In the case of the spin qubits considered, we observe that the total coherence in the system is always global coherence which implies that all the available form of coherence in a spin qubit can be used for quantum information processing tasks. In addition, the existence of several control parameters such as the spin–spin interaction parameter, the spin–lattice interaction parameter and the external parameters such as magnetic field and temperature helps us to modify the state of a system to improve the capacity of dense coding and the teleportation fidelity of quantum states. In Ref. [26] the authors only demonstrated the complementarity relations of the local coherence with the dense coding capacity and the teleportation fidelity. An important development in this direction would be to directly quantify the dense coding capacity and teleportation fidelity in terms of the global coherence. Such an improvement will be directly applicable to the spin systems we have considered in our work, where we can quantify the ability to perform quantum information processing tasks using the coherence of the spin system.

Declaration of competing interest

The authors declare that they have no known competing financial interests or personal relationships that could have appeared to influence the work reported in this paper.

Acknowledgments

TB and RC are supported by the Shanghai Research Challenge Fund; New York University Global Seed Grants for Collaborative Research; National Natural Science Foundation of China (61571301, D1210036 A); the NSFC Research Fund for International Young Scientists (11650110425, 11850410426); NYU-ECNU Institute of Physics at NYU Shanghai; the Science and Technology Commission of Shanghai Municipality (17ZR1443600); the China Science and Technology Exchange Center (NGA-16-001); and the NSFC-RFBR Collaborative grant (81811530112).

References

[1] R.J. Glauber, Phys. Rev. 131 (1963) 2766.
[2] E. Sudarshan, Phys. Rev. Lett. 10 (1963) 277.
[3] T. Baumgratz, M. Cramer, M. Plenio, Phys. Rev. Lett. 113 (2014) 140401.
[4] Y. Yao, X. Xiao, L. Ge, C. Sun, Phys. Rev. A 92 (2015) 022112.
[5] B. Yadin, J. Ma, D. Girolami, M. Gu, V. Vedral, 2015, arXiv preprint arXiv:1512.02085.
[6] J. Ma, B. Yadin, D. Girolami, V. Vedral, M. Gu, Phys. Rev. Lett. 116 (2016) 160407.
[7] B. Yadin, V. Vedral, Phys. Rev. A 93 (2016) 022122.
[8] T.R. Bromley, M. Cianciaruso, G. Adesso, Phys. Rev. Lett. 114 (2015) 210401.
[9] S. Du, Z. Bai, Y. Guo, Phys. Rev. A 91 (2015) 052120.
[10] D.P. Pires, L.C. Céleri, D.O. Soares-Pinto, Phys. Rev. A 91 (2015) 042330.
[11] S. Cheng, M.J. Hall, Phys. Rev. A 92 (2015) 042101.
[12] A. Streltsov, U. Singh, H.S. Dhar, M.N. Bera, G. Adesso, Phys. Rev. Lett. 115 (2015) 020403.
[13] H.-L. Shi, S.-Y. Liu, X.-H. Wang, W.-L. Yang, Z.-Y. Yang, H. Fan, Phys. Rev. A 95 (2017) 032307.
[14] M. Hillery, Phys. Rev. A 93 (2016) 012111.
[15] C. Zhang, T.R. Bromley, Y.-F. Huang, H. Cao, W.-M. Lv, B.-H. Liu, C.-F. Li, G.-C. Guo, M. Cianciaruso, G. Adesso, Phys. Rev. Lett. 123 (2019) 180504.
[16] J. Ma, Y. Zhou, X. Yuan, X. Ma, Phys. Rev. A 99 (2019) 062325.
[17] V. Narasimhachar, G. Gour, Nature Commun. 6 (2015) 1.
[18] A. Winter, D. Yang, Phys. Rev. Lett. 116 (2016) 120404.
[19] F.G. Brandão, G. Gour, Phys. Rev. Lett. 115 (2015) 070503.
[20] E. Chitambar, M.-H. Hsieh, 2015, arXiv preprint arXiv:1509.07458.
[21] E. Chitambar, G. Gour, Phys. Rev. Lett. 117 (2016) 030401.
[22] L. del Rio, L. Kraemer, R. Renner, 2015, arXiv preprint arXiv:1511.08818.
[23] E. Chitambar, G. Gour, Rev. Modern Phys. 91 (2019) 025001.
[24] C. Radhakrishnan, M. Parthasarathy, S. Jambulingam, T. Byrnes, Phys. Rev. Lett. 116 (2016) 150504.
[25] M. Lostaglio, D. Jennings, T. Rudolph, Nature Commun. 6 (2015) 1.
[26] F. Pan, L. Qiu, Z. Liu, Sci. Rep. 7 (2017) 43919.
[27] I.M. Georgescu, S. Ashhab, F. Nori, Rev. Modern Phys. 86 (2014) 153.
[28] B. Opanchuk, L. Rosales-Zárate, R. Teh, M. Reid, Phys. Rev. A 94 (2016) 062125.
[29] Q. Zheng, J. Xu, Y. Yao, Y. Li, Phys. Rev. A 94 (2016) 052314.
[30] N. Ishida, T. Byrnes, F. Nori, Y. Yamamoto, Sci. Rep. 3 (2013) 1180.
[31] G. Karpat, B. Çakmak, F. Fanchini, Phys. Rev. B 90 (2014) 104431.
[32] E. Lieb, T. Schultz, D. Mattis, Ann. Physics 16 (1961) 407.
[33] T. Niemeijer, Physica 36 (1967) 377.
[34] T. Niemeijer, Physica 39 (1968) 313.
[35] E. Barouch, B.M. McCoy, M. Dresden, Phys. Rev. A 2 (1970) 1075.
[36] E. Barouch, B.M. McCoy, Phys. Rev. A 3 (1971) 786.
[37] T. Giamarchi, Quantum Physics in One Dimension, Oxford university press, 2004.
[38] A. Malvezzi, G. Karpat, B. Çakmak, F. Fanchini, T. Debarba, R. Vianna, Phys. Rev. B 93 (2016) 184428.
[39] Y.-C. Li, H.-Q. Lin, Sci. Rep. 6 (2016).
[40] W. Cheng, Z. Zhang, L. Gong, S. Zhao, Eur. Phys. J. B 89 (2016) 1.
[41] B. Çakmak, G. Karpat, F.F. Fanchini, Entropy 17 (2015) 790.
[42] C. Radhakrishnan, I. Ermakov, T. Byrnes, Phys. Rev. A 96 (2017) 012341.
[43] I. Dzyaloshinsky, J. Phys. Chem. Solids 4 (1958) 241.
[44] T. Moriya, Phys. Rev. 120 (1960) 91.
[45] X. Wang, Phys. Rev. A 64 (2001) 012313.
[46] L. Zhou, H. Song, Y. Guo, C. Li, Phys. Rev. A 68 (2003) 024301.

[47] D.-C. Li, Z.-L. Cao, Eur. Phys. J. D 50 (2008) 207.
[48] F. Kheirandish, S.J. Akhtarshenas, H. Mohammadi, Phys. Rev. A 77 (2008) 042309.
[49] D.-C. Li, Z.-L. Cao, Opt. Commun. 282 (2009) 1226.
[50] Z.N. Gurkan, O.K. Pashaev, Internat. J. Modern Phys. B 24 (2010) 943.
[51] J.-L. Guo, Y.-J. Mi, J. Zhang, H.-S. Song, J. Phys. B: At. Mol. Opt. Phys. 44 (2011) 065504.
[52] N. Zidan, J. Quantum Inf. Sci. 2014 (2014).
[53] C. Yi-Xin, Y. Zhi, Commun. Theor. Phys. 54 (2010) 60.
[54] C. Radhakrishnan, M. Parthasarathy, S. Jambulingam, T. Byrnes, Sci. Rep. 7 (2017) 1.
[55] J. Lin, IEEE Trans. Inform. Theory 37 (1991) 145.
[56] P. Lamberti, A. Majtey, A. Borras, M. Casas, A. Plastino, Phys. Rev. A 77 (2008) 052311.
[57] J. Briët, P. Harremoës, Phys. Rev. A 79 (2009) 052311.
[58] F.-W. Ma, S.-X. Liu, X.-M. Kong, Phys. Rev. A 84 (2011) 042302.
[59] S. Miyahara, J.-B. Fouet, S. Manmana, R. Noack, H. Mayaffre, I. Sheikin, C. Berthier, F. Mila, Phys. Rev. B 75 (2007) 184402.
[60] R. Bruinsma, G. Aeppli, Phys. Rev. Lett. 50 (1983) 1494.
[61] M. Fujinaga, N. Hatano, J. Phys. Soc. Japan 76 (2007) 094001.

P93

Field Induced Enhancement of Spin Excitations in the Frustrated Magnet $LiYbW_2O_8$

Nishit Patel[1], Rahul Kumar[2], Rhea Stewart[3], Peter J. Baker[3], Ralf Feyerherm[4], Bella Lake[4,5] and A. Sundaresan[1]

[1] *School of Advanced Materials, and Chemistry and Physics of Materials Unit, Jawaharlal Nehru Centre for Advanced Scientific Research, Bangalore-560064, India*
[2]*Department of Physics and Astronomy, Seoul National University, Seoul 08826, Republic of Korea*
[3]*ISIS Facility, Rutherford Appleton Laboratory, Chilton, Didcot OX11 0QX, United Kingdom*
[4]*Institut für Festkörperphysik, Technische Universität Berlin, Hardenbergstraße 36,10623 Berlin, Germany*
[5]*Helmholtz-Zentrum Berlin für Materialien und Energie, Hahn-Meitner-Platz 1, 14109 Berlin, Germany*

Realizing a quantum spin liquid (QSL) in higher-dimensional spin systems is of considerable interest, as sustaining quantum fluctuations requires strong magnetic frustration to counteract their natural suppression relative to low-dimensional counterparts[1]. Rare-earth-based magnets, with strong spin–orbit coupling and localized 4*f* electrons, are promising candidates; in systems with an odd number of *f*-electrons, spin–orbit coupling and the crystal electric field (CEF) typically stabilize a Kramers doublet ground state describable by an effective pseudospin-½.

Here, we report the successful synthesis and comprehensive characterization of $LiYbW_2O_8$, a wolframite-type compound (space group *P2/n*) free from detectable site disorder between Yb^{3+} and Li^+ ions [2]. Magnetization measurements on polycrystalline samples reveal the absence of long-range magnetic order down to 0.4 K. Deviations from Curie-Weiss behaviour in the inverse susceptibility data indicate strong CEF effects, yielding an effective J_{eff} = ½ for Yb^{3+} with $\theta_{CW} = -0.14(4)$ K. Heat capacity measurements shown no magnetic ordering down to 0.35 K but reveal a Schottky whose analysis gives a small energy gap $\Delta(0)$~0.14 K, consistent with weak Yb^{3+}-Yb^{3+} interactions inferred from magnetization data. Zero-field μSR measurements reveal a finite relaxation rate λ = 2.76(8) μs^{-1} at 120 mK, indicating persistent low-energy spin fluctuations and the absence of static magnetic order down to the base temperature. The temperature dependence of λ follows an Orbach relaxation mechanism, suggesting a thermally activated transition between the ground state doublet & excited CEF levels. Longitudinal-field μSR at 100 mK shows that spin dynamics persist up to 3000 Oe, with the fluctuation rate increasing with field, pointing to a field-induced enhancement in the density of spin excitations [3].

These results demonstrate that $LiYbW_2O_8$ hosts a dynamic magnetic ground state, robust against applied magnetic fields, establishing it as a promising platform for investigating frustrated magnetism and correlated ground states in rare-earth-based systems.

[1] Gonzalez, M.G., Noculak, V., Sharma, A., Favre, V., Soh, J.R., Magrez, A., Bewley, R., Jeschke, H.O., Reuther, J., Rønnow, H.M., and Iqbal, Y., 2024. Dynamics of $K_2Ni_2(SO_4)_3$ governed by proximity to a 3D spin liquid model. *Nature Communications*, 15(1), p.7191.

[2] J. M. Postema, W. T. Fu, and D. J. W. Ijdo, Crystal structure of $LiLnW_2O_8$ (Ln=lanthanides and Y): An X-ray powder diffraction study, J Solid State Chem **184**, (2011).

[3] R. Kumar et al., Dynamic magnetic ground state in the dimer based compound $Yb_2Te_5O_{13}$, *Phys Rev B* **111**, L140411 (2025).

P94

Quantum phases of two-dimensional Z2 gauge theory coupled to Double-component spin-full fermionic matter in SSH model

Tunable topological protection in Rydberg lattices via a novel quantum Monte Carlo approach

Pranay Patil[1,3], **Owen Benton**[2,3]

[1]*(Presenting author underlined) Theory of Quantum Matter Unit, Okinawa Institute of Science and Technology Graduate University, Onna-son, Okinawa 904-0412, Japan*
[2] *School of Physical and Chemical Sciences, Queen Mary University of London, London, E1 4NS, United Kingdom*
[3] *Max Planck Institute for the Physics of Complex Systems, Nothnitzer Strae 38, 01187 Dresden, Germany*

Rydberg atom arrays have recently been conjectured to host Z_2 quantum spin liquids in certain parameter regimes. Due to the strong interactions between these atoms, it is not possible to analytically study these systems, and one must resort to Monte Carlo sampling of the path integral to reach definite conclusions. The complex landscape of path integral configurations prevents efficient sampling, and leads to a severe lack in ergodicity for the Monte Carlo simulation. Here we use the resonances expected between different configurations of a Z_2 spin liquid to design a sampling protocol which is especially suited to the expected path integral landscape. This allows us to reliably simulate Rydberg atoms on a triangular lattice in this regime, and identify a correlated paramagnetic phase at low temperatures which hosts topological protection similar to a Z_2 spin liquid upto a lengthscale tuned by Hamiltonian parameters.

[1] Pranay Patil, Owen Benton, arXiv:2503.12949 (2025).

P96

Effective Field Theory for Quantum Skyrmion Hall Effect

Vinay Patil[1], Rafael Flores Calderón[1,2], and Ashley M. Cook[2]

[1]*Max Planck Institute for the Physics of Complex Systems, Dresden, Germany*
[2]*Max Planck Institute for the Chemical Physics of Solids, Dresden, Germany*

We derive an effective field theory (EFT) description for the quantum skyrmion Hall effect (QSkHE) and related topologically non-trivial phases of matter. An almost point-like Landau level with small orbital degeneracy can host an intrinsically 2+1 D topological many-body state, meaning internal degrees of freedom can encode a finite number of spatial dimensions. This almost point-like 2+1 D many-body state plays the role, in the quantum skyrmion Hall effect (QSkHE), that a charged particle plays in the quantum Hall effect.

[1] V. Patil, R. Flores-Calderón, and A. M. Cook, Effective field theory of the quantum skyrmion hall effect (2024), arXiv:2412.19565 [hep-th]

P97

Functional Renormalization Group treatment of the spiral phase

Miriam Patricolo[1,2,3], Paulo Forni[3], Sabine Andergassen[1,2], Demetrio Vilardi[3]

[1] *Institute of Information Systems Engineering, Vienna University of Technology, Vienna, Austria*

[2] *Institute for Solid State Physics, Vienna University of Technology, Vienna, Austria*

[3] *Max Planck Institute for Solid State Research, Heisenbergstrasse 1, Stuttgart, Germany*

Spiral magnetic order is a natural instability of the doped two-dimensional Hubbard and t–J models, and has been proposed as a candidate for the incommensurate phases observed in high-temperature cuprate superconductors. With doping, for a wide coupling range and finite next-to-nearest hopping amplitude, the Nèel antiferromagnet becomes unstable as spins rearrange to maximize carrier kinetic energy, leading to an incommensurate spiral state with ordering vector $Q \neq (\pi/a, \pi/a)$. This state fully breaks SU(2) spin symmetry and gives rise to three Goldstone modes: two from out-of-plane and one from in-plane spin fluctuations.At finite temperature, magnetic fluctuations of the spiral order become strong enough to destroy the long-range order, as stated by the Mermin-Wagner theorem. A remaining short-range fluctuating spiral order competes or coexists with charge and pairing instabilities and is regarded as a promising candidate for the normal state of cuprates under strong magnetic fields.

In this project, we investigate the spiral phase and its interplay with superconducting and charge-order instabilities using the functional renormalization group (fRG). To this end, we recast the fRG formulation within the single-boson exchange (SBE) representation, which not only provides a transparent physical interpretation in terms of collective bosonic fluctuations but also yields significant computational advantages. A central element of our framework is the explicit treatment of the flow of the order parameter, which is essential to preserve the Goldstone theorem.

P98

Magnetic Anisotropies of RuX_3 (X = Br, I) Probed by Torque Magnetometry

Pearce J. S.[1], **Ma Z** [1], **Ni D** [2], **Cava R** [2], **Vignolles D** [3], **Badoux S** [3], **Coldea R** [1], **Coldea A. I.** [1]

[1] *University of Oxford, United Kingdom*
[2] *Princeton University, USA*
[3] *LNCMI Toulouse, France*

In the Kitaev model, bond-dependent Ising-like exchange on a 2D honeycomb lattice establishes an exactly solvable spin liquid ground state [1]. However, the competition of surplus Heisenberg and off-diagonal couplings often stabilises long-range magnetic order. In α-RuX_3 (X = Cl, Br, I), the choice of X tunes the relative strength of the Kitaev interaction and thus affects its ground state. We investigate magnetic anisotropies in two systems: α-$RuBr_3$, which stabilises zigzag antiferromagnetic (ZAFM) order below 34 K, and the isoelectronic α-RuI_3, which lacks long-range magnetic order and is a potential spin liquid [2]. We perform angle-dependent single-crystal torque magnetometry in fields up to 16 T and find that α-$RuBr_3$ possesses easy-plane anisotropy with the torque amplitude mimicking the temperature dependence of its magnetic susceptibility [3]. Meanwhile, we observe a torque sign change as a function of temperature in α-RuI_3, reflecting a transition from easy-axis to easy-plane anisotropy, and the development of a saw-tooth angular dependence at low temperatures where the strength of anisotropic interactions overcomes *g*-tensor anisotropy [4]. Angular-dependent studies in the honeycomb plane reveal a six-fold symmetric torque attributed to the trigonal symmetry of bond-dependent interactions in both systems [3, 4]. Field-dependent torque studies up to 55T show an expected parabolic behaviour in $RuBr_3$ in contrast to RuI_3 which develops a broad kink at a characteristic crossover field, H*, where a local maximum in saw-tooth anisotropy is observed. These studies offer insight into the field and temperature dependencies of magnetic anisotropies in two distinct Kitaev honeycombs, each with different ground states where Kitaev interactions have different strengths in relation to competing interactions.

[1] Kitaev, A. *Annal of Phys.* **321**, 2-111 (2006)
[2] Kaib, D.A.S. et al. *npj Quantum Mater.* **7**, 75 (2022)
[3] Pearce, J.S. et al. *Phys. Rev. B* **110**, 214404 (2024)
[4] Ma, Z. et al. *Commun Phys* **7**, 390 (2024)

P99

Spin susceptibility in a pseudogap state with fluctuating spiral magnetic order

Paulo Forni[1], **Pietro M. Bonetti**[2], **Henrik Müller-Groeling**[1], **Demetrio Vilardi**[1], and **Walter Metzner**[1]

[1] *Max Planck Institute for Solid State Research, D-70569 Stuttgart, Germany*
[2] *Department of Physics, Harvard University, Cambridge MA 02138, USA*

We compute the electron spin susceptibility in the pseudogap regime of the two-dimensional Hubbard model in the framework of a SU(2) gauge theory of fluctuating magnetic order [2]. The electrons are fractionalized in fermionic chargons with a pseudospin degree of freedom and bosonic spinons. The chargons are treated in a renormalized mean-field theory and order in a Néel or spiral magnetic state in a broad range around half-filling below a transition temperature T^*. Fluctuations of the spin orientation are captured by the spinons. Their dynamics is governed by a non-linear sigma model, with spin stiffnesses computed microscopically from the pseudospin susceptibility of the chargons [3]. The SU(2) gauge group is higgsed in the chargon sector, and the spinon fluctuations prevent breaking of the physical spin symmetry at any finite temperature. The electron spin susceptibility obtained from the gauge theory shares many features with experimental observations in the pseudogap regime of cuprate superconductors: the dynamical spin susceptibility $S(\mathbf{q},\omega)$ has a spin gap, the static uniform spin susceptibility κ_s decreases strongly with temperature below T^*, and the NMR relaxation rate T_1^{-1} vanishes exponentially in the low temperature limit if the ground state is quantum disordered [1]. At low hole doping, $S(\mathbf{q},\omega)$ exhibits nematicity below a transition temperature $T_{\mathrm{nem}} < T^*$, and at larger hole doping in the entire pseudogap regime below T^*.

[1] P. Forni, P. M. Bonetti, H. Müller-Groeling, D. Vilardi, and W. Metzner, arXiv:2509.07826 (2025).
[2] Pietro M. Bonetti and Walter Metzner, Phys. Rev. B **106**, 205152 (2022).
[3] Pietro M. Bonetti, Phys. Rev. B **106**, 155105 (2022).

P100

Anticommuting quantum spin liquids and eigenstate thermalization

Arnav Pushkar[1], **Sumiran Pujari**[1], **and Pranay Patil**[2]

[1]*(Presenting author underlined) Indian Institute of Technology Bombay, Mumbai, India.*
[2]*Indian Institute of Technology Madras, Chennai, India.*

We explore thermalization in quantum spin systems with local Z_2 conserved quantities that mutually anti-commute [1]. Using exact diagonalization within symmetry-resolved subspaces, we test the applicability of the Eigenstate Thermalization Hypothesis (ETH) in such constrained settings. Our analysis combines eigenstate expectation values of local observables with spectral diagnostics such as level spacing distributions and adjacent gap ratios, to distinguish between thermalizing (chaotic) and non-thermalizing (structured) regimes.

To assess the stability of ETH, we introduce controlled perturbations, such as external magnetic fields, that selectively break subsets of the local symmetries. This allows us to track how thermal behavior emerges as symmetry constraints are lifted. Ultimately, the project aims to understand how non-commuting local conservation laws shape the dynamics, chaos, and thermal properties of quantum many-body systems.

[1] S. Pujari, arXiv:2407.06236.

P101

Eliashberg theory and superfluid stiffness of band-off-diagonal pairing in twisted graphene

Bernhard Putzer[1,2], **and Mathias S. Scheurer**[2]

[1] *Institute for Theoretical Physics, University of Innsbruck, Innsbruck A-6020, Austria*
[2] *Institute for Theoretical Physics III, University of Stuttgart, 70550 Stuttgart, Germany*

Band-off-diagonal superconductivity has recently been proposed as a pairing state in twisted graphene systems [1]. Mean-field theory suggests it arises naturally from both intervalley electron-phonon coupling and fluctuations near correlated insulators, and it can exhibit both nodal and gapped regimes, consistent with scanning tunneling microscopy. Here [2], we study band-off-diagonal pairing within Eliashberg theory. Despite the additional frequency dependence, the leading-order description of both intervalley coherent fluctuations and intervalley phonons exhibits a symmetry prohibiting the admixture of an intraband component to the interband pairing state. A mixing of even- and odd-frequency components emerges due to the reduced flavor degrees of freedom in the normal state, and the superconducting phase transition can become discontinuous. Analytic continuation reveals an enhanced electronic spectral weight below the order-parameter energy compared to band-diagonal pairing. Finally, we also study the superfluid stiffness of band-off-diagonal pairing, taking into account multiband and quantum geometry effects. It is shown that for s-wave and chiral momentum dependencies - conventionally fully gapped - an interband structure reduces the temperature scale below which the stiffness saturates. For the chiral state, this scale can even be suppressed all the way to zero temperature, leading to a complex competition of multiple dispersive and geometrical contributions. These findings suggest that interband pairing could explain recent superfluid stiffness measurements in twisted multilayer graphene [3].

[1] Christos, M., Sachdev, S. & Scheurer, M.S. Nat Commun 14, 7134 (2023).
[2] Putzer, B. and Scheurer, Phys. Rev. B 111, 144513 (2025).
[3] Banerjee, A., Hao, Z., Kreidel, M. et al. Nature 638, 93–98 (2025).

P102

Kondo screening versus random singlet formation in highly disordered systems

Lucas G. Rabelo[1] and **Eric C. Andrade**[1]

[1]*Instituto de Física, Universidade de São Paulo, 05315-970 São Paulo, SP Brazil.*

In this work, we introduce the two-impurity Kondo problem as a minimal model to capture the anomalous thermodynamics observed across the metal-insulator transition (MIT) in doped semiconductors [1, 2, 3]. To this end, we investigate an ensemble of independent configurations, each consisting of two localized spins coupled to a highly disordered, non-interacting electronic bath that undergoes a MIT as a function of doping. This setting retains the essential competition between random-singlet formation —- predicted by the Bhatt–Lee theory [4, 5, 7] to dominate deep in the insulating phase – and Kondo screening, which prevails with the onset of metallic behavior [8, 9]. Using a large-$\mathcal{N}$ variational mean-field approach combined with an implementation of the two-fluid scheme [1, 10], we capture both the insulating random-singlet phase at low impurity concentrations and the inhomogeneous local Fermi-liquid at high doping. Our results show that the local moment susceptibility (χ) follows a well-defined power-law behavior at low temperatures, $\chi(T) \propto T^{-\alpha}$, where the exponent α evolves smoothly with doping and saturates in the metallic regime. This result is in striking accordance with experimental observations concerning Si:P, the prototypical doped semiconductor [2]. Furthermore, our analysis reveals that the fraction of Kondo screened sites (inert random singlets) increases (decreases) continuously with the impurity density. In this two-fluid scenario [1, 10], both fractions remain finite at the MIT, resulting in a smooth thermodynamic response – in contrast to the abrupt changes observed in the transport properties [3]. Our variational approach thus connects the random-singlet formation deep into the insulating regime to the disordered Fermi-liquid behavior expected in the metallic phase, emerging as a first step towards a self-consistent theory of MIT in doped semiconductors.

[1] M. Paalanen, J. Graebner, R. Bhatt, and S. Sachdev, Phys. Rev. Lett. **61**, 597 (1988).
[2] H. G. Schlager and H. v. Löhneysen, Europhys. Lett. **40**, 661 (1997).
[3] S. Kettemann, Ann. Phys. **456**, 169306 (2023).
[4] R. N. Bhatt and P. A. Lee, Phys. Rev. Lett. **48**, 344 (1982).
[5] S. Zhou, J. A. Hoyos, V. Dobrosavljević, and E. Miranda, Europhys. Lett. **87**, 27003 (2009).
[6] B. A. Jones, B. G. Kotliar, and A. J. Millis, Phys. Rev. B **39**, 3415 (1989).
[7] E. Miranda and V. Dobrosavljević, Rep. Prog. Phys. **68**, 2337 (2005).
[8] P. Coleman, *Introduction to Many-Body Physics*, Cambridge University Press (2015).
[9] A. C. Hewson, *The Kondo Problem to Heavy Fermions*, Cambridge Univ. Press (1993).
[10] R. N. Bhatt and D. S. Fisher, Phys. Rev. Lett. **68**, 3072 (1992).

P103

Variational study of the magnetization plateaux in the spin-1/2 kagome Heisenberg antiferromagnet: a neural network quantum state approach

Andreas Raikos[1], Sylvain Capponi[1], and Fabien Alet[1]

[1] *Univ Toulouse, CNRS, Laboratoire de Physique Théorique, Toulouse, France.*

We study the spin-1/2 kagome Heisenberg antiferromagnet in a magnetic field using Variational Monte Carlo with a Neural Quantum State ansatz. We construct the zero-temperature magnetization curve and resolve robust plateaux at $m = 1/3, 5/9, 7/9$. Local observables indicate $\sqrt{3} \times \sqrt{3}$ valence bond crystal states on these three high-magnetization plateaux, forming nine-site "hexagram" unit cells. We also obtain numerical evidence for a finite plateau near $m = 1/9$ and report state-of-the-art variational energies for this regime, surpassing previous results.

P104

A Hierarchy of Spectral Gap Certificates for Frustration-Free Spin Systems

Kshiti Sneh Rai [1,2] , **Ilya Kull** [3] , **Patrick Emonts** [1,2,4,5], **Jordi Tura** [1,2] , **Norbert Schuch** [3,6], **and Flavio Baccari** [7,8]

[1]*Instituut-Lorentz, Universiteit Leiden, P.O. Box 9506, 2300 RA Leiden, The Netherlands*
[2] *⟨aQa^L⟩ Applied Quantum Algorithms, Universiteit Leiden, The Netherlands*
[3] *University of Vienna, Faculty of Physics, Boltzmanngasse 5, A-1090 Vienna, Austria*
[4] *Institute for Complex Quantum Systems, Ulm University, 89069 Ulm, Germany*
[5] *Center for Integrated Quantum Science and Technology (IQST), Ulm-Stuttgart, Germany*
[6] *University of Vienna, Faculty of Mathematics, Oskar-Morgenstern-Platz 1, A-1090 Vienna, Austria*
[7] *Dipartimento di Fisica e Astronomia "G. Galilei", Universit`a di Padova, I-35131 Padova, Italy*
[8] *Padua Quantum Technologies Research Center, Universit`a degli Studi di Padova, Italy I-35131, Padova, Italy*

Estimating spectral gaps of quantum many-body Hamiltonians is a highly challenging computational task, even under assumptions of locality and translation-invariance. Yet, the quest for rigorous gap certificates is motivated by their broad applicability, ranging from many-body physics to quantum computing and classical sampling techniques. Here we present a general method for obtaining lower bounds on the spectral gap of frustration-free quantum Hamiltonians in the thermodynamic limit. We formulate the gap certification problem as a hierarchy of optimization problems (semidefinite programs) in which the certificate—a proof of a lower bound on the gap—is improved with increasing levels. Our approach encompasses existing finite-size methods, such as Knabe's bound [1] and its subsequent improvements [2], as those appear as particular possible solutions in our optimization, which is thus guaranteed to either match or surpass them. We demonstrate the power of the method on one-dimensional spin-chain models where we observe an improvement by several orders of magnitude over existing finite size criteria in both the accuracy of the lower bound on the gap, as well as the range of parameters in which a gap is detected. We believe that this technique will have a wide range of applications, including providing guarantees for state preparation methods that require gap estimates in advance and detecting phase transitions in systems previously inaccessible due to the absence of accurate gap estimation methods.

[1] S. Knabe, Energy gaps and elementary excitations for certain VBS-quantum antiferromagnets, Journal of Statistical Physics 52, 627 (1988).
[2] D. Gosset and E. Mozgunov, Local gap threshold for frustration-free spin systems, Journal of Mathematical Physics 57, 091901 (2016).

Spin-basis wavefunctions for 1D Kitaev Spin Models

Alwyn Jose Raja[1], Rajesh Narayanan[1], and R. Ganesh[2]

[1] *Department of Physics, Indian Institute of Technology Madras, Chennai 600036, India*
[2]*Department of Physics, Brock University, St. Catharines, Ontario L2S 3A1, Canada*

Frustrated magnets are a playground for exotic physics. They host quantum states that are disordered, entangled, topological or fractionalized. A broad class of such disordered states fall under the umbrella of quantum spin liquids (QSLs).

Resonating Valence Bond (RVB) theory posits QSL wavefunctions described as linear superpositions of singlet coverings[2]. A general method for studying such RVB QSLs is to treat the excitations as 'fractionalized' particles [2, 3]. The spin operators are rewritten in terms of these new entities, leading to emergent gauge theories [3, 4]. This typically involves a mean-field approximation, with a projection onto the physical Hilbert space [2]. This projection introduces non-trivial correlations in an otherwise ordinary Hartree-Fock ground state.

The parton construction has been validated by many successes including the Kitaev Honeycomb model [4]. However, it cannot be easily interpreted in terms of the physical spins that constitute the magnet. A recipe to construct an explicit wavefunctions in the spin-basis can bridge this gap. Moreover, it can demonstrate the character of valence bonds and resonance as promised by the RVB picture.

We provide a recipe for spin-basis wavefunctions for 1D and quasi-1D Kitaev-like models (and generalized compass models). Our work builds upon the results of [5]. The spin-$\frac{1}{2}$ models are Jordan-Wigner integrable, while higher spin versions are not. Our wavefunctions are inspired by a perturbative approach starting from the an anisotropic limit. They are validated by comparison with exact-diagonalization and a variational approach. We point to intriguing topological character that encodes long-ranged correlations.

Our approach generalizes the RVB picture to Hamiltonians that explicitly break spin-rotation symmetry. It can lead the way to spin-wavefunction-based approaches for 2D QSLs with topological order [4].

[1] Alwyn Jose Raja, Rajesh Narayanan, R. Ganesh (manuscript in preparation)
[2] Baskaran, G., Z. Zou, and P. W. Anderson. "The resonating valence bond state and high-T c superconductivity-a mean field theory." Solid State Communications 63, no. 11 (1987): 973-976.
[3] Affleck, Ian, Z. Zou, T. Hsu, and P. W. Anderson."SU (2) gauge symmetry of the large-U limit of the Hubbard model." Physical Review B 38, no. 1 (1988): 745.
[4] Kitaev, Alexei. "Anyons in an exactly solved model and beyond." Annals of Physics 321, no. 1 (2006): 2-111.
[5] Gordon, Jacob S., and Hae-Young Kee."Insights into the anisotropic spin-S Kitaev chain." Physical Review Research 4, no. 1 (2022): 013205.

P106

Dynamics of magnetic monopoles in the presence of domain walls

Anoop Raj[1], **Sumiran Pujari**[1], **and Ludovic D. C. Jaubert**[2]

[1] *Department of Physics, Indian Institute of Technology Bombay, Mumbai 400076, India*
[2]*CNRS, University of Bordeaux, LOMA, UMR 5798, F-33400 Talence, France*

Magnetic monopoles have long been sought after in fundamental physics. In recent years, spin ice materials have emerged as a canonical platform where emergent magnetic monopole-like excitations arise naturally from the underlying spin configurations [1]. These systems belong to the broader class of frustrated magnets, which, unlike conventional ferromagnets and antiferromagnets, show strong correlations without long-range order even at very low temperatures. The spin ice model has been instrumental in understanding such exotic phases, particularly the Coulomb spin liquid phase [2], where fractionalized excitations manifest as magnetic monopoles. The dynamics of these emergent monopoles have been studied before [3], but much less is known about their behaviour in inhomogeneous environments. In our work, we have looked at their dynamics in presence of domain wall within Fragmented Coulomb Spin Liquid (FCSL) phase. Particularly, we have focused on how the nature of magnetic-monopoles change and their departure from the pure Coulomb phase under different domain wall configurations.

[1] C. Castelnovo, R. Moessner, and S. L. Sondhi, "Magnetic monopoles in spin ice," *Nature*, **451**, 42–45 (2008).

[2] C. L. Henley, "The Coulomb phase in frustrated systems," *Annu. Rev. Condens. Matter Phys.* **1**(1), 179–210 (2010).

[3] L. D. C. Jaubert, "Monopole Holes in a Partially Ordered Spin Liquid," *SPIN* **5**, 1540005 (2015).

P107

Characterising Quantum Magic in Topological Many-Body Quantum Systems

P108

Abstract for Poster

<u>Malo Rouxel</u>[1], Sylvain Capponi[2], and Andreas Honecke[1]

[1]*(Presenting author underlined) Laboratoire de Physique Théorique et Modélisation, CY Cergy Paris Université, CNRS, 95302 Cergy-Pontoise, France*
[2]*Laboratoire de Physique Théorique, Université de Toulouse and CNRS, UPS (IRSAMC), F-31062, Toulouse, France*

The spin-1 bilinear-biquadratic chain represents the most general model for an isotropic exchange interaction within such a chain. The Hamiltonian of this chain can be expressed as a function of θ, the chain exhibiting several phases depending on the value of its value. To characterize the different phases while avoiding the entire spectral decomposition computation, entanglement within the ground state is investigated. This ground state is obtained by diagonalizing the Hamiltonian using an algorithm similar to the Lanczos algorithm. As the ground state can be degenerate, symmetries and conservations are also studied to achieve a non-degenerate ground state. It is demonstrated that proper multipartite entanglement measures enable the differentiation of various behaviors and the identification of the corresponding phases.

P109

Unveiling Floquet Skin Modes via Generalized Brillouin zone in a Driven Non-Hermitian Ladder

Koustav Roy*[1], Koustabh Gogoi[2], and Saurabh Basu[1]

[1]*Department of Physics, Indian Institute of Technology Guwahati, 781039, Assam, India*
[2]*Department of Physics, Indian Institute of Technology Gandhinagar, 382055, Gujarat, India*

Abstract

Here, we study a non-Hermitian (NH) ladder subjected to a variety of driving protocols. The driven system loses chiral symmetry (CS) whose presence is indispensable for its topological characterization. Further, the bulk-boundary correspondence (BBC) gets adversely affected due to the presence of non-Hermitian skin effect (NHSE). Here, we present a formalism that retrieves the lost CS, and subsequently restores the BBC via the construction of a generalized Brillouin zone (GBZ). Specifically, we employ delta and step drives to compare and contrast between them with regard to their impact on NHSE. Further, a widely studied harmonic drive is invoked in this context, not only for the sake of completeness, but its distinct computational framework offers valuable insights on the properties of out-of-equilibrium systems. While the delta and the harmonic drives exhibit unidirectional skin effect in the system, the step drive may show bi-directional skin effect. Also, there are specific points in the parameter space that are devoid of skin effect. These act as critical points that distinguish the skin modes to be localized at one boundary or the other. Moreover, for the computation of the non-Bloch invariants, we employ GBZ via a pair of symmetric time frames corresponding to the delta and the step drives, while a high-frequency expansion was carried out to deal with the harmonic drive. Finally, we present phase boundary diagrams that demarcate distinct NH phases obtained via tracking the trajectories of the exceptional points. These diagrams demonstrate a co-existence of the zero and π energy modes in the strong NH limit and thus may be relevant for studies of Floquet time crystals.

*koustav.roy@iitg.ac.in

P110

Emergence of Nematic Ordering from Two-Magnon Bound States on Frustrated Triangular Lattices

László Rudner[1,2], **Karlo Penc**[2]

[1] *Budapest University of Technology and Economics*
[2] *HUN-REN Wigner Research Centre for Physics*

Excitations, known as magnons in magnetic systems, determine low-temperature properties such as specific heat and magnetic susceptibility and provide insights into the nature of the ground state. Magnons can interact strongly, potentially forming two-magnon bound states whose behavior remains less well understood compared to single-magnon excitations. The nature of this interaction determines the resulting ordered phase: repulsive interactions lead to antiferromagnetic phases upon magnon condensation, whereas attractive interactions can induce condensation of two-magnon bound states, resulting in nematic phases without breaking time-reversal symmetry.
This study investigates two-magnon excitations in the Heisenberg model on a triangular lattice incorporating ferromagnetic and antiferromagnetic interactions between first-, second-, and third-nearest neighbors. Using the Luttinger-Tisza method, I constructed the model's phase diagram and calculated magnon dispersion relations starting from the ferromagnetic regime, including the phase boundaries to antiferromagnetic phases. Subsequently, I derived and solved the Schrödinger equation describing two-magnon interactions via a self-consistent approach, decomposing the interaction into partial-wave components. At high-symmetry Γ and K points in the Brillouin zone, the self-consistent equations simplify according to irreducible representations of the D_6 point group. I identified parameter regimes where nematic phases can arise by analyzing conditions under which the bound-state energy gap closes at the ferromagnetic phase boundary. Finally, I validated the analytical findings using exact diagonalization calculations and provided additional insights into effective interactions between the two-magnon bound states by studying the behavior of three- and four-magnons.

P111

Majorana Bound States in Nanowires: Identifying Topological Signatures and Overcoming Transport Challenges

Dibyajyoti Sahu[1], **Vipin Khade**[1], **and Suhas Gangadharaiah**[1]

[1] *Department of Physics, IISER Bhopal, India*

Majorana bound states (MBSs) in semiconductor-superconductor nanowires offer a promising route to topological quantum computation, yet experimental identification is challenged by the overlap of conductance signatures with trivial Andreev bound states (ABSs). We employ moving protocols that systematically reduce the topological length in nanowires, revealing that topological zero-bias peaks (ZBPs) arising from spatially separated MBSs remain pinned at zero bias, while trivial ZBPs from ABSs split at finite bias due to increased overlap of their Majorana components. This protocol, which can be implemented via tuned Zeeman or potential profiles, robustly distinguishes topological from trivial bound states through tunneling conductance measurements[1].

Building on these distinguishing capabilities, we investigate the dynamical transport of MBSs using piano-key setups, wherein wire segments are tuned stepwise from topological to trivial phases. Analytical and numerical studies address diabatic errors arising from drive times, temporal noise, and disorder, uncovering scaling laws and optimal protocols for minimizing error in realistic environments[2]. Our results provide design principles for noise-resilient movement and control of MBSs, informing future implementation of topological qubits. By integrating identification and robust transport schemes, this work advances the realization of fault-tolerant quantum architectures based on Majorana modes.

[1] D. Sahu, V. Khade, S. Gangadharaiah, Effect of topological length on bound state signatures in a topological nanowire, Phys. Rev. B **108**, 205426 (2023).

[2] D. Sahu, S. Gangadharaiah, Transport of Majorana bound states in the presence of telegraph noise, Phys. Rev. B **111**, 235306 (2025).

P112

Z_2 Spin liquid in Bilayer Kagome

Krushna Chandra Sahu [1], **Harsh Nigam**[1], **Rohit Deb** [2], **Sambuddha Sanyal** [2], **Subhro Bhattacharjee** [1]

[1] *International Center for Theoretical Sciences TIFR Bengaluru, India*
[2] *Indian Institute of Science Education and Research Tirupati, India*

We present a detailed Projective Symmetry Group (PSG) analysis of two bilayer Kagome stackings: the AA stacking and a shifted stacking configuration. Our analysis identifies 120 distinct Z_2 spin liquid states for the AA stacking and 32 for the shifted stacking. Using parton mean-field theory, we further compute the specific heat and dynamical structure factor for these solutions.

Our results offer a potential explanation for the linear temperature dependence of the specific heat observed at low temperatures in the AA-stacked bilayer Kagome material $Ca_{10}Cr_7O_{28}$ [1]. The shifted stacking configuration, on the other hand, is found in intermetallic compounds of the form M_3Sn_2 [2], where M denotes a transition metal. For these systems, we explore the interplay between metallic behavior and spin liquid correlations.

[1] J. Sonnenschein et al. Phys. Rev. B 100, 174428 (2019)
[2] S. Baidya et al. Phys. Rev. Lett. 125, 026401 (2020)

P113

Spin Dynamics Approach to Thermal Hall Conductivity in Kitaev Magnets

Ignacio Salgado-Linares[1,2], **Alexander Mook**[3], **Léo Mangeolle**[1,2], **and Johannes Knolle**[1,2,4]

[1] *Technical University of Munich, TUM School of Natural Sciences, Physics Department, TQM, 85748 Garching, Germany*
[2] *Munich Center for Quantum Science and Technology (MCQST), Schellingstr. 4, 80799 München, Germany*
[3] *Department of Physics, Johannes Gutenberg University Mainz, 55128 Mainz, Germany*
[4] *Blackett Laboratory, Imperial College London, London SW7 2AZ, United Kingdom*

We investigate thermal Hall transport in ordered magnetic systems using classical spin dynamics simulations based on the Landau–Lifshitz–Gilbert equation. Building on a linear response framework, we compute the thermal Hall conductivity from real-time energy current correlations and we apply this methodology to the Kitaev model in a field. We find a finite Hall response emerging from thermally activated magnon modes in the magnetically ordered regime. Our results establish a unified approach to thermal Hall transport beyond harmonic approximations, and offer a benchmark for comparison with experiments in regimes where magnon-magnon interactions and strong thermal fluctuations play a crucial role.

P114

Dynamics of Periodically Driven Spin Liquid

Diganta Samanta[1], **Pinaki Dutta**[1], **and Vishwanath Shukla** [1]

[1]*Department of Physics, Indian Institute of Technology Kharagpur, Kharagpur - 721 302, India*

Periodic driving of quantum spin liquids offer a unique window into nonequilibrium physics shaped by fractionalized excitations. We investigate the Kitaev Honeycomb model subject to a driving protocol and analyse the resulting dynamics of emergent Majorana fermions and Z_2 gauge fluxes. Our study reveals that the drive leads to qualitatively distinct heating behaviour and a prethermal regime where energy absorption behaviour is oscillatory in matter sector but flux sector does not absorb energy. Our results provide theoretical insights into how tailored drive protocols can be used to control non-equilibrium phases in spin liquid platforms.

[1] A. Kitaev, Annals of Physics 321 (2006) 2-111.
[2] Hui-Ke Jin, Johannes Knolle, and Michael Knap, Phys. Rev. Lett. 133, 069901 (2024).
[3] Arnab Sen et al 2021 J. Phys.: Condens. Matter 33 443003.

P115

Defect poisoning in quantum spin ice

Alaric Sanders, [1,2], Gautam Naik[3], Jonathan Hallén[3,4], and Robin Schäfer[3,4]

[1]*TCM Group, Cavendish Laboratory, University of Cambridge, Cambridge CB3 0HE, United Kingdom*

[2]*Helmholtz-Zentrum Berlin für Materialien und Energie, Hahn-Meitner Platz 1, D-14109 Berlin, Germany*

[3]*Department of Physics, Boston University, Boston, Massachusetts 02215, USA*

[4]*Department of Physics, Harvard University, Cambridge, Massachusetts 02138, USA*

Recent, exciting experimental results on $Ce_2Zr_2O_7$ [1] have brought the quantum spin ice community tantalisingly close to declaring a discovery. Interpreting such experiments is, however, made very difficult by a general lack of understanding regarding disorder in these systems. In this poster, we consider the highly experimentally relevant question of site disorder in quantum spin ice, exhibiting a mechanism by which a small number of non-magnetic impurities can nucleate strongly gapped singlets that effectively deactivate large regions of the system. This 'diluted QSI' model provides an upper bound on the allowable disorder levels that QSI can survive. Our model shows signs of a localised, gapped photon even at the modest 9% impurity concentration reported in experiments, underscoring the critical importance of ultra-clean samples to seeing spin-liquid physics in experiment.

[1] Gao, B.; Desrochers, F.; Tam, D. W.; Kirschbaum, D. M.; Steffens, P.; Hiess, A.; Nguyen, D. H.; Su, Y.; Cheong, S.-W.; Paschen, S.; Kim, Y. B.; Dai, P. Neutron Scattering and Thermodynamic Evidence for Emergent Photons and Fractionalization in a Pyrochlore Spin Ice. Nat. Phys. 2025.

P116

Anomalous dynamics of a fermion coupled to a constrained gauge background

P117

Geometry of tensor network varieties for quantum condensed matter physics

P118

Properties of Krylov State Complexity in Qubit Dynamics

Siddharth Seetharaman, Chetanya Singh, and Rejish Nath

Indian Education of Science Education and Research, Pune 411008, India

The concept of complexity has various implications in physics, ranging from quantum information and computing to black holes [1]. Krylov state complexity is a measure of the complexity of the dynamics of an initial state under a generator of time-evolution, which has been formulated recently in [2]. Compared to other measures of complexity that have been proposed, such as Nielsen complexity [3], the advantages of Krylov complexity are twofold. First, given an initial state and a Hamiltonian, the complexity is unambiguously defined using the Krylov basis obtained via the Lanczos algorithm [4], unlike other measures of complexities that invariably suffer from ambiguities in their definition. Second, the Krylov basis has been shown to minimize the spread of an initial state among all choices of ordered bases [2]. The Krylov complexity further gained attention in studying quantum chaos and integrability [5] and quantum phase transitions (see [6, 7], for instance), among various other applications [5].

In our work [8], we study the Krylov complexity in single-qubit and two-qubit systems in search of fundamental insights into the Krylov state complexity in qubit dynamics. We discuss a geometrical interpretation of the Krylov complexity, which has implications for potentially establishing a correspondence with Nielsen complexity, which is associated with a distance measure [9]. While we demonstrate a geometrical interpretation for the square root of the Krylov complexity in the single-qubit case, we show that it becomes impossible to generically do so in the two-qubit case precisely because the overall Krylov complexity is more than just a sum of the individual complexities. Further, considering the particular example of interacting Rydberg two-level atoms, we show that the Krylov basis may actually not always be optimal (except at very early times) as a practical measure of complexity of time-evolution, and discuss when such a case may arise. We also give an example where two states that are effectively related by time-evolution do not exhibit near-identical complexity behaviour as one would expect, which is a consequence of the former fact. We show that the Krylov basis, that is instead obtained using an effective Hamiltonian, minimizes the time-averaged spread complexity compared to that obtained from the original Hamiltonian. Finally, we generalize this to an arbitrary Hamiltonian in which the entire Hilbert space comprises of two subspaces provided a weak coupling between them.

[1] S. Chapman, G. Policastro, Eur. Phys. J. C **82**, 128 (2022).
[2] V. Balasubramanian, P. Caputa, J. M. Magan, Q. Wu, Phys. Rev. D **106**, 046007 (2022).
[3] M. A. Nielsen, M. R. Dowling, M. Gu, A. C. Doherty, Science **311**, 1133 (2006).
[4] V. S. Viswanath, G. Mueller, Springer **23** (1994).
[5] P. Nandy, A. S. Matsoukas-Roubeas, P. Martínez-Azcona, A. Dymarsky, A. del Campo, Physics Reports **1125-1128**, 1 (2025).
[6] P. Caputa, S. Liu, Phys. Rev. B **106**, 195125 (2022).
[7] P. Caputa, N. Gupta, S. S. Haque, S. Liu, J. Murugan, H. J. R. Van Zyl, J. High Energ. Phys. **2023**, 120 (2023).
[8] S. Seetharaman, C. Singh, R. Nath, Phys. Rev. D **111**, 076014 (2025).
[9] S. E. Aguilar-Gutierrez, A. Rolph, Phys. Rev. D **109**, L081701 (2024).

P119

Fermionic Bands of the Heisenberg Antiferromagnetic Spin-$\frac{1}{2}$ Trimer Chain

Snehasish Sen[1], Sudhansu S. Mandal[1]

[1] *Department of Physics, Indian Institute of Technology, Kharagpur, West Bengal 721302, India*

A spin-1/2 chain with inhomogeneous nearest neighbor antiferromagnetic Heisenberg interaction given by $J(1+\delta) - J(1+\delta) - J(1-\delta) - J(1+\delta) - \cdots$ is attempted to solve by converting the Hamiltonian in terms of three species of fermions corresponding to three sublattices through Jordan-Wigner transformation [1, 2]. A mean field is employed for finding energy dispersions for three species of fermions with three different bands separated by gaps which close when parameter $\delta = 0$. We calculate magnetization, magnetic susceptibility, specific heat and dynamical spin structure factors for comparing with numerical and experimental data [3].

[1] Jordan P., Wigner E., Z. Phys. **47**, 631 (1928).
[2] Bulaevskii L.N., Sov. Phys. JETP **17**, 684 (1963).
[3] Bera, A.K., Yusuf, S.M., Saha, S.K. *et al.* Nat Commun **13**, 6888 (2022).

P120

Machine learning symmetry protected topological phases from randomized measurements

Anastasiia Skurativska, Vedran Dunjko, and Evert van Nieuwenburg

LIACS, Universiteit Leiden, Niels Bohrweg 1, 2333 CA Leiden, Netherlands

Topological phases of matter are characterized by unconventional nature of entanglement. Unlike conventional phases, they cannot be described using local observables, which makes them hard to detect in experiments. In the presence of symmetries, there exist short-range entangled symmetry-protected topological (SPT) phases. Topological invariant for detecting these phases usually requires performing a global transformation of the many-body wave function [1]. Approaches based on randomized measurements have been successful in characterizing many-body states prepared on a quantum device [2]. In particular, classical shadows, obtained from randomized measurements, provide an efficient framework for extracting information about quantum states and predicting their properties with guaranteed precision [3]. Building on this approach, we propose a machine learning algorithm to diagnose phases of matter directly from measurement outcomes. To benchmark our method, we demonstrate its application to detecting the phases present in the XXZ spin chain.

[1] J. Haegeman, Y. Jinlong et al. PRL 109.5 (2012)
[2] A. Elben, Y. Jinlong et al. Science Advances 6.15 (2020)
[3] H. Y. Huang, R. Kueng, et al. Science, 377(6613) (2022)

P121

Phase diagram of the Kitaev-Heisenberg model on the Amorphous and hyperbolic lattices

P122

Entanglement Signatures of Gapless Topological Phases in a 2D BdG Superconductor

Srinidhi S.[1], Jayendra N. Bandyopadhyay[1]

[1]Department of Physics, Birla Institute of Technology and Science Pilani, Pilani Campus, Vidya Vihar, Pilani, Rajasthan 333031, India

Abstract:
We explore gapless topological phases in a time-reversal symmetric Kitaev chain on a two-dimensional square lattice [1]. By analyzing the entanglement properties of the system, we demonstrate the presence of bulk-boundary correspondence even in the absence of a full bulk gap. The entanglement entropy follows an area law, consistent with two-dimensional gapless behavior. Notably, the topological entanglement entropy is not quantized, reflecting a complex interplay between criticality and topology [2, 3]. These results highlight the effectiveness of entanglement-based diagnostics in identifying unconventional topological order in gapless quantum systems.

References

[1] S. Srinidhi et al., Quasi-Majorana modes in p-wave Kitaev chains on a square lattice, *Journal of Physics: Condensed Matter*, **37**, 205403 (2025).

[2] A. Kitaev and J. Preskill, Topological entanglement entropy, *Phys. Rev. Lett.* **96**, 110404 (2006).

[3] M. Levin and X. G. Wen, Detecting Topological Order in a Ground State Wave Function, *Phys. Rev. Lett.* **96**, 110405 (2006).

P123

Revealing Flat-Band Tunability through Orbital-Selective Hopping in Kagome Materials

Pritesh Srivastava [1] , **Bikash Patra** [1] , **and Bahadur Singh** [1]

[1] *Department of Condensed Matter Physics and Materials Science,*
Tata Institute of Fundamental Research, Colaba, Mumbai 400005, India

Flat bands, van Hove singularities, and Dirac bands in kagome lattice materials make them ideal platforms for exploring correlated many-body phenomena such as superconductivity, nematic order, and charge density waves, intertwined with nontrivial topology [1, 2]. While these features are intrinsic to the kagome lattice, their positions relative to the Fermi level depend sensitively on material- and orbital-dependent hopping interactions. Using Slater-Koster tight-binding modeling with symmetry-allowed d-orbital configurations [3, 4], we show that a nodal arrangement places flat bands below the Fermi level, while an antinodal configuration shifts them above. A continuous transition occurs between these states as orbital character evolves. First-principles calculations reveal that materials such as CoSn and $CsTi_3Bi_5$, featuring kagome nets formed by d orbitals, support these findings. Our results, which incorporate orbital hybridization while preserving kagome symmetry, demonstrate tunable flat bands across materials. This work not only enables the design of flat-band states with controllable energy placement but also guides the search for systems hosting correlated phases and directional-interaction-driven states.

[1] Z. Liu et al., Nat. Comm. **11**, 4002 (2020).
[2] B. Patra, A. Mukherjee, B. Singh, Phys. Rev. B **111**, 045135 (2025).
[3] J. C. Slater, G. F. Koster, Phys. Rev. **94**, 1498 (1954).
[4] D. Kim, F. Liu, Phys. Rev. B **107**, 205130 (2023).

P124 Signatures of the Fermi surface reconstruction of a doped Mott insulator in a slab geometry

Gregorio Staffieri, Michele Fabrizio

International School for Advanced Studies (SISSA), Via Bonomea 265, I-34136 Trieste, Italy

Keywords : Fermi surface reconstruction, open boundary conditions, Friedel oscillations

In the underdoped regime of high−Tc superconductors, the Fermi surface consists of Fermi pockets that coexist with a pseudogap at the antinodal point [1]. Conversely, in the overdoped regime, the Fermi surface is large and electron-like [2]. Evidence of this doping-driven reconstruction of the Fermi surface has been found in the two-dimensional single-band Hubbard model using various numerical methods [3, 4, 5].

In this work [6], we explore the reconstruction of the Fermi surface that emerges when a Mott insulator is hole-doped in a slab geometry, employing the Dynamical Cluster Approximation (DCA). We show that the enhancement of the correlation strength at the surface of the slab [7] results in the remarkable evolution of the layer-projected Fermi surface, which exhibits hole-like pockets in the superficial layers, but gradually evolves into a single electron-like surface in the innermost layers. We further investigate the behavior of the Friedel oscillations induced by the surface as a function of hole-doping. We identify distinct signatures of the Fermi surface reconstruction in the periodicity of the oscillations. In addition, we introduce a computationally tractable quantity that diagnoses the same Fermi surface variation by the concurrent breakdown of Luttinger's theorem. Both the latter quantity and the Friedel oscillations serve as reliable indicators of the change in Fermi surface topology, without the need for any periodization in momentum space.

[1] M. R. Norman et al., Nature 392, 157 (1998).
[2] B. Vignolle et al., Nature 455, 952 (2008).
[3] L. F. Tocchio et al., Phys. Rev. B 86, 035102 (2012).
[4] R. Rossi et al., Phys. Rev. Res. 6, L032058 (2024).
[5] W. Wu et al., Phys. Rev. X 8, 021048 (2018).
[6] G. Staffieri and M. Fabrizio, arXiv:2506.04155 [cond-mat.str-el] (2025).
[7] G. Borghi, M. Fabrizio, and E. Tosatti, Phys. Rev. Lett. 102, 066806 (2009).

Classical Fracton Spin Liquid on the Octochlore Lattice

Matthew Stern, Michael D. Burke, Michel J. P. Gingras, Judit Romhányi, and Kristian Tyn Kai Chung

For nearly three decades, research in frustrated magnetism in three dimensions (3D) has prominently centered on the pyrochlore geometry of corner-sharing tetrahedra and the classical spin liquid (CSL) known as spin ice. We propose that a lattice of corner-sharing octahedra, octochlore lattice, may provide a next-generation platform for 3D frustrated magnetism with realizations in anti-perovskites and certain potassium-fluoride compounds with magnetic rare-earth ions. We study the phase diagram of Ising spins on the octochlore lattice with first- and second-neighbor interactions within each octahedron. In addition to a spin ice CSL [1], we identify a novel fracton CSL with excitations restricted to move on one-dimensional lines, which is a classical U(1) analog of the celebrated X-cube model [2] of fracton topological order. We characterize this fracton liquid from multiple perspectives—via its flat bands with nodal line touchings; as a condensate of spinon bound states; as a cage-net liquid; as a foliated fracton phase of intersecting spin vorticity models; and as a bionic spin liquid of intersecting square ice sheets. This work paves the way for the potential realization of fracton CSLs in real materials.

[1] A. Szabó, F. Orlandi, and P. Manuel, Fragmented Spin Ice and Multi-k Ordering in Rare-Earth Antiperovskites, Phys. Rev. Lett.129, 247201 (2022).

[2] Vijay, J. Haah, and L. Fu, Fracton topological order, generalized lattice gauge theory, and duality, Phys. Rev. B 94, 235157 (2016).

The work at the University of Waterloo was funded by the NSERC of Canada. M.B. acknowledges a CSG-M scholarship from NSERC. M.S. and J.R. were supported by the NSF through grant DMR-2142554. This work was in part supported by the Deutsche Forschungsgemeinschaft under the cluster of excellence ct.qmat (EXC-2147, project number 390858490).

P126

Kondo effect in atomic gases: suppression of screening clouds by potential scattering

Lidia Stocker[1,2], **Jeff Maki** [3], **and Oded Zilberberg**[3]

[1] *Institute for Theoretical Physics, ETH Zurich, 8093 Zurich, Switzerland*
[2]*Max Planck Institute for the Physics of Complex Systems, 01187 Dresden, Germany*
[3]*Department of Physics, University of Konstanz, 78464, Konstanz, Germany*

The Kondo effect is a paradigmatic example of strongly correlated physics, in which a magnetic impurity forms a many-body singlet with its bath. Ultracold gases of Ytterbium atoms, where an impurity interacts magnetically with its bath, have recently been proposed for the experimental realization of Kondo states. However, in these systems, an impurity interacts with the bath also via potential scattering, which competes with the Kondo effect. In this work, we investigate the competition between these two scattering mechanisms in one-dimensional Ytterbium gases. Using a renormalization-group analysis, we show that the Kondo temperature decreases with increasing potential scattering. Complementarily, a DMRG-based approach allows us to characterize the screening cloud, whose extent is reduced until a crossover to a Mott-insulating state for strong potential scattering. Our results identify parameter regimes where Kondo correlations remain observable in Ytterbium gases, highlighting their promise as a platform for realizing exotic Kondo impurities and other strongly correlated states in ultracold atomic systems.

P127

Accurate conformal data from entanglement in rainbow chains

Attila Szabó[1]

[1]*Physik-Institut, Universität Zürich*

Obtaining details of the underlying 2D conformal field theory (CFT) from wave functions is a challenge both for edges of chiral topological orders and for critical spin chains.

In this talk, I will discuss a method to overcome the latter challenge [1]. By mapping CFT reduced density matrices to thermal ones, I show that the ground-state entanglement spectra of chains with exponentially decaying terms recover conformal towers of the associated boundary CFT, which have the same structure as chiral conformal towers. Crucially, the logarithmic finite-size scaling of entanglement spectra in uniform chains [2] is replaced by power laws for these “rainbow chains” [3], thus yielding sharp conformal multiplets using much smaller system sizes.

Through free-fermion and interacting examples, I will demonstrate that such chains are an efficient tool for obtaining detailed CFT spectra from single wave functions without access to the parent Hamiltonian. This makes them promising for studying the edge physics of, e.g., chiral spin liquids, which are routinely described in terms of projected parton wave functions.

I will also discuss an MPS-based Wilsonian numerical renormalisation group (NRG) scheme for solving interacting rainbow chains, which can handle chains with Hamiltonian terms spanning several orders of magnitude without numerical instabilities. I will show that the fixed-point tensor of this NRG also encodes scaling dimensions of the full CFT, thus making it a promising tool for extracting additional CFT data, such as fusion and OPE coefficients and modular matrices. I will demonstrate the power of this approach for both such standard models as the Potts chain and characterising poorly understood critical points in more challenging models. Finally, I will show examples of the particular usefulness of the method for CFT wave functions from, e.g., parton constructions [4], which have no readily available parent Hamiltonian.

[1] A. Szabó. Rainbow chains and numerical renormalisation group for accurate chiral conformal spectra. SciPost Phys. **19,** 075 (2025).

[2] A. Läuchli. Operator content of real-space entanglement spectra at conformal critical points. arxiv:1303.0741 (2013).

[3] G. Vitagliano, A. Riera, and J. I. Latorre. Volume-law scaling for the entanglement entropy in spin-1/2 chains. New J. Phys. **12,** 113049 (2010)

[4] T. Liu, Y. H. Wu, H. H. Tu, and T. Xiang. Bridging conformal field theory and parton approaches to $SU(n)_k$ chiral spin liquids. Phys. Rev. B **111,** 205137 (2025).

P128

revealing spinons by proximity effect

P129

Adiabatic gauge potential approach to characterize the onset of chaos in a many-body quantum system with a quasiperiodical potential

Texca-Garcia J. C. [1], **and Torres-Herrera E. J.**[1]

[1] *Physics Institute of Puebla, IFUAP; Benemérita Universidad Autónoma de Puebla, Mexico.*

The behavior of integrable and non-integrable classical Hamiltonian systems, including those that present chaotic behavior, are now well understood. In contrast, chaos in quantum systems have been a puzzle for a long time, especially in recent times for interacting systems. Classical chaos is usually described in terms of an exponential sensitivity of trajectories in phase space to initial conditions [1]. However, the quantum world excludes any definition of chaos in terms of physical trajectories due to the Heisenberg uncertainty principle. The understanding of quantum chaos is very important in part because nowadays it is accepted as a fundamental ingredient for the application of statistical mechanics and thermodynamics [2, 3]. In the broad field of non-equilibrium many body quantum physics, the evolution of isolated systems after an instantaneous perturbation has become a prominent subject.

Traditional methods for studying chaos in quantum systems have been applied to study the transition between integrable and chaotic behavior in quantum systems. These methods are mainly based in energy level statistics and structure of energy eigenstates. However, the involved tools are, in many cases, not enough sensitive to detect the onset of chaos when an integrability breaking term is included in the system. Specifically, traditional diagnostics of quantum chaos can fail to detect the onset of chaos when the strength of an integrability breaking term is weak.

An alternative method to detect chaos in quantum systems was proposed in [5]. It was claimed and demonstrated that so-called adiabatic gauge potential (AGP) [4], which generates adiabatic deformations between eigenstates and encodes information on both level spacings and the matrix elements of local operators, is significantly more sensitive in detecting the onset of quantum chaos compared to traditional methods.

In this work we study the so-called adiabatic gauge potential (AGP) [5] as a diagnostic of quantum many-body chaos. For our purposes we employ a paramagnetic model of many-body quantum systems, the one-dimensional Aubry-Andre model [6]. The first part of the work consists in characterizing the behavior of this model with conventional tools of random matrix theory. In particular, we focus on describing the spectrum as well as the eigenstates structure. Finally, we study the transition to chaos in the model by means of the adiabatic gauge potential (AGP).

[1] A. Vulpiani, F. Cecconi, and M. Cencini. Chaos: From Simple Models To Complex Systems. Series On Advances In Statistical Mechanics. WSPC, 2009.

[2] F. Borgonovi, F. M. Izrailev, L. F. Santos, and V. G. Zelevinsky. Quantum chaos and thermalization in isolated systems of interacting particles. Phys. Rep., 626:1–58, 2016.

[3] L. D'Alessio, Y. Kafri, A. Polkovnikov, and M. Rigol. From quantum chaos and eigenstate thermalization to statistical mechanics and thermodynamics. Adv. Phys., 65(3):239–362, 2016.

[4] Michael Kolodrubetz, Dries Sels, Pankaj Mehta, and Anatoli Polkovnikov. Geometry and non-adiabatic response in quantum and classical systems. Phys. Rep., 697:1–87, June 2017.

[5] Mohit Pandey, Pieter W. Claeys, David K. Campbell, Anatoli Polkovnikov, and Dries Sels. Adiabatic eigenstate deformations as a sensitive probe for quantum chaos. Phys. Rev. X, 10:041017, Oct 2020.

[6] S. Aubry and G. André. Analyticity breaking and Anderson localization in incommen- surate lattices. Ann. Israel Phys. Soc, 3(133):18, 1980.

P130

In altermagnetic materials, the underlying spin group symmetry allows for the spin-splitting of the electronic bands even in the absence of a net magnetization. While the effect is well understood from a symmetry point of view, the detailed microscopic mechanisms responsible for the altermagnetic phase remain to be understood. We introduce a minimal two-dimensional square-lattice model containing two inequivalent d-orbitals per site, along with the conventional on-site and nearest-neighbor four-fermion interactions. Following the identification of the symmetry-allowed octupolar order parameter, a mean-field analysis reveals the possible interaction terms required for stabilizing the altermagnetic phase.

P131

Anisotropic spin models on frustrated lattices: from spin liquids to supersolids

Martin Ulaga[1]

[1]*Max Planck Institute for the Physics of Complex Systems, 01187 Dresden, Germany*

Recent experiments on novel materials, which are described by easy-axis spin models on a triangular lattice, stimulated renewed theoretical interest in basic properties of anisotropic spin models on frustrated planar lattices. While the thermodynamic properties of the model on the kagome lattices [1] are consistent with the spin-liquid scenario in the whole range of anisotropies, the case of the triangular lattice is more complex. Spin-wave theory and several numerical studies indicate that the anisotropic systems should follow the supersolid scenario with ground-state broken translational symmetry, as well as the transverse magnetic order, implying a gapless Goldstone mode. Confirming this scenario at finite magnetic fields, we find numerically that at zero field, the available evidence points instead to a solid with a finite gap [2].

[1] MU, J. Kokalj, A. Wietek, A. Zorko, P. Prelovšek, Phys. Rev. B **109**, 035110 (2024).
[2] MU, J. Kokalj, T. Tohyama, P. Prelovšek, Phys. Rev. B **111**, 174442 (2025).

Strain-induced Ettingshausen effect in spin-orbit coupled noncentrosymmetric metals

Gautham Varma K[1], Azaz Ahmad[1] and Gargee Sharma[2]

[1]School of Physical Sciences ,Indian Institute of Technology Mandi, Kamand, Himachal Pradesh – 175075,India

[2] Department of Physics, Indian Institute of Technology Delhi, New Delhi-110016,India

ABSTRACT

Recent studies have revealed that CA is not necessarily only a Weyl-node property, but is rather a Fermi surface property, and is also present in a more general class of materials, for example, in spin-orbit-coupled noncentrosymmetric metals (SOC-NCMs). Using a tight-binding model for SOC-NCMs, we first demonstrate that strain in SOC-NCMs induces anisotropy in the spin-orbit coupling and generates an axial electric field. Then, using the quasi-classical Boltzmann transport formalism with momentum-dependent intraband and interband scattering processes, we show that strain in the presence of external magnetic field can generate temperature gradients via the Nernst-Ettingshausen effect, whose direction and behavior depends the on interplay of multiple factors: the angle between the applied strain and magnetic field, the presence of the chiral anomaly, the Lorentz force, and the strength of interband scattering.

INTRODUCTION

- Chiral anomaly have been observed in SOC-NCMs, which renders it to be a Fermi surface property rather than a Weyl-node property.
- SOC-NCMs have an additional k^2 dependence in the hamiltonian. As a result, there will be two fermi surfaces associated with a single node.
- Strain induces anisotropy in the spin-orbit coupling and generates an axial electric field.
- Strain in the presence of external magnetic field can generate temperature gradients via the Nernst-Ettingshausen effect whose direction and behavior depends on the angle between the applied strain and magnetic field, and the strength of interband scattering.

MATHEMATICAL MODELLING

- For SOC-NCMs under strain, we consider the Hamiltonian:

$$\frac{\hbar^2 k^2}{2m} + \alpha k \cdot \sigma + b_z k_z \sigma_z$$

We have taken into account the effect of Berry curvature on the semi-classical dynamics of Bloch electrons as per the equations:

$$\dot{\mathbf{r}}^\lambda = D^\lambda\left(\frac{e}{\hbar}(\mathbf{E}\times\mathbf{\Omega}^\lambda + \frac{e}{\hbar}(\mathbf{v}^\lambda\cdot\mathbf{\Omega}^\lambda)\mathbf{B} + \mathbf{v}_k^\lambda)\right)$$

$$\dot{\mathbf{p}}^\lambda = -eD^\lambda(\mathbf{E} + \mathbf{v_k}^\lambda \times \mathbf{B} + \frac{e}{\hbar}(\mathbf{E}\cdot\mathbf{B})\mathbf{\Omega}^\lambda)$$

- We solved the Maxwell-Boltzmann Equation for a given distribution function without loss of generality.

$$\frac{\partial f^\lambda}{\partial t} + \dot{\mathbf{r}}^\lambda \cdot \nabla_{\mathbf{r}} f^\lambda + \dot{\mathbf{k}}^\lambda \cdot \nabla_{\mathbf{k}} f^\lambda = I_{coll}[f^\lambda]$$

and in accordance with Fermi-Golden rule we have,

$$I_{\text{coll}}[f_{\mathbf{k}}^m] = \sum_p \sum_{\mathbf{k}'} W_{\mathbf{k},\mathbf{k}'}^{mp}(f_{\mathbf{k}'}^p - f_{\mathbf{k}}^m)$$

Where,

$$W_{\mathbf{k},\mathbf{k}'}^{mp} = \frac{2\pi}{\hbar}\frac{n}{\mathcal{V}}|\langle\psi_{\mathbf{k}'}^p|U_{\mathbf{kk}'}^{mp}|\psi_{\mathbf{k}}^m\rangle|^2\delta(\epsilon_{\mathbf{k}'}^p - \epsilon_F)$$

- In the presence of finite temperature, the Maxwell Boltzmann equation is modified as:

$$\left[\left(\frac{\partial f_{\mathbf{k}}^\lambda}{\partial \epsilon_{\mathbf{k}}^\lambda}\right)\left(e\mathbf{E} + \frac{\epsilon_{\mathbf{k}}^\lambda - \mu}{T}\nabla T\right)\cdot\left(\mathbf{v}_{\mathbf{k}}^\lambda + \frac{e\mathbf{B}}{\hbar}(\mathbf{\Omega}^\lambda\cdot\mathbf{v}_{\mathbf{k}}^\lambda)\right)\right] = -\frac{1}{\mathcal{D}^\lambda}\sum_{\lambda'}\sum_{\mathbf{k}'} W_{\mathbf{kk}'}^{\lambda\lambda'}(g_{\mathbf{k}'}^\lambda - g_{\mathbf{k}}^\lambda)$$

- The distribution function is obtained by solving the above equation, and is substituted in the current density equation:

$$\mathbf{J} = -\frac{e}{\mathcal{V}}\sum_{\lambda,k}\dot{\mathbf{r}} f_{\mathbf{k}}^\lambda.$$

- From the above equation we get the Hall and Peltier coefficients driven by electric and temperature gradient responses.
- At the steady state, the current density vanishes and we get the following equation:

$$\frac{\nabla T}{E_5} = \hat{\alpha}^{-1}\hat{\sigma}$$

RESULTS

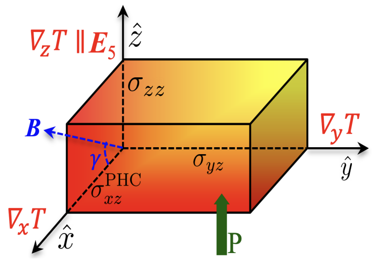

Fig1: Schematic that shows the strain-induced Ettingshausen effect

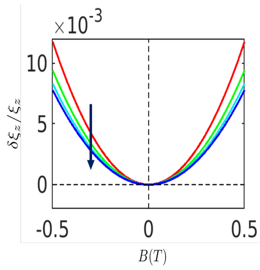

Fig 2: Temperature gradient for the case when direction of strain and magnetic field are parallel.

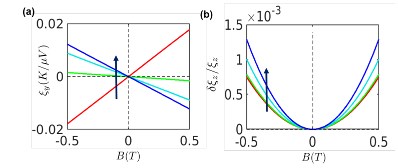

Fig 3:Temperature gradients for the case when strain and magnetic field are perpendicular.

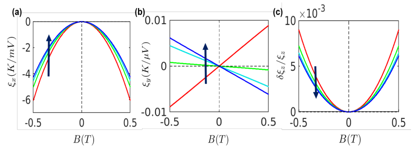

Fig 4: temperature gradient for an arbitrary angle.

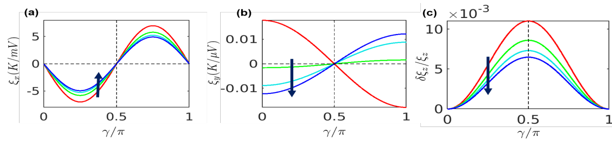

Fig 5: Dependence of temperature gradients on the angle between strain direction and magnetic field.

CONCLUSIONS

- SOC-NCMs will have anisotropy in the spin-orbit coupling due to strain.
- Strain generates an axial electric field in SOC-NCMs along the direction of application.
- At the steady state, strain generates temperature gradients whose direction depends on the angle between the strain direction and magnetic field and the strength of interband scattering.
- Temperature gradient along x-direction is purely induced by chiral anomaly via PHC, while that along the y- and z-directions are generated by Lorentz Hall and LMC(chiral anomaly induced) respectively.

REFERENCES

1. S. Cheon, G. Y. Cho, K.-S. Kim, and H.-W. Lee, Chiral anomaly in noncentrosymmetric systems induced by spin-orbit coupling, Physical Review B 105, L180303(2022).
2. S. Das, K. Das, and A. Agarwal, Chiral anomalies in three-dimensional spin-orbit coupled metals: Electrical, thermal, and gravitational anomalies, Physical Review B 108, 045405 (2023).
3. G. Varma K, A. Ahmad, S. Tewari, and G. Sharma, Magnetotransport in spin-orbit coupled noncentrosymmetric and weyl metals, Physical Review B 109, 165114 (2024).

ACKNOWLEGEMENTS

I wish to extend my gratitude to my supervisor Dr. Gargee Sharma for her valuable insights and discussions. I wish to thank IIT Mandi for providing me with HTRA funding for my work. I also thank my group members for their valuable discussions.

P133

Probing Topological Phase Transitions in Disordered SSH Chains via Entanglement Entropy and Lyapunov Exponents

Manish Kumar[1], **Bharadwaj Vedula**[1], **Suhas Gangadharaiah**[1], **and Auditya Sharma**[1]

[1]*Department of Physics, Indian Institute of Science Education and Research, Bhopal, Madhya Pradesh 462066, India.*

Entanglement entropy (EE) has emerged as a useful tool to study quantum phases of matter. In this work, we examine its role in detecting topological phase transitions in systems where disorder can make conventional diagnostics difficult. Focusing on variants of the Su–Schrieffer–Heeger (SSH) model, we present an EE-based framework that separates topological and trivial phases in a clear way.

Our key finding is that the difference in EE between half-filled and near-half-filled ground states, denoted as $\Delta S^{\mathcal{A}}$, provides a robust signature of topology: it vanishes in the topological phase, while remaining finite in the trivial phase due to edge-state localization. This behavior holds even in the presence of quasiperiodic and binary disorder.

We also find close agreement between phase boundaries obtained from Lyapunov exponents (via transfer matrices), EE-based diagnostics, and the topological quantum number $\mathcal{Q}$. In some cases, $\Delta S^{\mathcal{A}}$ gives a clearer signal than $\mathcal{Q}$.

These results show that EE can serve as a reliable diagnostic for disordered topological systems, providing a bridge between quantum information approaches and condensed matter perspectives on quantum phases.

[1] M. Kumar, B. Vedula, S. Gangadharaiah, A. Sharma (arXiv:2508.15897).
[2] I. C. Fulga, F. Hassler, A. R. Akhmerov, and C. W. J. Beenakker, Phys. Rev. B **83**, 155429 (2011).
[3] I. Peschel, Brazilian Journal of Physics **42**, 267 (2012).

P134

Quantum Imaging With Undetected Photons

Balakrishnan Viswanathan[1], Gabriela Barreto Lemos[2], and Mayukh Lahiri[3]

[1]*Center for Quantum Information, Communication and Computing, Indian Institute of Technology Madras, India*

[2]*Instituto de Física, Universidade Federal do Rio de Janeiro, Brazil*

[3]Department of Physics, Oklahoma State University, USA

Quantum Imaging with Undetected Photons (QIUP) is a novel interferometric imaging technique where the light that illuminates the object is not detected [1]. Since there is no coincidence detection or post-selection involved here, this method allows the sample to be probed at wavelengths for which efficient detectors are not yet available. QIUP requires a correlated pair of photons, and the imaging is enabled by detecting the companion photon that never interacted with the object. More specifically, the image is constructed from the single-photon interference pattern on the camera.

We will discuss the imaging process in near-field and far-field configurations. In the near-field configuration, both the object and the camera are in the image plane with respect to the bi-photon source. However, in the far-field configuration, both the object and the camera are in the Fourier plane with respect to the source.

The image acquisition, in the near-field configuration, is enabled by the position correlation between the twin photons [2]. In the complementary scenario, i.e., the far-field configuration, the image is constructed due to the momentum correlation between the two photons [3]. Furthermore, we will also discuss the resolution limit in both these configurations [4, 5, 6] and do a comparative study between them.

[1] Gabriela Barreto Lemos, Victoria Borish, Garrette D. Cole, Sven Ramelow, Radek Lapkiewicz and Anton Zeilinger, "Quantum imaging with undetected photons," Nature **512**, 409–412 (2014)

[2] Balakrishnan Viswanathan, Gabriela Barreto Lemos, and Mayukh Lahiri, "Position correlation enabled quantum imaging with undetected photons," Opt. Lett. **46**, 3496-3499 (2021)

[3] Mayukh Lahiri, Radek Lapkiewicz, Gabriela Barreto Lemos, and Anton Zeilinger, "Theory of quantum imaging with undetected photons," Phys. Rev. A **92**, 013832 (2015)

[4] Balakrishnan Viswanathan, Gabriela Barreto Lemos, and Mayukh Lahiri, "Resolution limit in quantum imaging with undetected photons using position correlations," Opt. Express **29**, 38185-38198 (2021)

[5] Marta Gilaberte Basset, René Sondenheimer, Jorge Fuenzalida, Andres Vega, Sebastian Töpfer, Elkin A. Santos, Sina Saravi, Frank Setzpfandt, Fabian Steinlechner, and Markus Gräfe, "Experimental analysis of image resolution of quantum imaging with undetected light through position correlations", Phys. Rev. A **108**, 052610 (2023)

[6] Jorge Fuenzalida, Armin Hochrainer, Gabriela Barreto Lemos, Evelyn A. Ortega, Radek Lapkiewicz, Mayukh Lahiri and Anton Zeilinger, "Resolution of quantum imaging with undetected photons," Quantum **6**, 646 (2022)

P135

Realisaton of the ancilla concept in cuprate-like systems

Mikołaj Walicki[1], **Johannes Knolle**[2], **and Krzysztof Wohlfeld**[1]

[1]*(Presenting author underlined) Faculty of Physics, University of Warsaw, Ludwika Pasteura 5, 02-093 Warsaw, Poland*

[2]*Department of Physics, Technische Universität München TQM, Garching, Germany.*

Since its first appearance in 2020 [1] the ancilla model has been at the cutting edge of new research because of the variety of quantum phases that it can host. However, the ancilla qubits largely remain a theoretical concept with its application to the real systems still under debate.
In this work we revisit the effective model for the superconducting cuprates. We start from the three-band Emery model with Hubbard interactions on both copper and oxygen atoms [2]. By going to the symmetry basis for the oxygen orbitals [3, 4] the higher oxygen band decouples from the copper atoms, creating a layered structure. Then we systematically remove the high energy processes by repeatedly applying the Schrieffer-Wolff transformation, while still keeping all three bands present. At the end we arrive at a Hamiltonian that is clearly separated into successive layers with fixed number of particles, as in the ancilla concept. Those layers are coupled together by antiferromagnetic superexchange couplings, as well as the three-site processes. This suggests that a physical ancilla might be realised for a cuprate-like system with high enough hole doping.

[1] Y. Zhang, S. Sachdev, Phys. Rev. Research **2**, 2 (2020).
[2] V. J. Emery, Phys. Rev. Lett. **58**, 26 (1987).
[3] J. H. Jefferson, H. Eskes, L. F. Feiner, Phys. Rev. B **45**, 14 (1992).
[4] L. F. Feiner, J. H. Jefferson, R. Raimondi, Phys. Rev. B **53**, 13 (1996).

P136

Sierpiński Spin Ice

J. Walkling[1] **and R. Moessner**[1]

[1] *Max-Planck-Institut für Physik komplexer Systeme, Nöthnitzer Straße 38, 01187 Dresden, Germany*

Artificial spin ice [1, 2] permits the exploration of novel geometries with tunable couplings. Most directly, it enables the study of planar lattices in 2D. This motivates our investigation of the Sierpinski gasket fractal. With a fractal dimension $d = \ln(3)/\ln(2) \approx 1.5$, this structure can host spin ice physics in fractional dimensions. Building on previous work calculating the Pauling entropy [3], we employ Monte Carlo methods to show that magnetic monopole excitations are confined at zero temperature. The system exhibits quasi-one-dimensional behaviour, with flux lines connecting oppositely charged excitations strongly bunched in a flux-lensing effect. We extract the entropic confinement potential analytically by leveraging the hierarchical dilation symmetry inherent in the fractal. Finally, we propose experimental parameters to locally realise the spin ice Hamiltonian, enabling spin ice physics to be probed in the laboratory in fractional dimensions.

[1] R. F. Wang, C. Nisoli, P. Schiffer, Rev. Mod. Phys. 85, 1473 (2013).
[2] P. Schiffer, C. Nisoli, Appl. Phys. Lett. 118, 110501 (2021).
[3] Shu-Chiuan Chang, Lung-Chi Chen, Hsin-Yun Lee, Physica A 392, 1776 (2013).

P137

Persistence of the BKT transition with long-range couplings

Luis Walther[1], Josef Willsher[1], and Johannes Knolle[2,3,4]

[1]*Max-Planck-Institut für Physik komplexer Systeme, Nöthnitzer Straße 40, 01187 Dresden*
[2]*Physics Department, TUM School of Natural Sciences, Technical University of Munich, 85748 Garching, Germany*
[3]*Munich Center for Quantum Science and Technology (MCQST), Schellingstrasse 4, 80799 München, Germany*
[4]*Blackett Laboratory, Imperial College London, London SW7 2AZ, United Kingdom*

The BKT phase transition is an archetypal example of a topological phase transition, which is driven by the decoupling of vortices. In this letter, we analyze the persistence of this phase transition in the XY model under the influence of long-range algebraically decaying interactions of the form $\sim \frac{1}{r^{2+\sigma}}$. We find that the transition persists for arbitrary values of σ. Crucially, in the presence of long-range interactions, spin waves renormalize the vortex interactions, which pushes the BKT to larger temperatures. As a conclusion, we find a rich phase diagram of the model, which is topologically distinct from previously known results. We use both Landau-Peierls-type arguments and Renormalization Group calculations and compare their results, emphasizing that the former are a powerful tool to analyze spin models. Our findings could be observed in state-of-the-art experiments, such as Rydberg simulators, and highlight the importance of long-range couplings for topological defects.

P138

Dynamics and stability of critical spin liquids

P139

QRCTM: Efficient iPEPS Simulation for Quantum Spin Models

Qi Yang[1], Yining Zhang[1], and Philippe Corboz[1]

[1]*Institute for Theoretical Physics, University of Amsterdam,
Science Park 904, 1098 XH Amsterdam, The Netherlands*

Infinite projected entangled-pair states (iPEPS) are a powerful tool for studying two-dimensional quantum spin systems, but standard CTMRG becomes prohibitively expensive at large bond dimensions. We introduce **QRCTM**, a QR-based CTMRG scheme that replaces costly SVD/EVD steps with QR factorizations *and* exploits lattice symmetries (e.g., C_{3v} on the honeycomb and C_{4v} on the square lattice), achieving *up to one–two orders of magnitude* acceleration *without loss of accuracy*.

On the honeycomb lattice, benchmarks for the $S = \frac{1}{2}$ antiferromagnetic Heisenberg and isotropic Kitaev models yield energies and magnetizations comparable to SVD-based CTMRG, and applications to the Kitaev–Heisenberg model show dimer–dimer correlations consistent with $1/r^4$ decay in the Kitaev QSL regime [1]. On the square lattice, our approach attains state-of-the-art results for the Heisenberg and $J_1 - J_2$ models in about one hour on a single H100 GPU [2]. These results establish QRCTM as a scalable, GPU-friendly route to exploring the physics of quantum spin models.

[1] Q. Yang and P. Corboz, Efficient iPEPS Simulation on the Honeycomb Lattice via QR-based CTMRG, arXiv:2509.05090. (2025)

[2] Y. Zhang*, Q. Yang*, and P. Corboz, Accelerating two-dimensional tensor network contractions using QR-decompositions, arXiv:2505.00494. (2025)

P140

Abstract for the Advanced School and Conference on Quantum Matter (smr 4114)

Polaron formation in bosonic flux ladders

Selma Youcef Khodja[1], **Laurens Vanderstraeten**[1], **Nathan Goldman**[1,2,3], **and Ivan Amelio**[1,2,4]

[1]*Center for Nonlinear Phenomena and Complex Systems, Université Libre de Bruxelles, CP 231, Campus Plaine, B-1050 Brussels, Belgium*
[2]*International Solvay Institutes, 1050 Brussels, Belgium*
[3]*Laboratoire Kastler Brossel, Collège de France, CNRS, ENS-Université PSL, Sorbonne Université, 11 Place Marcelin Berthelot, 75005 Paris, France*
[4]*Institute of Quantum Electronics, ETH Zurich, CH-8093 Zurich, Switzerland*

Understanding how a mobile impurity interacts with a quantum many-body environment is an active area of research in condensed matter physics [1]. This work studies the dressing of a particle immersed in a weakly interacting Bose-Einstein condensate, forming a polaron. The host system is a quasi one-dimensional bosonic flux ladder, which serves as a minimal model for two-dimensional systems under magnetic flux [2, 3]. The system is described by the Bose-Hubbard Hamiltonian with Peierls substitution and is studied at zero temperature in the thermodynamic limit. It exhibits three phases: Meissner, vortex, and biased ladder, each characterized by distinct current patterns and symmetry-breaking properties [4]. The phase diagram is obtained using mean-field theory and is confirmed numerically by Gross-Pitaevskii evolution. Bogoliubov theory [5] is used to compute the collective excitations of the bath above the condensate, and the corresponding dynamical structure factor is computed in each phase.

An impurity is then introduced and treated within the Chevy approximation, a variational truncation of the many-body wavefunction [6]. The polaron spectral function is computed across all three phases. To isolate the role of flux, the spectral function is also computed for the one-dimensional Bose gas on a lattice. In this case, the impurity-boson correlation function is used to identify the nature of the dressed quasi-particles. The spectral functions show clear signatures of the underlying background. These are new results and are testable in cold-atom experiments.

[1] F. Grusdt, N. Mostaan, E. Demler, L. A. Peña Ardila, *Impurities and polarons in bosonic quantum gases: a review on recent progress*, 2024.

[2] M. Atala, M. Aidelsburger, M. Lohse, et al., *Observation of chiral currents with ultracold atoms in bosonic ladders*, Nature Physics, 10:588–593, 2014.

[3] J. Dalibard, F. Gerbier, G. Juzeliūnas, P. Öhberg, *Colloquium: Artificial gauge potentials for neutral atoms*, Reviews of Modern Physics, 83(4):1523–1543, November 2011.

[4] S. Greschner, M. Piraud, F. Heidrich-Meisner, I. P. McCulloch, U. Schollwöck, T. Vekua, *Symmetry-broken states in a system of interacting bosons on a two-leg ladder with a uniform abelian gauge field*, Phys. Rev. A, 94:063628, Dec 2016.

[5] N. N. Bogolyubov, *On the theory of superfluidity*, J. Phys. (USSR), 11:23–32, 1947.

[6] W. Li and S. Das Sarma, *Variational study of polarons in Bose-Einstein condensates*, Phys. Rev. A, 90:013618, Jul 2014.

P141

Adiabatic echo protocols for robust quantum many-body state preparation

Zhongda Zeng,[1,2,*] Giuliano Giudici,[1,2,*] Aruku Senoo,[3]
Alexander Baumgärtner,[3] Adam M. Kaufman,[3] and Hannes Pichler[1,2,†]

[1] *Institute for Theoretical Physics, University of Innsbruck, Innsbruck 6020, Austria*
[2] *Institute for Quantum Optics and Quantum Information, Austrian Academy of Sciences, Innsbruck 6020, Austria*
[3] *JILA, University of Colorado and National Institute of Standards and Technology, and Department of Physics, University of Colorado, Boulder, Colorado 80309, USA*

Entangled many-body states are a key resource for quantum technologies. Yet their preparation through analog control of interacting quantum systems is often hindered by experimental imperfections. Here, we introduce the adiabatic echo protocol, a general approach to state preparation designed to suppress the effect of static perturbations. We provide an analytical understanding of its robustness in terms of dynamically engineered destructive interference. By applying quantum optimal control methods, we demonstrate that such a protocol emerges naturally in a variety of settings, without requiring assumptions on the form of the control fields. Examples include Greenberger-Horne-Zeilinger state preparation in Ising spin chains and two-dimensional Rydberg atom arrays, as well as the generation of quantum spin liquid states in frustrated Rydberg lattices. Our results highlight the broad applicability of this protocol, providing a practical framework for reliable many-body state preparation in present-day quantum platforms.

* These authors contributed equally to this work.

† hannes.pichler@uibk.ac.at

P142

Second order phase transition in dissipative Cat Qubits

Martina Zündel[1], Sebastian Diehl[2]

[1] *Université Grenoble Alpes, CNRS, LPMMC, 38000 Grenoble, France*
[2] *Institut fur Theoretische Physik, Universität zu Köln, 50937 Cologne, Germany*

Dynamically protected cat qubits[1] are realized through a coherent two-body drive and incoherent two-body loss. The dynamics inherits a strong parity symmerty which implies a symmetry between classical and quantum field within the Schwinger-Keldysh formalism. We show that the mean field phase diagram exhibits a second order phase transition where both modes go to zero and an additional first order transition. For vanishing Kerr non-linearity, there is an exceptional point where the first order transition becomes second order.

[1] M. Mirrahimi et al, New J. Phys. 16 045014